The Pennsylvania State University

The Graduate School

College of Agricultural Sciences

ENHANCED TECHNIQUES FOR DETERMINING CHANGES TO SOILS RECEIVING WASTEWATER IRRIGATION FOR OVER FORTY YEARS

A Thesis in

Soil Science

by

Charles W. Walker

Submitted in Partial Fulfillment
of the Requirements
for the Degree of

Doctor of Philosophy

December 2006

The thesis of Charles W. Walker was reviewed and approved* by the following:

Hangsheng Lin
Associate Professor of Hydropedology/
Soil Hydrology
Thesis Adviser
Chair of Committee

Daniel D. Fritton
Professor of Soil Physics

Maxim J. Schlossberg
Assistant Professor of Turfgrass Nutrition
and Soil Fertility

Gary W. Petersen
Distinguished Professor Emeritus of
Soil and Land Resources

Richard R. Parizek
Professor of Geology and Geo-
Environmental Engineering

David M. Sylvia
Professor of Soil Microbiology and
Head of the Department of Crop and
Soil Science

*Signatures are on file in the Graduate School.

ABSTRACT

It is the goal of the present study to use the framework set out by the emerging hydropedology concepts and techniques to better understand a real world practice, wastewater irrigation. The objectives are twofold, 1) to evaluate and modify selected hydraulic conductivity measurement techniques to enhance their reliability and accuracy; and 2) to comprehensively evaluate the changes in soil properties after receiving over forty years of wastewater irrigation, including the use of improved methodologies addressed in the first objective.

The tension infiltrometer is a standard tool for measuring near-saturated soil hydraulic properties. We examined the dynamics of the supply tension at the interface between the tension infiltrometer and the measured soil using a pressure transducer under different soil conditions and raised some cautions needed for proper use of this standard device. Infiltration experiments were conducted on a tension table, a large sand column, and in two field soils of contrasting textures and structures to test the performance of the standard two-piece infiltrometer. Results showed that during high flow rates (> 200 cm^3 min^{-1}) the tension at the infiltrometer/soil interface started to deviate by as much as 15 mm from the desired tension. However, during field experiments the high flow rates were not experienced, and thus no deviation was observed between the pre-set desired tension and the actual measured tension at the infiltrometer/soil interface. To alleviate the problem of tension deviation under high flow, the water supply tubing and fitting diameters of the standard infiltrometer were successfully increased to yield a higher flow rate (~300-400 cm^3 min^{-1}) without elevated tensions.

The constant head method for determining saturated hydraulic conductivity is a classical laboratory method for measuring the soil's ability to conduct water. One error commonly associated with this technique occurs when there is flow between the edge of the soil sample and the cylindrical ring holding the soil sample. We developed a method to minimize the effects of this artificial boundary flow. A new simple permeameter was constructed to separate flow between the outer and inner portions of the soil core. Intact core samples from the surface and subsurface Hagerstown silt loam series were analyzed to quantify the edge flow phenomenon. Outer saturated hydraulic conductivity (associated with possible edge flow) was found to be significantly higher than the inner saturated hydraulic conductivity (p = 0.038, n = 153). The A-horizon surface samples were found to have significant edge flow (n=110, p =0.049), whereas the subsurface soil samples did not experience significant edge flow because of possible clay expansion. In addition, brilliant blue dye was used to visually confirm the edge flow phenomenon. This study also investigated the length of saturation time needed to saturate the soil cores, and found that the heavier textured cores should be saturated for at least a week. A long term experiment was conducted for eight days to determine if and when the outflow volume reaches steady-state. The results indicated that, although the core appeared to be at steady-state during short time periods, true steady-state conditions were not achieved until approximately five days into the experiment. Furthermore, the new permeameter's results were compared with *in situ* hydraulic conductivity methods. Taken altogether, these results suggest that the hydraulic conductivity values from the inner portion of the soil core are more comparable to the *in situ* tension and double ring infiltrometer conductivity values observed in the field.

For over 40 years, The Pennsylvania State University (PSU) has irrigated its wastewater onto both cropped and forested lands. While this method of wastewater disposal has gained popularity in water-deficit regions, it is not widely used in areas that have a surplus of water. Despite local weather conditions, PSU sprays two inches of wastewater a week. This irrigation, combined with the natural precipitation, amount to approximately 140 inches of water per year, which is equivalent to tropical rainfall. The objective of this study was to investigate the morphological and functional changes in soils as a result of this increased water load.

Previous studies conducted at this site provided an estimate of the original soil properties. Soil morphological parameters, such as structure, horizonation and redoximorphic features, were evaluated from the soil cores and *in situ* soil pits. In addition, soil functional parameters, such as saturated hydraulic conductivity, bulk density, texture, organic matter content, and pH, were evaluated to determine the longevity of the wastewater irrigation system.

Results indicate that the soils are experiencing periods of saturation and local erosion, which are explained by redoximorphic features and over thickened A-horizons found on the site. Although redoximorphic features were found to experience a significant increase in size since the last description in 1978, they did not increase in frequency. The site was also evaluated based on three different landscape positions: summit, side-slope, and depression. These positions were found to be statistically different when describing morphological features (i.e., manganese coating percentage, A-horizon depth, soil structure) and physical features (i.e., bulk density). As a result of prolonged irrigation, soil functionality has also changed. Visual observations of

increased runoff amounts are supported by laboratory findings of reduced saturated hydraulic conductivity in some regions of the study area. Collectively, these findings indicate that the summit areas may be the cause of excess runoff, having the lowest hydraulic conductivity values and most eroded A-horizon. Conversely, while the depressional areas are the most saturated, a result of receiving extra runon from the summit positions, laboratory hydraulic conductivity results indicate these depressions can transmit the greatest amount of water. We therefore propose remediation to increase the hydraulic conductivity of the summit areas in order to keep this area sustainable for future years to come.

TABLE OF CONTENTS

LIST OF TABLES

LIST OF FIGURES

ACKNOWLEDGEMENTS

I would like to dedicate this dissertation to my family. They have provided me with never ending support throughout my very long college career. I truly believe that I have the greatest family in the world. I love you guys.

Dad: Thank you for your endless words of wisdom, motivation and inspiration.
Mom: Thank you for all of your confidence, believing in me, and for your engineering talent.

To my wife, Susan: Four years ago, I wrote "Together we can accomplish anything." I believe in that more and more each day. Thank you for keeping me in the program, being by my side through everything, and for being the love of my life.

I would like to thank Dr. Lin for being my advisor throughout my journey as a Ph.D. student and for the opportunities that he has provided me with.
.
I would also like to thank my graduate committee for all of their helpful suggestions and insight. Their knowledge intimidated me, their friendship comforted me.

Eight years ago, Mr. Randall Bock hired me as a shop assistant in the Agricultural and Biological Engineering Department. I cannot find words to express how important to my life that experience has been. Thank you, Randy.

There are many others that helped to make this degree possible for me including: The Hydropedology Lab Group, Jake Eckenrode, Dr. Ciolkosz, Ray Crew, Scott Harkcom, Shaun Heinbaugh and The Farm Operations Crew.

Finally, I would like to thank everyone in the Crop and Soil Science Department for providing such an enjoyable learning atmosphere.

This project was partially supported by USDA-National Needs Initiative Grant #2002-35102-12547 and the National Cooperative Soil Survey Program.

CHAPTER 1

INTRODUCTION

In 1883, V. Dokuchaev was the first person to classify soils based on their properties and forming factors such as climate. This information was introduced to the Western world by one of Dokuchaev's most influential students, K.D. Glinka, who focused on concepts such as soil geography, formation, and weathering (Buol et al., 1997). The next major advancement in soil science was in 1941 when Hans Jenny put forth the state-factor model of soil formation. Jenny's state-factor model suggests that soil formation is a function of climate, organisms, relief, parent material, and time. Jenny was one of the first scientists to suggest the concept of quantification for the soil science discipline (Soil Survey Staff, 1993). Although individual aspects of soil science can be quantified, such as soil physics, soil hydrology, soil morphology, soil biology, and soil chemistry, a great challenge that we face today is linking all of the different sub-disciplines of soil science in an integrated way (Wilding and Lin, 2006)

The concept of hydropedology has been defined as the "interwoven branch of soil science and hydrology that embraces interdisciplinary and multi-scale approaches to study interactive pedological and hydrological processes in the Earth's Critical Zone" (Lin, 2003). The interactions of soil and water control many soil-forming processes at multiple scales that are studied by pedologists; whereas hydrologists use the interactions between soil and water to gain a better understanding of water quality and quantity. The concept of hydropedology therefore suggests a synergy to be formed when these two disciplines are combined. Hydropedology also advocates the use of the landscape

perspective, commonly used by pedologists, and combines that information with hydrologic data to better define soil uses and limitations (Lin et al., 2006).

It is the goal of the present study to use the framework set out by the emerging hydropedology concepts and approaches to better understand a real world practice, wastewater irrigation. Many researchers have investigated the effects of wastewater on soils (Filip et al., 1999; Friedel et al., 2000; Magesan et al., 2000; Presley et al., 2004) . However, few studies have integrated soil morphology and physics at multiple scales to determine the effects of the prolonged period of irrigation. The objectives of this research are twofold. 1) to evaluate and modify selected hydraulic conductivity measurement methods to enhance their reliability and accuracy; and 2) to comprehensively evaluate the changes in soil properties after receiving over forty years of wastewater irrigation, including the use of improved methodology addressed in the first objective. The changes in soil properties are evaluated on both pedon and landscape scales. At the pedon scale, we describe the soil's morphological and physical properties and how they have changed as a result of wastewater irrigation. At the landscape scale, individual pedons are spatially linked together to diagnose select areas that are in need of remediation to keep the entire system functional.

Before analyzing a particular system, it is necessary to validate the tools used for analysis. This research not only evaluates how the soils have changed over the long period of irrigation, it also evaluates two common methods used for determining soil hydraulic properties, i.e., the tension infiltrometer and soil core saturated hydraulic conductivity measurement.

The second chapter of this dissertation verifies the assumptions made while using a tension infiltrometer for the determination of unsaturated hydraulic conductivity. The tension infiltrometer is a popular tool for soil scientists to describe unsaturated water flow through soils, pore size contribution to flow, and sorptivity (Angulo-Jaramillo et al., 2000; Casanova et al., 2000; Lin and McInnes, 1995; Lin et al., 1996; Lin et al., 1997). One of the main assumptions, a constant tension between the soil and instrument boundary, has never been verified in real time. The constant tension assumption plays a critical role for solving the unsaturated hydraulic conductivity function. If the assumptions are not satisfied, the results will be unreliable at best.

The third chapter addresses the perpetual issue of boundary flow in intact soil cores during the laboratory measurements of saturated hydraulic conductivity. The edge flow phenomenon has been documented in nearly all of the standard protocols for performing tests of laboratory saturated hydraulic conductivity (Dane and Topp, 2002; Klute, 1986). However, little has been done to correct this issue. This research utilizes soil samples from the Pennsylvania State University's Spray Irrigation Facility to demonstrate the capability of a new device to separate the boundary flow from the inner flow. Dye tracing was used to visually verify the edge-flow phenomenon, the concept of steady-state flow, and soil core saturation time. Recommendations are provided to eliminate some of the variability commonly found with this standard procedure and to document the caution that should be taken when utilizing data from this analysis.

The fourth chapter investigates the effects of over 40 years of wastewater irrigation on soil properties. The local climate makes this system very different from the surrounding environment. As mentioned earlier, there has been a number of research

efforts investigating the effects of wastewater irrigation (Shahalam et al., 1998; Vinten et al., 1983; Wang et al., 2003); however, most of the research sites are in areas that require irrigation for crop growth. Our study area receives 30 to 40 inches of precipitation annually with natural rainfall. Combining natural and artificial precipitation, the area receives a total of 140 inches of water annually. This climate alteration and the use of hydropedological framework make this research unique.

The advanced methods described in the first two chapters, along with traditional methods, were used to analyze the soils for the spray irrigation field. Previous research in the same area was established as a control (Simpson and Cunningham, 1978; Sopper and Richenderfer, 1978). Soil morphological, physical, and chemical properties were analyzed to develop possible recommendations for sustaining the area for wastewater irrigation. Recommendations were also made on the key soil properties that need to be investigated at other sites in the Penn State Spray Irrigation System to determine the health of the whole system.

The final chapter explains the overall conclusions of this research. Summaries for each of the chapters are provided along with the direction for future research.

REFERENCES

Angulo-Jaramillo, R., J. Vandervaere, S. Roulier, J. Thony, J. Gaudet, and M. Vauclin. 2000. Field measurement of soil surface hydraulic properties by disc and ring infiltrometers A review and recent developments. Soil and Tillage Research 55:1-29.

Buol, S.W., F.D. Hole, R.J. McCracken, and R.J. Southard. 1997. Soil genesis and classification *In* (ed.). Iowa State University Press, Ames, Iowa.

Casanova, M., I. Messing, and A. Joel. 2000. Influence of aspect and slope gradient on hydraulic conductivity measured by tension infiltrometer. Hydrological Processes 14:155-164.

Dane, J., and G. Topp, (eds.) 2002. Methods of Soil Analysis: Part 4 Physical Methods, pp. 1-1692. Soil Science Society of America, Madison, Wisconsin.

Filip, Z., S. Kanazawa, and J. Berthelin. 1999. Characterization of effects of a long-term wastewater irrigation on soil quality by microbiological and biochemical parameters. Journal of Plant Nutrition and Soil Science 162:409-413.

Friedel, J., T. Langer, C. Siebe, and K. Stahr. 2000. Effects of long-term waste water irrigation on soil organic matter, soil microbial biomass and its activities in central Mexico. Biology and Fertility of Soils 31:414-421.

Klute, A., (ed.) 1986. Methods of soil analysis, Vol. 2nd edition. ASA and SSSA, Madison, WI.

Lin, H. 2003. Hydropedology: Bridging disciplines, scales and data. Vadose Zone Journal 2:1-11.

Lin, H., and K. McInnes. 1995. Water flow in clay soil beneath a tension infiltrometer. Soil Science 159:375-382.

Lin, H., K. McInnes, L. Wilding, and C. Hallmark. 1996. Effective porosity and flow rate with infiltration at low tensions into a well-structured subsoil. Transactions of the ASAE 39:131-133.

Lin, H., K. McInnes, L. Wilding, and C. Hallmark. 1997. Low tension water flow in structured soils. Canadian Journal of Soil Science 77:649-654.

Lin, H., J. Bouma, Y. Pachepsky, A. Western, J. Thompson, R.v. Genuchten, H. Vogel, and A. Lilly. 2006. Hydropedology: Synergistic integration of pedology and hydrology. Water Resource Research 42:1-13.

Magesan, G., J. Williamson, G. Yeates, and A. Lloyd-Jones. 2000. Wastewater C:N ratio effects on soil hydraulic conductivity and potential mechanisms for recovery. Bioresource Technology 71:21-27.

Presley, D.R., M.D. Ransom, G.J. Kluitenberg, and P.R. Finnell. 2004. Effects of thirty years of irrigation on the genesis and morphology of two semiarid soils in Kansas. Soil Science Society of America Journal 68:1916-1926.

Shahalam, A., B.A. Zahra, and A. Jaradat. 1998. Wastewater irrigation effect on soil, crop and environment: A pilot scale study at Irbid, Jordan. Water, Air, and Soil Pollution 106:425-445.

Simpson, T., and R. Cunningham. 1978. Soil Morphologic and Hydraulic Changes Associated with Wastewater Irrigation. Institute for Research on Land and Water Resources, The Pennsylvania State University, University Park, PA.

Soil Survey Staff, N.R.C.S. 1993. Soil Survey: Early Concepts of Soil [Online]. Available by Natural Resources Conservation Service. U.S. Department of Agriculture (verified July 2006).

Sopper, W., and J. Richenderfer. 1978. Effects of spray irrigation of municipal wastewater on the physical properties of the soil. Institute for Research on Land and Water Resources, The Pennsylvania State University, University Park, PA.

Vinten, A., U. Mingelgrin, and B. Yaron. 1983. The effect of suspended solids in wastewater on soil hydraulic conductivity: II. Vertical distribution of suspended solids. Soil Science Society of America Journal 47:408-412.

Wang, Z., A. Chang, L. Wu, and D. Crowley. 2003. Assessing the soil quality of long-term reclaimed wastewater-irrigated cropland. Geoderma 114:261-278.

Wilding, L., and H. Lin. 2006. Advancing the frontiers of soil science towards a geoscience. Geoderma 131:257-274.

CHAPTER 2

IS THE TENSION BENEATH THE TENSION INFILTROMETER WHAT WE THINK IT IS?*

ABSTRACT

The tension infiltrometer has become a standard tool for measuring near-saturated soil hydraulic properties. The objective of this study was to examine the dynamics of the supply tension at the interface between the tension infiltrometer and the measured soil using a pressure transducer under different soil conditions and to raise some cautions needed for proper use of this standard device. Infiltration experiments were conducted on a tension table, a large sand column, and in two field soils of contrasting textures and structures to test the performance of the standard two-piece infiltrometer. Results showed that during high flow rates (> 200 cm^3 min^{-1}) the tension at the infiltrometer/soil interface started to deviate by as much as 15 mm from the desired tension. However, during field experiments the high flow rates were not experienced, and thus no deviation was observed between the pre-set desired tension and the actual measured tension at the infiltrometer/soil interface. To alleviate the problem of tension deviation under high flow, the water supply tubing and fitting diameters of the standard infiltrometer were successfully increased to yield a higher flow rate (~300-400 cm^3 min^{-1}) without elevated tensions.

***This chapter has been published in the Vadose Zone Journal, 5:860-866 (2006)**

INTRODUCTION

Tension infiltrometers are widely used for determining soil hydraulic parameters such as saturated and unsaturated hydraulic conductivity, sorptivity, and macropore flow contribution (Angulo-Jaramillo et al., 2000; Ankeny et al., 1991; Casanova et al., 2000; Evett et al., 1999; Lin et al., 1997; Perroux and White, 1988; Watson and Luxmoore, 1986; White et al., 1992). The non-destructive nature of this instrument also allows for temporal investigations of soil hydraulic conductivity (Lin et al., 1998). The easy of use and relatively short operating times have provided the flexibility of making a large number of measurements to determine the spatial variability of hydraulic properties in different landscape settings and soil types (Lin et al., 1998; Watson and Luxmoore, 1986). The widespread use of the tension infiltrometer has facilitated field measurements of *in situ* soil hydraulic properties, inspired continued instrument improvements (Ankeny et al., 1988; Casey and Derby, 2002; Wang et al., 1998), and stimulated new analytical procedures for determining hydraulic properties from infiltrometer measurements (Ankeny et al., 1991; Logsdon and Jaynes, 1993; Reynolds and Elrick, 1991; Smettem and Clothier, 1989).

Wooding's solution for steady-state, three-dimensional flow into the soil from a circular source is the basis for unsaturated hydraulic conductivity calculations from infiltrometer measurements (Wooding, 1968). From this equation, many techniques have been developed to obtain various hydraulic parameters from steady-state tension infiltrometer measurements (Angulo-Jaramillo et al., 2000). A common solution to the Wooding's equation involves the use of simultaneous equations through a pair of supply tensions (Ankeny et al., 1991; Smettem and Clothier, 1989). All calculations of

hydraulic properties from tension infiltrometer data rely on the assumption that the supply tension at the infiltrometer disc-soil interface is constant and is not dependant on soil conditions.

This study investigates the assumption of constant supply tension at the interface between infiltrometer disc and the contacted soil of the standard two-piece tension infiltrometer. We also investigated the upper flow limit of the two-piece tension infiltrometer and potential modifications designed to increase the flow of water without increasing the tension in the disc.

MATERIALS AND METHODS

The tension infiltrometer utilized in this study was a two-piece unit (Fig. 2.1), which was designed after the specifications described by Perroux and White (1988) and consistent with commercially available models. However, to improve flow-monitoring accuracy, the unit was adapted to accommodate multiple reservoir sizes. The reservoir base, constructed from 51 mm diameter PVC pipe, was attached to a flexible coupling (American Valve, Greensboro, NC) to allow for a quick change between different sizes of reservoirs. The reservoirs were equipped with an Omega PX26-005 DV differential pressure transducer (Omega Engineering, Stanford, CT) to monitor water height change in the reservoir. The inner diameter (I.D.) of the air entry tube in the bubbling tower was 3.2 mm. The tubing and fittings that linked the bubbling tower to the reservoir also had a 3.2 mm I.D. The 600 mm section of tubing and barbed fittings used to connect the reservoir to the infiltration disc had an inner diameter of 12.7 mm and 8.7 mm, respectively. The infiltration disc had an effective diameter of 232 mm.

To monitor the tension between the infiltrometer disc and the contacted soil surface, we attached an Omega PX26-001 DV pressure transducer to the disc, using a 100mm section of plastic tubing (3.2 mm I.D.) (Fig. 2.1). The tubing was used to prevent the transducer from getting wet while the disc was submerged to remove air bubbles. The transducer was installed 30 mm from the center of the disc. With this setup, it was possible to monitor the actual tension applied to the soil surface using a datalogger and a laptop and to make real-time adjustments to the tension setting so that the desired tension can be achieved. This study used a Campbell CR-10 datalogger (Campbell Scientific,

Logan, UT) to monitor the water tension transducer as well as the water height transducer attached to the water reservoir.

We calibrated the water tension transducer by placing it on a pre-saturated tension table equipped with grade 470 filter paper (S & S Filter Paper, Keene, N.H.). To ensure a zero tension in the disc, the infiltrometer's water supply valve was opened before calibration started. However, during calibration the valve remained closed. The tension settings on the infiltrometer were calibrated by using a U-tube manometer and then were verified with the pressure transducer. The slope and intercept from the calibration linear regression equation was programmed into the datalogger to provide a real-time tension monitoring capability.

Laboratory experiments were carried out both on the tension table and on a large sand column. The tension table was chosen to provide a method of controlling the flow rate, whereas the large sand column provided a natural but controlled high-flow setting. Laboratory setup for the infiltrometer mimicked a field situation. The tension infiltrometer was placed at an even elevation with the tension table and was set to the desired tension. The infiltrometer was turned on and the tension table was adjusted to simulate different flow rates. We were able to increase and decrease the flow rates for the experiment by varying the height of the tension table. The tension setting on the tension infiltrometer was kept constant while the height of the tension table was varied. Tension measurements from the pressure transducer were recorded every 2 seconds with the datalogger. Each tension was measured for at least 5 minutes after steady-state had been achieved. The sand column experiments were performed on a drained cylinder of medium sand (cylinder 550 mm in diameter by 700 mm in height). Measurements were

carried out on the sand column at 120, 60, 30, 20, 10, and 0 mm tensions sequentially (with 10 min for 120 mm tension, 5 min for 60 to 20 mm, and 3 min for 10 and 0 mm), following the procedures similar to that of Lin et al. (1997). The sand column had a laboratory-measured saturated hydraulic conductivity of 2.0 cm min^{-1}.

To verify the constant tension assumption, we conducted field measurements on two different soil types. These measurements were carried out using three identical tension infiltrometers as replicates. Each infiltrometer was equipped with two pressure transducers, one to measure water height change in the reservoir (flow) and the other to measure the actual tension in the disc. Site preparation followed that of Lin et al. (1997), and included trimming vegetation, installing a retention ring, placing a layer of cheesecloth on the soil surface, and making the area even with thin layer of very fine sand. The water reservoir was placed next to the infiltration area and was even with the tension disc. The infiltration measurements were conducted at the same sequence of supply tensions as the sand column experiments, but the time period for each supply tension was longer (with 30 min for 120 and 60 mm tensions, 20 min for 30 and 20 mm tensions, and 15 min for 10 and 0 mm tensions). The pressure transducer in the infiltration disc was used solely to record the actual tension in the disc during the infiltration, not to make real time adjustments.

The field studies were conducted on two soils of contrasting textures and structures. The Hagerstown series (*Typic Hapludalf*) in a cropland was a limestone-derived residual soil that was very deep and well drained with a moderate permeability. The surface texture of the soil was silt loam and the surface structure was fine subangular blocky to granular. The Morrison series (*Ultic Hapludalf*) in a forest was a non-

calcareous sandstone-derived residual soil that was very deep and well drained with moderate to moderately-rapid permeability. The surface texture was loamy sand with a granular to single grain structure. Both of these soils had laboratory-measured saturated hydraulic conductivity values less than 0.1 cm min^{-1}.

To increase the maximum flow rate of the two-piece tension infiltrometer, this study evaluated modifications to the water supply tube. The I.D. of the tube connecting the water reservoir to the tension plate was increased from 12.7 mm to 15.9 mm, and the I.D. of the barbed fittings were also enlarged from 8.7 mm to 13.2 mm. The water supply valve was replaced with a 15.9 mm PVC plumbing valve attached directly to the reservoir. By retrofitting the infiltrometer with the larger fittings and tubing, we increased the smallest orifice diameter from 8.7 mm to 13.2 mm.

To mathematically solve for head loss through the water supply orifices in the tension infiltrometer, both the orifice equation and the Darcy-Weisbach equation were used. The different components were considered to be in series with each other, and plotted as total head loss. The orifice equation is described as (Jarrett, 2000):

$$q = ca\sqrt{2gh}\,, \qquad [1]$$

where q = flow (m^3 s^{-1}), c = orifice coefficient (0.6, based on the shape of the orifice), a = area of the orifice (m^2) (barbed tube fittings), g = gravity (m s^{-2}), and h = pressure difference (m). The Darcy-Weisbach equation is described as (Viessman and Hammer, 1998):

$$\Delta t = \lambda(L / d_n)(v^2 / 2g)\,, \qquad [2]$$

where Δt = change in tension (m), λ = friction factor (64/ Reynolds number), L = length of pipe (m), d_n = diameter (m), v = velocity (m s^{-1}), and g = gravity (m s^{-2}). It was

determined that the flow through this instrument was laminar flow (Reynolds number < 2000), so the equations are valid.

RESULTS AND DISCUSSION

Figure 2.2 shows the response of the infiltrometer's infiltration disc when subjected to different flow rates on the tension table. As the flow rate increased beyond ~200 cm^3 min^{-1}, the disc's tension started to increase by as much as 15 mm over the desired tensions. This elevated tension occurred even though the tension-setting tube was not changed during the experiment. These results suggest that, depending on the soil type being measured and its permeability, the two-piece tension infiltrometer has the possibility of voiding one of the primary assumptions of the instrument, i.e., maintaining a constant supply tension. The increase in tension at the disc was positively related to the flow rate under all of the supply tensions tested (Fig. 2.2). However, the standard deviation of the tension was roughly inversely related to the increase in the flow rate. This increase in the standard deviation of the measured tension at low flows visually corresponded to the air bubbling through the air entry tube. The 200 cm^3 min^{-1} threshold was chosen because the tension had a noticeable increase shortly after reaching this value.

The elevated tension with respect to flow rate was also detected in the sand column experiments. Figure 2.3 depicts the measured tension in the tension disc during the sand column experiments. When the instrument was set to a tension of 120 mm the measured and the desired tensions were similar. However, when the instrument was set to lower tensions of 60, 30, 20, 10, and 0 mm, the calibrated and the measured tensions started to deviate from each other more and more (Fig. 2.3). Even though the instrument was set to 0 mm tension, the actual tension was recorded to be approximately 30 mm (Fig. 2.3). The flow rates for the 120 mm tension were below the ~200 cm^3 min^{-1}

threshold flow rate, whereas the flow rates for the lower tensions were between 400 cm^3 min^{-1} and 750 cm^3 min^{-1}.

Field experiments were conducted to determine if there was any tension deviation from the calibrated value. Figures 2.4 and 2.5 show the results obtained from the Hagerstown silt loam and Morrison loamy sand, respectively. Overall, the tensions measured with the pressure transducer match up within a 10 mm range of the calibrated tension throughout all the tensions tested (120-0 mm range). The small deviation (< 10 mm) from the calibrated tensions may be attributed to a combination of several factors, including small difference in height between the base of the infiltrometer reservoir and the tension disc, air bubbling, and temperature fluctuation during the field measurements. We noticed that the tension disc has a slight tendency to sink after the measured soil has been moistened, which contributed to the difference between the actual and calibrated tensions. The flow rates calculated for each infiltrometer were all below 200 cm^3 min^{-1} threshold value. These results indicate that the present design for the infiltrometer works well in these two natural conditions. Nevertheless, cautions should be taken when conducting measurements in areas of faster flow, such as golf greens, recently tilled soils, or other highly permeable soils, because there may be restrictions on flow caused by inadequate tubing sizes leading to tension deviations as those shown in Fig. 2.3.

From observations made during the tension table and the sand column experiments, the volume of water flowing from the infiltrometer reservoir to the disc appeared to have a direct influence on the measured tension in the tension disc. It was hypothesized that the barbed tube fitting connecting the piece of 12.7 mm tubing from the reservoirs to the valve may be limiting the water flow to the tension disc. To substantiate

this idea, both the orifice equation (Eq. [1]) and the Darcy Weisbach equation (Eq. [2]) were used to calculate the increase in tension through the pipe network due to friction. These calculations were performed for a range of flow rates and the results are depicted in Fig. 2.6. The increase in tension shown from the calculations is similar to the laboratory results reported previously.

To determine if the water supply tube was the problem, the tubing, barbed fittings, and the water supply valve were all replaced with larger ones. The results from such increased diameters of the tubing, barbed fittings, and valves indicated that the tension remained steady beyond the ~200 cm^3 min^{-1} flow rate, but started to rise (drift away from calibrated tension) after > 300-400 cm^3 min^{-1} flow rate (Fig. 2.7). This suggests that the water supply tube and fittings may be the cause of the rising tension under high flow rates in the standard two-piece infiltrometer. There did not appear to have any adverse effects of increasing the tubing diameter, except a slight increase in the standard deviation of the tension at 60 mm supply tension as compared to the smaller tube.

SUMMARY

This study suggests that in many field situations, the present standard design of the two-piece tension infiltrometer is fully capable of maintaining a constant tension at the infiltrometer/soil boundary, if used properly. However, in some circumstances, where flow rates are very high (e.g., in golf greens, cracked soils, and soils with a coarse sandy texture), cautions should be taken to avoid the drift of supply tensions. This is important to the accurate use and interpretation of tension infiltrometer measurements since these devices are most frequently used for determining near-saturated hydraulic parameters in macroporous soils where flow rate could be high. Retrofitting the infiltrometer with larger tubing and fittings will help maintain a constant tension under conditions of high flow rates.

Proper infiltrometer setup is also important to accurate measurements. If the infiltrometer water reservoir is not level with the tension disc when using the two-piece unit, then there will be a discrepancy between the calibrated tension and the actual tension at the instrument/soil boundary. In such situations, it would be desirable to use a pressure transducer to monitor the actual tension on a real-time basis. The addition of a pressure transducer on the tension disc, as used in this study, allows for flexible tensions to be applied to the soil. This added pressure transducer is also helpful during measurement to detect any problems that may be occurring (such as leaks or air bubbles) and to make real-time adjustment.

References

Angulo-Jaramillo, R., J. Vandervaere, S. Roulier, J. Thony, J. Gaudet, and M. Vauclin. 2000. Field measurement of soil surface hydraulic properties by disc and ring infiltrometers A review and recent developments. Soil and Tillage Research 55:1-29.

Ankeny, M., T. Kaspar, and R. Horton. 1988. Design for an automated tension infiltrometer. Soil Science Society of America Journal 52:893-895.

Ankeny, M., M. Ahmed, T. Kaspar, and R. Horton. 1991. Simple field method for determining unsaturated hydraulic conductivity. Soil Science Society of America Journal 55:467-470.

Casanova, M., I. Messing, and A. Joel. 2000. Influence of aspect and slope gradient on hydraulic conductivity measured by tension infiltrometer. Hydrological Processes 14:155-164.

Casey, F., and N. Derby. 2002. Improved design for an automated tension infiltrometer. Soil Science Society of America Journal 66:64-67.

Evett, S., F. Peters, O. Jones, and P. Unger. 1999. Soil hydraulic conductivity and retention curves from tension infiltrometer and laboratory data, p. 541-551, *In* M. v. Genuchten, et al., eds. Proc. Int. Workshop Characterization and Measurement of Hydraulic Poperties of Unsatrated Porous Media. University of California, Riverside, Riverside California.

Jarrett, A. 2000. Water Management410. *In* (ed.). Kendall/Hunt Pub. Co., Dubuque, Iowa.

Lin, H., K. McInnes, L. Wilding, and C. Hallmark. 1997. Low tension water flow in structured soils. Canadian Journal of Soil Science 77:649-654.

Lin, H., K. McInnes, L. Wilding, and C. Hallmark. 1998. Macroporosity and initial moisture effects on infiltration rates in vertisols and vertic intergrades. Soil Science 163:2-8.

Logsdon, S., and D. Jaynes. 1993. Methodology for determining hydraulic conductivity with tension infiltrometers. Soil Science Society of America Journal 57:1426-1431.

Perroux, K., and I. White. 1988. Designs for disc permeameters. Soil Science Society of America Journal 52:1205-1215.

Reynolds, W., and D. Elrick. 1991. Determination of hydraulic conductivity using a tension infiltrometer. Soil Science Society of America Journal 55:633-639.

Smettem, K., and B. Clothier. 1989. Measuring unsaturated sorptivity and hydraulic conductivity using multi-disc permeameters. Journal of Soil Science 40:565-568.

Viessman, W., and M. Hammer. 1998. Water Supply and Pollution Control *In* (ed.). Addison Wesley Longman, Inc., Menlo Park, CA.

Wang, D., S. Yates, and F. Ernst. 1998. Determining soil hydraulic properties using tension infiltrometers, time domain reflectometry and tensionmeters. Soil Science Society of America Journal 62:318-325.

Watson, K., and R. Luxmoore. 1986. Estimating macroporosity in a forest watershed by use of a tension infiltrometer. Soil Science Society of America Journal 50:578-782.

White, I., M. Sully, and K. Perroux. 1992. Measurement of surface-soil hydraulic properties: Disk permeaters, tension infiltrometers, and other techniques, p. 69-103, *In* W. D. R. G. Clarke Topp, and Richard E. Green, ed. Advances in Measurement of Soil Physical Properties: Bringing Theory into Practice, Vol. Special Publication Number 30. Soil Science Society of America, Madison, Wisconsin.

Wooding, R. 1968. Steady infiltration from a shallow circular pond. Water Resource Research 4:1259-1273.

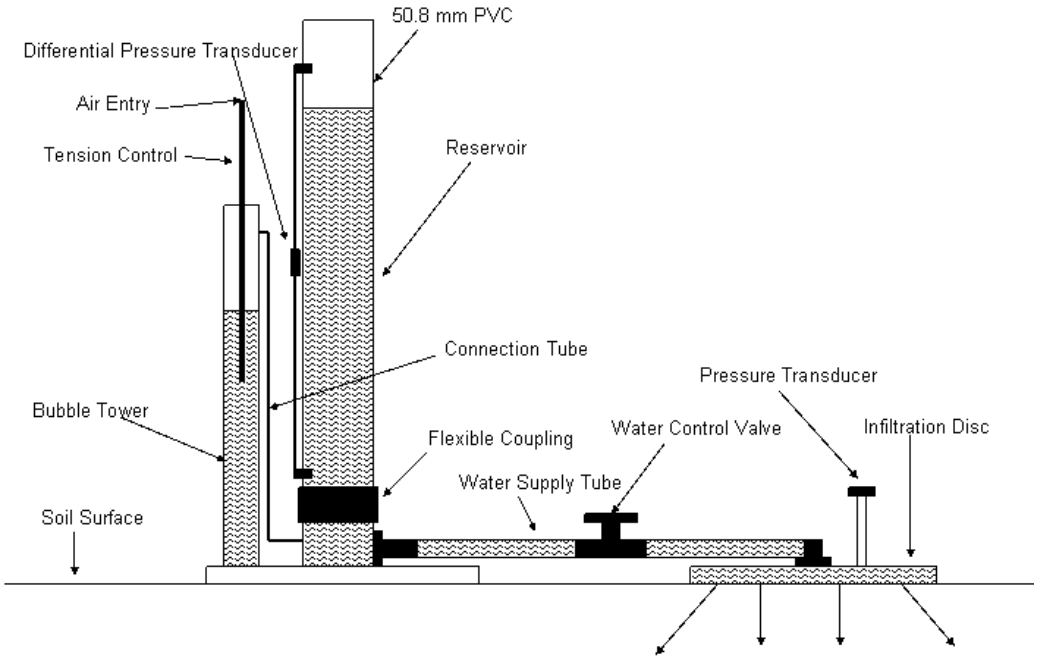

Fig. 2.1. Schematic a two-piece tension infiltrometer. The two-piece tension infiltrometer includes an additional pressure transducer on the infiltration disc. The flexible coupling allows for quick changes between different reservoir diameters, providing for more accurate water height measurements for different flow rates.

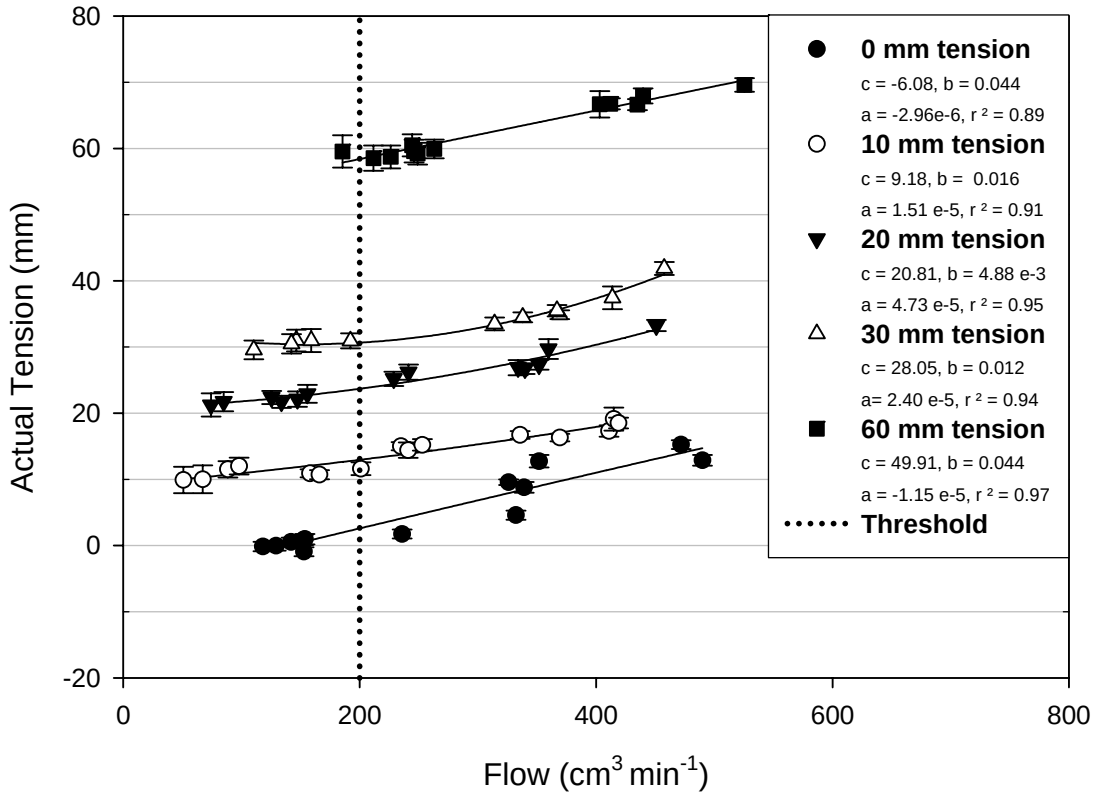

Fig. 2.2 Measured tension at the infiltration disc versus flow rate for the tension infiltrometer on a tension table using the standard water supply tube and fittings (12.7 and 8.7 mm, respectively). The tension control was set to the desired tension of either 0, 10, 20, 30 or 60 mm and remained so while the flow rates were varied. The starting point for each curve was the lowest constant flow rate measured and then the flow rate was increased by elevating the tension on the tension table. The error bars represent the standard deviation of the measured tension during each steady-state measurement. The coefficients of the quadratic equation, which was fitted to the points of each desired tension, are shown in the legend of the graph [$(a)x^2 + (b)x + (c)$]. The dotted vertical line (threshold) represents the approximate flow rate in which the tension starts to increase considerably.

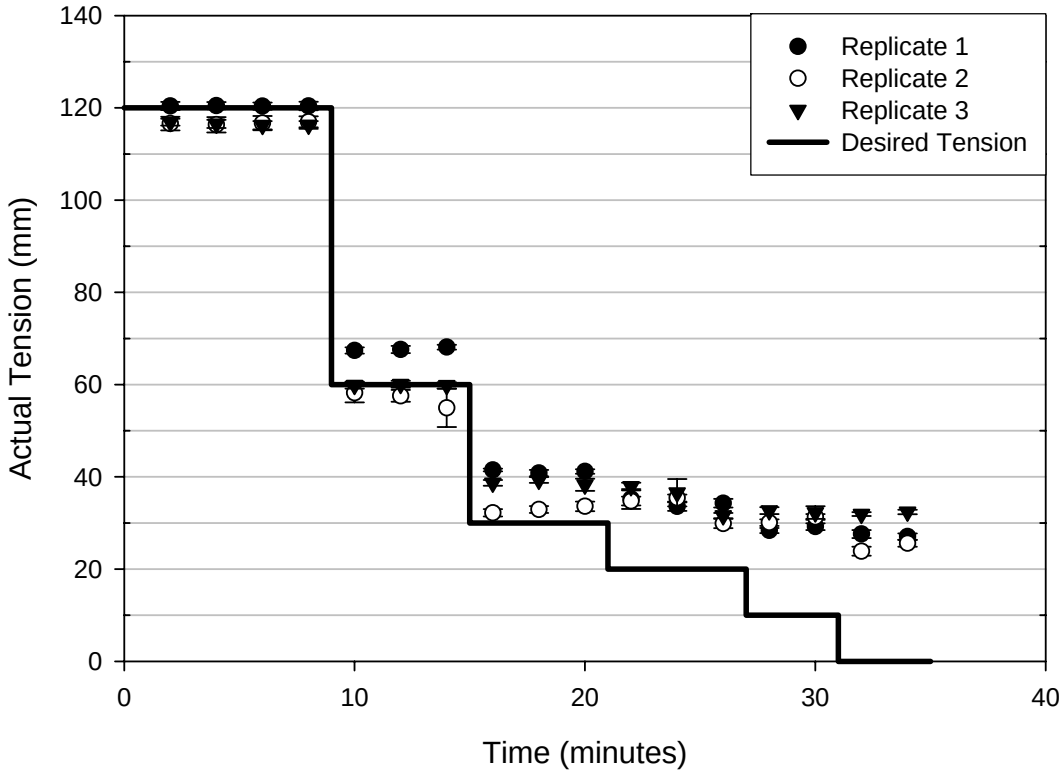

Fig. 2.3. Replicate measurements of tension in the infiltration disc while on a sand column for six desired tensions, 120, 60, 30, 20, 10, and 0 mm, respectively. Each point on the graph represents two minute tension averages with the standard deviation shown by error bars. The solid line represents the desired tension setting of the infiltrometer.

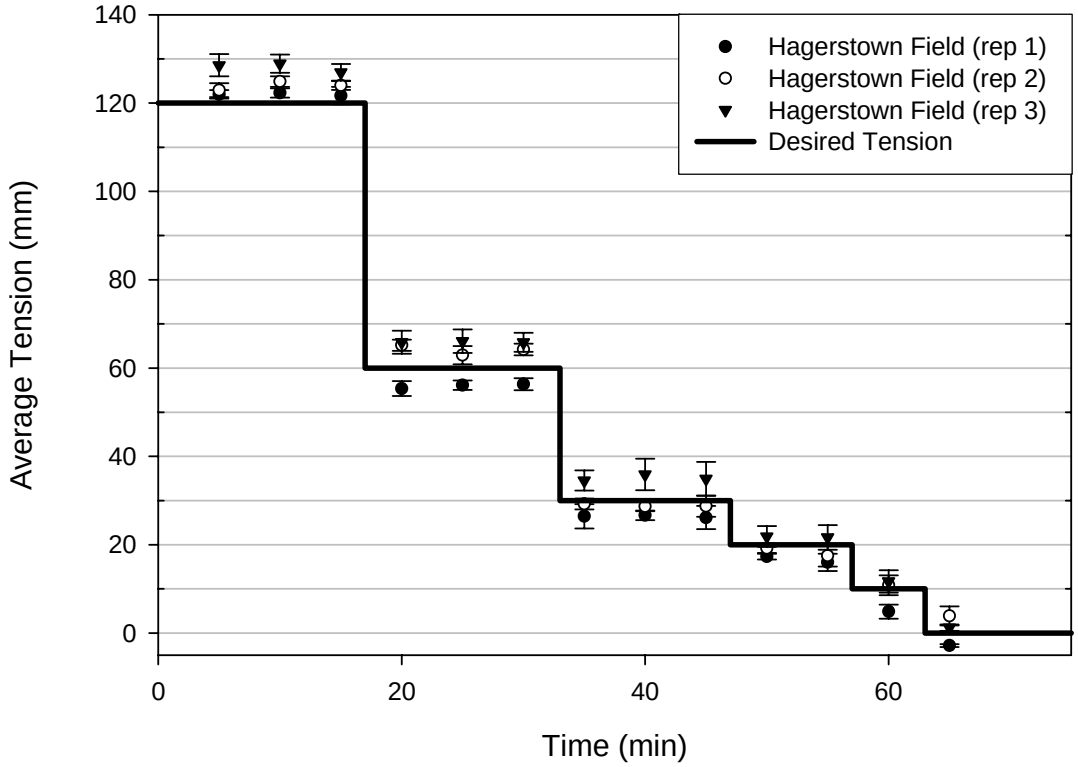

Fig. 2.4. Replicate measurements of tension in the infiltration disc placed on the Hagerstown silt loam soil for six desired tensions, 120, 60, 30, 20, 10, and 0 mm, respectively. Each point on the graph represents five minute tension averages with the standard deviation shown by error bars. The solid line represents the desired tension setting of the infiltrometer.

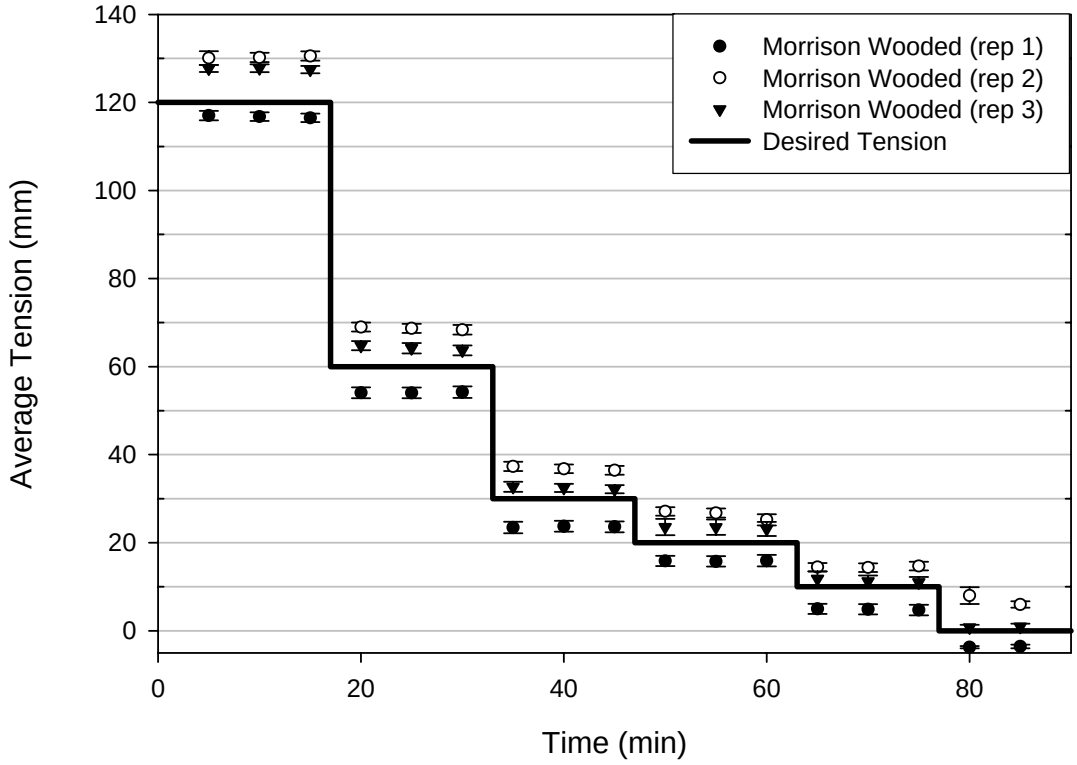

Fig. 2.5. Replicate measurements of tension in the infiltration disc placed on the Morrison sandy loam soil for six desired tensions, 120, 60, 30, 20, 10, and 0 mm, respectively. Each point on the graph represents five minute tension averages with the standard deviation shown by error bars. The solid line represents the desired tension setting of the infiltrometer.

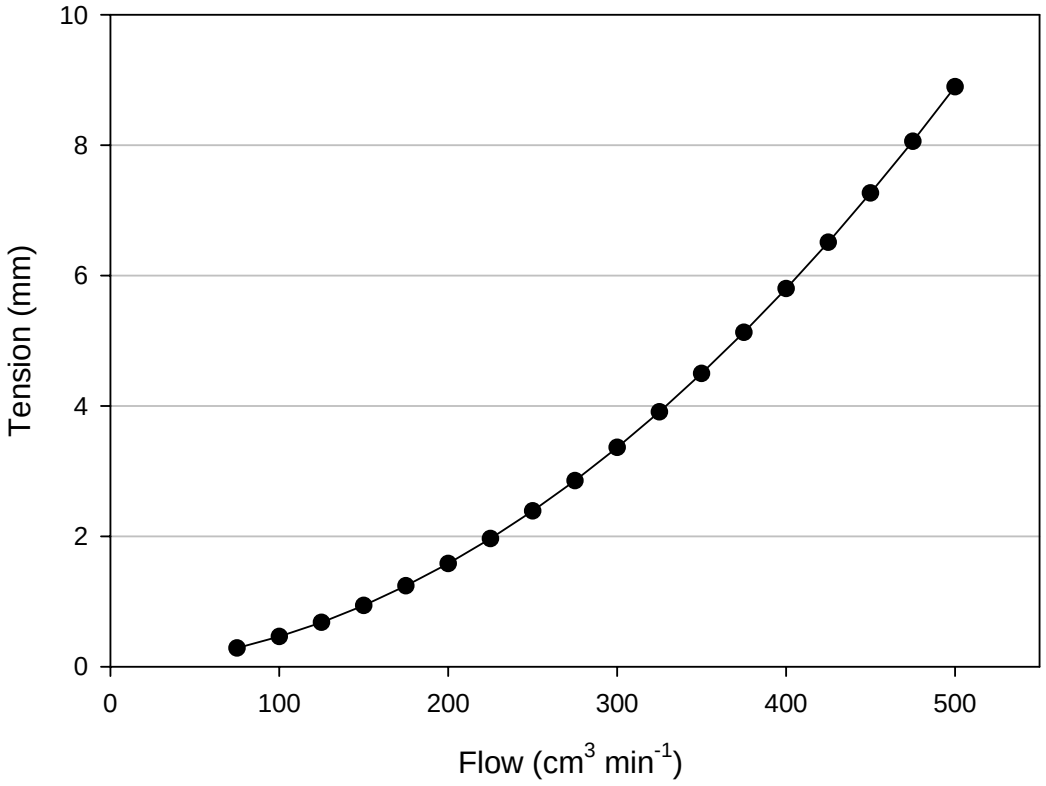

Fig. 2.6. Results from the tension calculations. The increase in tension, due to friction, was calculated using the orifice equation and the Darcy-Weisbach equation. The tension increase was calculated for flow rates from 75 to 500 cm^3 min^{-1}.

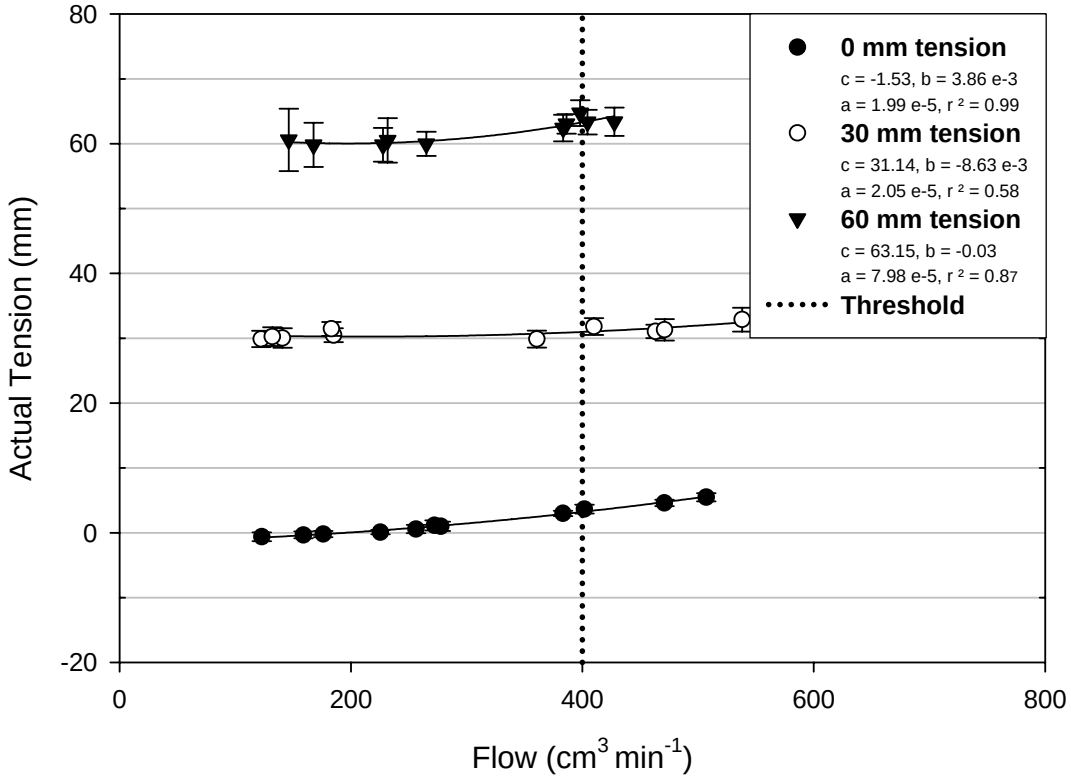

Fig. 2.7. Measured tension at the infiltration disc versus flow rate for the tension infiltrometer on a tension table using the larger water supply tube and fittings (15.9 and 13.2 mm, respectively). The tension control was set to the desired tension of either 0, 10, 20, 30 or 60 mm and remained so while the flow rates were varied. The starting point for each curve was the lowest constant flow rate measured and then the flow rate was increased by elevating the tension on the tension table. The error bars represent the standard deviation of the measured tension during each steady-state measurement. The coefficients of the quadratic equation, which was fitted to the points of each desired tension, are shown in the legend of the graph [$(a)x^2 + (b)x + (c)$]. The dotted vertical line (threshold) represents the approximate flow rate in which the tension starts to increase considerably.

CHAPTER 3

QUANTIFICATION OF BOUNDARY FLOW IN INTACT SOIL CORES DURING LABORATORY SATURATED HYDRAULIC CONDUCTIVITY MEASUREMENTS

ABSTRACT

The constant head method for determining saturated hydraulic conductivity is one of the traditional laboratory analyses for measuring the soil's ability to conduct water. One of the errors commonly associated with this technique occurs when there is flow between the outer edge of the soil sample and the cylindrical ring. The objective of this study was therefore to develop a method to minimize the effects of this artificial boundary flow during saturated hydraulic conductivity measurements. A new permeameter was constructed to separate flow between the outer and inner portions of the core. Intact core samples from the surface and subsurface Hagerstown silt loam series were analyzed to quantify the edge flow phenomenon. Outer saturated hydraulic conductivity (edge flow) was found to be significantly higher than the inner saturated hydraulic conductivity ($p = 0.038$, $n = 153$). The A-horizon surface samples were found to have significant edge flow ($n=110$, $p=0.049$), whereas the subsurface soil samples did not experience significant edge flow. In addition, brilliant blue dye was used to visually confirm the edge flow phenomenon. This study also investigated the length of saturation time needed to saturate the soil cores, and found that the heavier textured cores should be saturated for at least a week. Dye was utilized to determine if the entire core was conducting water when

the core reached steady-state flow. These results indicated that, although the core appeared to be at steady-state conditions during the early stages of the experiment, true steady-state conditions started to occur approximately 5 days into the experiment. Furthermore, the new permeameter's results were compared with *in situ* hydraulic conductivity methods. Taken together, these results suggest that the hydraulic conductivity values from the inner portion of the core are more comparable to the *in situ* tension and double ring infiltrometer conductivity values observed in the field.

INTRODUCTION

Our ability to determine soil-water relationships is essential to understanding the landscape hydrology. One of the key soil-water relationships was first described in 1856, while Henry Darcy was trying to determine the amount of water that could pass through a porous sand media (Hillel, 2004). Over a hundred and fifty years later, researchers are still trying to develop, improve, and compare methods to determine the soil's hydraulic conductivity (Campbell and Fritton, 1994; Evett et al., 1999; Joel and Messing, 2001; Lin et al., 1997; McNeal and Reeve., 1964; Reynolds and Elrick, 1991; White et al., 1992). Various field and laboratory methods have been developed to determine the soil's hydraulic conductivity, both saturated and unsaturated (Dane and Topp, 2002). Although the methodology is abundant, the reliability of these tests is sometimes lacking. Soil variability in the field often requires a large sample size to characterize even small area (Warrick and Nielsen, 1980). Compounded by methodology variability and associated uncertainty, the comparison and interpretation of soil hydraulic conductivity values can be confusing.

Laboratory measurements of saturated hydraulic conductivity (Ksat) using the constant head method is one of the traditional analyses for determining the soil's ability to conduct water (Reynolds et al., 2000). The constant head permeameter was essentially the same device that Darcy used in his classical experiments (Johnson et al., 2005). However, it is now more desirable to use intact soil cores rather than the packed sand columns of Darcy's time. These intact soil cores have a much more complex pore network than packed cores, resulting in higher Ksat values (Tuli et al., 2005). Along with

the complex pore network, it is also necessary to consider the disruption caused by using intact core samples, especially between the soil and ring boundary.

When comparing field techniques to laboratory techniques for measuring Ksat, some research has found that field techniques often yield results approximately fifty percent lower than laboratory techniques (Reynolds and Elrick, 2002). However, other investigations have found that field methods for determining Ksat yield higher values than laboratory core methods (Gribb et al., 2004; Zhang et al., 2006). Part of this deviation is attributed to the difficulty of achieving a fully saturated soil in the field, hence the term field-saturated (Reynolds et al., 1983). Another reason for such a difference in field and laboratory measurements may be the result of increased flow at the edge of soil cores that is challenging to completely eliminate at the contact between the soil core and ring.

Boundary flow, edge flow, and short circuit flow are terms often used to describe the flow regime between the outer edge of the soil sample and the cylindrical ring. This phenomenon is well recognized when performing laboratory Ksat tests (Dane and Topp, 2002; Hill and King, 1982; Hillel, 2004; Klute and Dirksen, 1986; McNeal and Reeve., 1964; Reynolds et al., 2000). In addition, several attempts have been made to eliminate the boundary flow from this method. McNeal et al. (1964) successfully designed a permeameter to divide outer and inner flow from a soil ring. However, this permeameter was designed to only be used with disturbed laboratory packed samples. Hill and King (1982) adapted McNeal's design to be able to accept either disturbed laboratory packed samples or undisturbed soil cores, yet the permeameter was never evaluated using undisturbed intact soil cores. Our study here follows the designs of McNeal (1964) and

Hill and King (1982) in constructing a hydraulic conductivity permeameter, but specifically designed to accommodate intact soil cores collected from the field in association with bulk density measurements. The edge-flow and inner-flow separation device will enable us to quantify the amount of edge flow that occurs in intact soil core samples, while measuring Ksat. This research also investigates the saturation process and the steady-state flow assumption used in measuring Ksat, as well as some *in situ* field hydraulic conductivity measurements including double ring infiltrometer and tension infiltrometer.

The goal of this study is to improve the accuracy of the standard laboratory saturated hydraulic conductivity measurement. This research focuses on four main objectives. The first objective is to remove edge-flow (artificial preferential flow) between the soil core and the wall of the ring. The second objective determines if steady-state flow is truly obtained in laboratory Ksat measurement. The third objective evaluates level of saturation based on length of core saturation time. The final objective was to compare the laboratory Ksat methods with several field methods.

MATERIALS AND METHODS

Permeameter Construction

The permeameter (Fig. 3.1) was constructed from 31.75 mm I.D. schedule 80 PVC pipe and 51 mm I.D. schedule 40 PVC pipe. The 51 mm pipe was machined to receive a 57 mm brass bulk density core with a snug fit. The 31.75 mm pipe was machined to have a 3 mm tapered cutting edge, to separate the inner and outer flow. These two pieces of pipe were then centered and cemented to a piece of flat PVC, 6.35 mm thick. A 15 mm barbed tubing fitting was used to direct flow from the center sampling area, and a 6.35 mm barbed tubing fitting was used to direct flow from the outer sampling area. A piece of wire screening with 6.35 mm openings was used in the center to help support the soil.

Permeameter Evaluation

Intact soil cores were taken with an Uhland-type soil core sampler (Soilmoisture Equipment Corporation, Santa Barbara, CA) from a wastewater irrigated field in Central Pennsylvania. The brass rings used were 60 mm in height with an inner diameter of 54 mm. The samples were kept at field moisture levels until they were presaturated for the Ksat test. Vertical cores were taken perpendicular with the soil surface at various locations within the field and at the soil trench locations. Subsurface cores were taken during trench descriptions both parallel with the surface (horizontal cores) and

perpendicular with the surface (vertical cores). The subsurface cores were taken at several depths, which were based on soil horizonation.

Soils from the Hagerstown silt loam series were analyzed in this research. The Hagerstown soil series (*Typic Hapludalf*) is a limestone derived residual soil that is very deep and well drained with a moderate permeability. Morphological and physical characteristics of the soils used for this analysis can be found in Table 4.1. The texture of the surface soils ranged from loam to silt loam and the surface structure was granular. The subsurface samples had silty clay loam, clay loam, silty clay, and clay textures. The structure of the subsurface samples was subangular blocky. Iron and manganese stains were also common within the pedon. The soils were sampled based on three landscape positions, depression, side-slope and summit.

The methodology used to determine the saturated hydraulic conductivity followed the classical method prescribed by Klute (1986) with slight modifications. Samples in this study were saturated for at least 24 h prior to running Ksat, whereas Klute and Dirksen (1986) suggest only 12 hour saturation or until visibly saturated (p. 695). Although not specifically mentioned in Klute and Dirksen (1986), care was taken to saturate the samples slowly from the bottom of the sample to the top. The water used for this method was de-aired and treated with 0.005 M $CaSO_4$ solution to help reduce clay dispersion (Klute and Dirksen, 1986). After saturation, we placed a piece of filter paper atop of the sample followed by an empty, but exact same size ring to allow for ponding (Fig. 3.2). The sample was moved to a constant head apparatus that was constructed to maintain a constant head on samples at all times (Fig. 3.2). Flow was recorded by collecting the effluent and weighing it every 10 to 20 minutes, depending on flow rate.

The core remained ponded for approximately 6 to 24 hours, based on time needed to reach steady-state conditions. Steady-state conditions were assumed when there was no observable trend in the last three measurements. Samples were evaluated first using the traditional method (Klute and Dirksen, 1986), then were immediately placed into the inner-flow and outer-flow separating device. Saturated hydraulic conductivity (Ksat) was then determined by Darcy's equation [1]

$$K_s = \frac{V * L}{A * T * (H_2 - H_1)} \qquad [3.1]$$

Where:

K_s = Saturated hydraulic conductivity (cm min^{-1})
V = Steady-state volume of water flowing through the core (cm^3)
L = Sample length (cm)
A= Cross section area of the core (cm^2)
T = Time (min)
$(H_2 - H_1)$ = Hydraulic head difference (cm)

For inner Ksat calculations, the area (A) was assumed to be the area of the inner sampling region. The area (A) for the outer Ksat was calculated by subtracting the area of the inner region from the total area of the core. To determine if the permeameter had any type of effect on the core's Ksat values, comparisons were made between the traditional method and both the inner and outer Ksat values (new method average) for the new permeameter using the same cores. For the new method average calculations, the entire area of the core was used for the calculations, along with the sum of the inner and outer flow measurements. It is recognized that the area (A) assumptions may not capture the complexity of the pore network within the soil core; however, the use of a dye solution, to indicate the flow pattern, may help indicate if the area assumption is valid.

To verify if edge-flow was occurring, we used a 3 g/kg brilliant blue dye (Company Brand: Permalon Blue VSG, Standard Dyes Inc., Highpoint, NC) solution to visualize the flow pattern of water. The 3g/kg solution was chosen to represent the main flow paths of the water through the core and following the methods and recommendations of Flury and Fluhler(1994); Flury and Wai (2003); and Lin et al. (1996). After the saturated hydraulic conductivity tests had been performed, the samples were then dried at 105^{o}C until a constant weight to obtain the soil's bulk density. After drying, select cores were split vertically and photographed to document the flow patterns of dyed areas. The statistical analyses used to determine significance were non-parametric 1-sample Wilcoxin analysis (Minitab 13, State College, PA), performed on the differences between the inner, outer, inner/outer average, and old method saturated hydraulic conductivity values.

To determine the effect of time on saturation and hydraulic conductivity the following experiment was conducted. A total of 24 replicate core samples were taken from a Hagerstown Bt subsurface horizon, samples were taken randomly within a 1 meter by 1.5 meter area. The samples were immediately weighed to determine initial soil moisture content, and then separated into 3 L plastic containers with lids. The samples were saturated using the de-aired water treated with 0.005 M Ca_2SO_4 and 3 grams of thymol (to prevent bacteria buildup). The cores were inundated gradually, by 1/3 core length increments, evenly spaced over the desired saturation time of 24 hours, four days, one week and two weeks, respectively. The cores designated for Ksat measurements were then evaluated with the constant head saturated hydraulic conductivity procedure, using a dye solution. These samples were dried and photographed after the Ksat

measurements were complete. At the same time, the samples not used for Ksat measurements were removed from the solution and dried at 105^{o}C. Bulk density and total porosity were determined on all samples. To more accurately determine the total porosity, the particle density was determined for the horizon, using the pycnometer method (Dane, 2002). To determine the degree of saturation for the cores, a percent saturation calculation was calculated based on volumetric water content and total porosity (Eq. 3.2).

$$\text{Percent Saturation (\%)} = \frac{Volumetric Water\ Content\ (cm^3 / cm^3)}{Total\ Porosity\ (cm^3 / cm^3)} \qquad [3.2]$$

The long term steady-state experiment was conducted by using an automated flow measurement device. Pressure transducers (Omega PX26-005 DV) were attached to PVC pipe which received the effluent from the cores. Measurements were then taken every 10 minutes with a CR-10 Data Logger (Campbell Scientific, Logan, Utah). The volume of water was determined by multiplying the difference in height by the cross-sectional area of the PVC pipe.

To compare the new method and old method with *in situ* field data, both the tension infiltrometer and the double ring infiltrometer were selected for the comparison at six field sites where lab Ksat samples were collected from two transects, each containing summit, side slope and depression landscape positions (Fig. 3.3). Procedures for the operation of each instrument followed the standard methodologies (Dane and Topp, 2002). Three modified tension infiltrometers (Walker et al., 2006) were setup with pressure transducers to measure both the height of water and the tension in the infiltrometer disc, as described in the previous chapter. Site preparation was kept to a minimum and followed the protocol of Lin et al., (1997). Sequential tensions of 12, 6, 3,

2, and 1 cm were utilized to determine unsaturated flow characteristics of the site and a zero tension measurement for the field-saturated hydraulic conductivity. Saturated and unsaturated hydraulic conductivity calculations [Eq. 3.3] were made using two supply tensions. (Ankeny et al., 1991; Lin and McInnes, 1995; Lin et al., 1997; Walker et al., 2006).

$$K(\psi_o) = \frac{Q(\psi_o)}{[\pi r^2 + 4r/\alpha]} \qquad [3.3]$$

Where:

Q = Steady-State Infiltration rate ($m^3 s^{-1}$)
ψ_o = Soil water potential at infiltration surface (m)
r = radius of the infiltration (m)
K= Hydraulic Conductivity ($m\ s^{-1}$)
α = Solved for by using two water supply potentials

The double ring infiltrometers consisted of inner and outer concentric rings with diameters of 16 cm and 50 cm, respectively. Water was kept to a constant level using marriotte supplies, equipped with 2 inch clear acrylic tubing, which allowed for ease of measurement. Two infiltrometers were run simultaneously at each site and calculations (Eq. 3.5) were based on Dane and Topp (2002).

$$K_{fs} = \frac{q_s}{[H/(C_1 d + C_2 a)] + \{1/[\alpha * (C_1 d + C_2 a)]\} + 1} \qquad [3.5]$$

Where:

K_{fs}= Field saturated hydraulic conductivity ($cm\ s^{-1}$)
q_s = Measured quasi-steady infiltration rate ($cm\ s^{-1}$)
H = Depth of water ponding (cm)
d = cylinder insertion depth (cm)
a = measuring cylinder radius (cm)
α = estimated tortuosity parameter
C_1 = Quasi-empirical constant
$C2$ = Quasi-empirical constant

RESULTS AND DISCUSSION

As expected, there was significant edge flow (n = 153, p = 0.038) for the samples taken at the study site (Fig. 3.4). On an individual basis, 79 cores displayed greater Ksat values for the boundary flow collection, whereas 68 cores had greater Ksat values for the inner flow region (Fig. 3.5). Six cores had equal values between the inner and the outer flow regions. Separating the cores between surface soil and subsoil samples, the surface A-horizon also had significant amount of edge flow (n=110, p=0.049), whereas the subsurface soil samples did not experience significant edge flow. These results are similar to previous findings using hand-packed soil cores (McNeal and Reeve, 1964, Hill and King, 1982). McNeal and Reeve (1964) found the boundary flow to be three to six time higher than the center flow. Hill and King (1982) also found that boundary flow exceeded center flow by 23 to 54%. This indicates a high amount of variability within individual surface and subsurface vertical core samples themselves, not to mention between site variability. Horizontally sampled cores displayed the same high degree of variability between inner and outer flow regions (Fig. 3.6).

Although edge flow was not significant in the subsurface horizons (n=43), there were nineteen cases that did experience a higher edge flow conductivity value when compared with the inner flow value. The reduction of edge flow observed in the subsurface horizons may be due to swelling of clays in the subsurface horizon. The Pennsylvania State Soil Characterization Laboratory Database System lists the Hagerstown subsurface soils having an average COLE value of 0.036, indicating the ability of the soil to shrink and swell, whereas, the surface COLE value is 0.01, which shows less of a shrink/swell potential (Ciolkosz, 2000). The small amount of swelling in

the subsurface horizons could reduce gaps between the soil and the core wall, which would in turn lower the amount of edge flow occurring within the cores.

Figure 3.7 shows the differences between the inner Ksat values and the traditional method values for vertically sampled cores. The surface samples have predominately lower Ksat values than when compared with the traditional method. The subsurface samples display the same trend, but it is not as great a difference, which can be related to a lower amount of edge flow that was measured for the subsurface samples. The lower values experienced for the inner sampling region, when compared to the traditional method values, indicate how the artificial flow between the soil and the core wall can overestimate Ksat values. The same patterns can also be observed for the horizontally sampled cores, again with the subsurface cores having a lesser degree of edge flow (Fig. 3.8).

While comparing the old method with the new method averages (calculated based on sum of the inner and outer flow) there was a significant difference (Fig. 3.9). This is thought to be due to the dividing ring at the bottom of the sample. By inserting the dividing ring, the outer edge of soil at the bottom of the sample may slightly reduce gaps between the soil and the cylinder wall, causing a reduction in outer flow. However, the dividing ring is sharpened in a manner that all compaction would occur on the edge flow portion, keeping the middle sample intact. Although there is a difference between the traditional method and the new method average, there is still a high correlation between the two methods (Fig 3.9).

To verify if flow between the soil and the cylinder wall was causing the edge-flow phenomenon, we added 3 g/kg brilliant blue dye to our de-gassed solution which was

then used for constant head analyses on selected cores. Fig 3.10 displays representative examples of cores that had experienced high edge flow. The two cores in figure 3.10 (A-D) experienced large amounts of edge flow and little inner flow. Figure 3.11 (A-F) displays cores that had very little edge flow and a more substantial amount of inner flow. Most of the inner flow in the third core was around a 2 mm cylindrical pore running through the centre of the core, which stained light blue in Figure 3.11 (B-C). The other core shown in Figure 3.11 (D-F) had nearly equal portions of edge flow and inner flow. The dye shows up quite well in the top portion of the core and becomes fainter towards the bottom. Most of the inner flow portion observed in the last core (Figure 3.11 D-E) can be traced backed to several macropores pictured in Figure 3.11 F. In most cores, the most significant dye accumulations were found between the wall of the cylinder and the intact soil sample. Dye patterns within the inside of the core were lighter than expected, which inspired follow-up procedures to better understand the concept of steady-state and complete saturation.

The saturation experiment found a significant difference between saturation time and percent saturation (Fig. 3.12). The 12 hour or 24 hour saturation time suggested by Klute and Dirksen (1986) does not appear to be optimal. Klute and Dirksen (1986) does express the option to wait until the samples are visibly saturated; however, between the 12 hr and 24 hr time period, our samples did appear to be fully saturated with water films vividly appeared on the soil core surface. While observing the cores during the saturation process, it was evident that the water was not only traveling through larger pores in the soil, but also through the space between the soil core and the ring wall as well. Klute and Dirksen do recognize that the samples may not be fully saturated after the 12 hour

saturation period, however, they indicate that if total saturation is desired, a vacuum or carbon dioxide should be used to accomplish this. The four day saturation period suggested by Dane and Topp (2002) was not significantly different ($p = 0.49$) from the 24 hour period, but was significantly less than the two week period. Our research suggests that a saturation period of approximately 1 to 2 weeks will yield a significantly higher saturation percentage than a 12 hour saturation period.

. There was a not significant difference between the saturated hydraulic conductivity values for the various lengths of saturation. However, it is evident from the dye staining patterns that the length of saturation does affect the portion of the core that conducts water (Fig. 3.13). The dye patterns are more uniform for the replicates that have been saturated for at least a week. Although the Ksat values are similar, it is evident that the samples, which are saturated for one or four days, have much larger areas that are not dyed. Whereas for cores that were saturated for one or two weeks, the dye patterns indicated a more uniform flow. These qualitative results also matched the quantitative percent saturation results. The bulk densities of the soils were not significantly different (Table 3.1).

Figure 3.14 represents data collected from an eight day constant head experiment. Each core was subjected to a constant head of brilliant blue dye for a period of eight days. The overall pattern for both of the cores that were evaluated was a sharp increase in flux density followed by an exponential decrease. Core A in Fig. 3.14 experienced the highest flux density and reached it maximum before core B, which experienced a lower flux density. This pattern matched the second (sharp increase) and third phase (decline) of a three phase hydraulic conductivity system described by Faybishenko (1995). The first

phase in Faybishenko's system was an initial decline due to entrapped air, this was not observed in our research. However, they used much larger soil columns that would be much more difficult to saturate than the small cores used in this study. The increase in flux could have been due to an increase in pores that were conducting water. The decrease in flux may have been caused by swelling of clays and/or resistant bacterial growth.

Throughout the measurements, there were periods of time that could have been considered steady-state; however, during the course of the eight days it is evident that the cores did not reach steady-state conditions until the 5^{th} or 6^{th} day. The conditions may not have been representative after the true steady-state conditions were achieved due to the swelling and bacterial factors.

Data from the laboratory and field comparison are shown in Figure 3.16. In all six sites, the traditional method for determining laboratory Ksat had the highest values. The higher values for the traditional laboratory method when compared with field methods were also noted by Reynolds and Elrick (2002). However, the inner flow region has values that are much closer, to the field methods. Over the entire field, there was a significant difference between methods ($p = 0.001$), with the old method having the highest average Ksat value of 18.5 cm/hour ($n = 18$). The inner flow Ksat measurement, without edge flow effects, had a mean saturated hydraulic conductivity of 5.2 cm/hour ($n = 18$). The tension infiltrometer had a mean saturated hydraulic conductivity value of 8.97 cm/hour ($n = 13$) and the double ring infiltrometer yielded a mean saturated hydraulic conductivity value of 3.53 cm/hr ($n = 12$). Although the trends in conductivity values were similar, variability within the site may have been caused by different

representative sampling sizes. The influence of macropores within the sample could heavily alter the results based on the size of the sample. A macropore in a small sample could skew the results; however, a larger sample is likely to include more macropores. All measurements for this experiment were conducted within a 1 meter radius of the northeast side of the soil trench.

CONCLUSIONS:

The traditional constant head soil core laboratory method for determining saturated hydraulic conductivity has the potential to overestimate the actual values of saturated hydraulic conductivity. The main cause of this overestimate is due to the preferential flow of water between the soil core and the cylindrical ring used to hold the soil core. This study has shown both qualitatively and quantitatively the effects of the boundary flow while determining saturated hydraulic conductivity in the laboratory. With the use of the new permeameter, the inner and boundary flow regimes were successfully separated. This separation allowed for the boundary flow error to be removed from the data. After the removal of the boundary flow, the results were much more comparable to the field determinations of saturated hydraulic conductivity. Although the results from the new laboratory method do appear to be more representative of the field methods, the dye results indicate that flow through the soil cores is not uniform, as often assumed.

Although the soil sample may appear to be at steady-state, a considerable portion of water passing through the core is traveling between the soil and core wall, not through the actual soil. When the boundary flow of the soil is bypassed, steady-state conditions are very dependent of the time scale. Conducting the measurement for several hours will lead to pseudo steady-state conditions; however, over the period of several days to a week, it is evident that the flow through the soil core is not experiencing steady-state conditions. The concept of steady-state flow may need to be further investigated and standardized. Soils with different structures and textures should be examined over a period of several days to determine the "minimum" time required to reach steady-state

conditions. From this type of investigation, the methods should be standardized so that results can be more comparable to each other.

Along with standardizing the time it takes to reach steady-state conditions, presaturation time should also be standardized. Based on our results fine textured soil samples should be saturated for at least one week prior to running the conductivity analysis on them. Although there was not a significant difference between conductivity values, the dye tracing patterns were much more uniform on the cores that were saturated for one to two weeks than those saturated for one or four days. Future experiments should also be conducted to determine the minimum length of time the soils should be saturated based on their texture and soil structure.

REFERENCES

Ankeny, M., M. Ahmed, T. Kaspar, and R. Horton. 1991. Simple field method for determining unsaturated hydraulic conductivity. Soil Science Society of America Journal 55:467-470.

Campbell, C., and D. Fritton. 1994. Factors affecting field-saturated hydraulic conductivity measured by the borehole permeameter technique. Soil Science Society of America Journal 58:1354-1357.

Ciolkosz, E. 2000. Pennsylvania State University Soil Characterization Laboratory Database. Agronomy Department, Penn State University, University Park, PA.

Dane, J., and G. Topp, (eds.) 2002. Methods of Soil Analysis: Part 4 Physical Methods, pp. 1-1692. Soil Science Society of America, Madison, Wisconsin.

Evett, S., F. Peters, O. Jones, and P. Unger. 1999. Soil hydraulic conductivity and retention curves from tension infiltrometer and laboratory data, p. 541-551, *In* M. v. Genuchten, et al., eds. Proc. Int. Workshop Characterization and Measurement of Hydraulic Poperties of Unsatrated Porous Media. University of California, Riverside, Riverside California.

Faybishenko, B. 1995. Hydraulic behavior of quasi-saturated soils in the presence of entrapped air: Laboratory experiments. Water Resources Research 31:2421-2435.

Flury, M., and H. Fluhler. 1994. Brilliant Blue FCF as a dye tracer for solute transport studies-- A toxicological overview. Journal of Environmental Quality 23:1108-1112.

Flury, M., and N. Wai. 2003. Dyes as tracers for vadose zone hydrology. Reviews of Geophysics 41:2.1 - 2.37.

Gribb, M., R. Kodesova, and S. Ordway. 2004. Comparison of soil hydraulic property measurement methods. Journal of Geotechnical and Geoenvironmental Engineering 130:1084-1095.

Hill, R.L., and L.D. King. 1982. A permeameter which eliminates boundary flow errors in saturated hydraulic conductivity measurements. Soil Science Society of America Journal 46:877-880.

Hillel, D. 2004. Introduction to Environmental Soil Physics.494. *In* (ed.). Elsevier, San Diego, CA.

Joel, A., and I. Messing. 2001. Infiltration rate and hydraulic conductivity measured with rain simulator and disc permeameter on sloping arid land. Arid Land Research and I 15:371-384.

Johnson, D.O., F.J. Arriaga, and B. Lowery. 2005. Automation of a falling head permeameter for rapid determination of hydraulic conductivity of multiple samples. Soil Science Society of America Journal 69:828-833.

Klute, A., and C. Dirksen. 1986. Hydraulic conductivity and diffusivity: laboratory methods, p. 687-697, *In* A. Klute, ed. Methods of Soil Analysis, Part 1. Physical and Mineralogical Methods, 2nd ed. American Society of Agronomy--Soil Science Society of America, Madison, WI.

Lin, H., and K. McInnes. 1995. Water flow in clay soil beneath a tension infiltrometer. Soil Science 159:375-382.

Lin, H., K. McInnes, L. Wilding, and C. Hallmark. 1996. Effective porosity and flow rate with infiltration at low tensions into a well-structured subsoil. Transactions of the ASAE 39:131-133.

Lin, H., K. McInnes, L. Wilding, and C. Hallmark. 1997. Low tension water flow in structured soils. Canadian Journal of Soil Science 77:649-654.

McNeal, B., and R. Reeve. 1964. Elimination of boundary flow errors in laboratory hydraulic conductivity measurements. Soil Science Society of America Journal 28:713-714.

Reynolds, W., and D. Elrick. 1991. Determination of hydraulic conductivity using a tension infiltrometer. Soil Science Society of America Journal 55:633-639.

Reynolds, W., and D. Elrick. 2002. Saturated and field-saturated water flow parameters: Principles and parameter definitions, p. 797-801, *In* J. Dane and G. C. Topp, eds. Methods of Soil Analysis: Part 4, Physical Methods. Soil Science Society of America, Madison, Wisconsin.

Reynolds, W., E. Elrick, and G. Topp. 1983. A reexamination of the constant head well permeameter method for measuring saturated hydraulic conductivity above the water table. Soil Science 136:250-268.

Reynolds, W.D., B.T. Bowman, R.R. Brunke, C.F. Drury, and C.S. Tan. 2000. Comparison of tension infiltrometer, pressure infiltrometer, and soil core estimates of saturated hydraulic conductivity. Soil Science Society of America Journal 64:478-484.

Tuli, A., J. Hopmans, D. Rolston, and P. Moldrup. 2005. Comparison of air and water permeability between disturbed and undisturbed soils. Soil Science Society of America Journal 69:1361-1371.

Walker, C., H. Lin, and D.D. Fritton. 2006. Is the tension beneath a tension infiltrometer what we think it is? Vadose Zone Journal 5:860-866.

Warrick, A., and D. Nielsen. 1980. Spatial variability of soil physical properties in the field *In* D. Hillel (ed.) Applications of soil physics. Acadmic Press, Toronto, Canada.

White, I., M. Sully, and K. Perroux. 1992. Measurement of surface-soil hydraulic properties: Disk permeaters, tension infiltrometers, and other techniques, p. 69-103, *In* W. D. R. G. Clarke Topp, and Richard E. Green, ed. Advances in Measurement of Soil Physical Properties: Bringing Theory into Practice, Vol. Special Publication Number 30. Soil Science Society of America, Madison, Wisconsin.

Zhang, S., L. Lovdahl, H. Grip, and Y. Tong. 2006. Soil Hydraulic properties of two loess soils in China measured by various field-scale and laboratory methods. Catena In Press.

Table 3.1 Bulk density, initial water content, total porosity, and percent saturation for the samples used in the saturation experiment.

Core Number	Time Saturated	Bulk Density	Initial Water Content (%)	Total Porosity (%)	Percent Saturation (%)
Saturated Cores					
13	24 hr	1.34	30.54	48.93	81.85
14	24 hr	1.41	32.49	46.13	89.00
15	24 hr	1.41	28.75	46.41	81.76
16	4 days	1.40	32.25	46.70	87.76
17	4 days	1.37	31.25	47.84	87.75
18	4 days	1.42	28.40	45.84	79.92
19	1 Week	1.44	32.61	45.04	92.12
20	1 Week	1.55	34.51	41.07	99.17
21	1 Week	1.40	30.85	46.76	89.64
22	2 Weeks	1.43	31.71	45.50	94.77
23	2 Weeks	1.55	33.49	40.79	98.22
24	2 Weeks	1.43	31.51	45.69	89.18
Ksat Cores					
3	24 hr	1.55	29.21	40.92	81.31
1	24 hr	1.46	32.35	44.17	87.38
2	24 hr	1.50	31.10	42.82	93.39
6	4 days	1.55	31.21	40.90	89.11
5	4 days	1.47	33.34	43.89	85.83
4	4 days	1.38	33.36	47.46	85.36
9	1 Week	1.42	33.77	45.73	89.58
7	1 Week	1.34	31.62	48.75	82.90
8	1 Week	1.17	48.46	55.57	75.73
11	2 Weeks	1.56	32.34	40.68	99.67
10	2 Weeks	1.40	32.42	46.67	94.33
12	2 Weeks	1.51	31.65	42.54	93.70

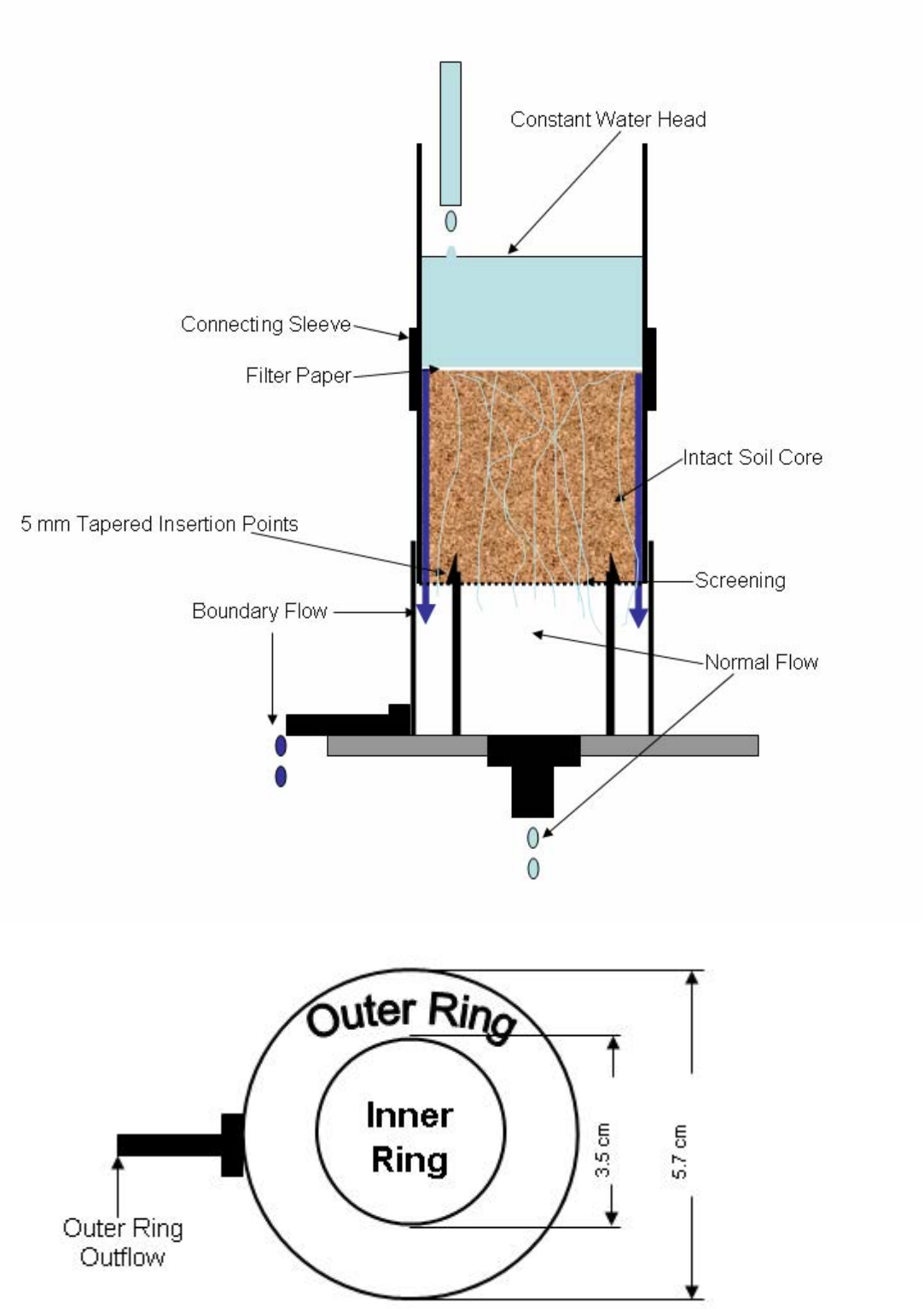

Fig. 3.1. Side view and top view of the permeameter designed to separate edge flow from inner flow.

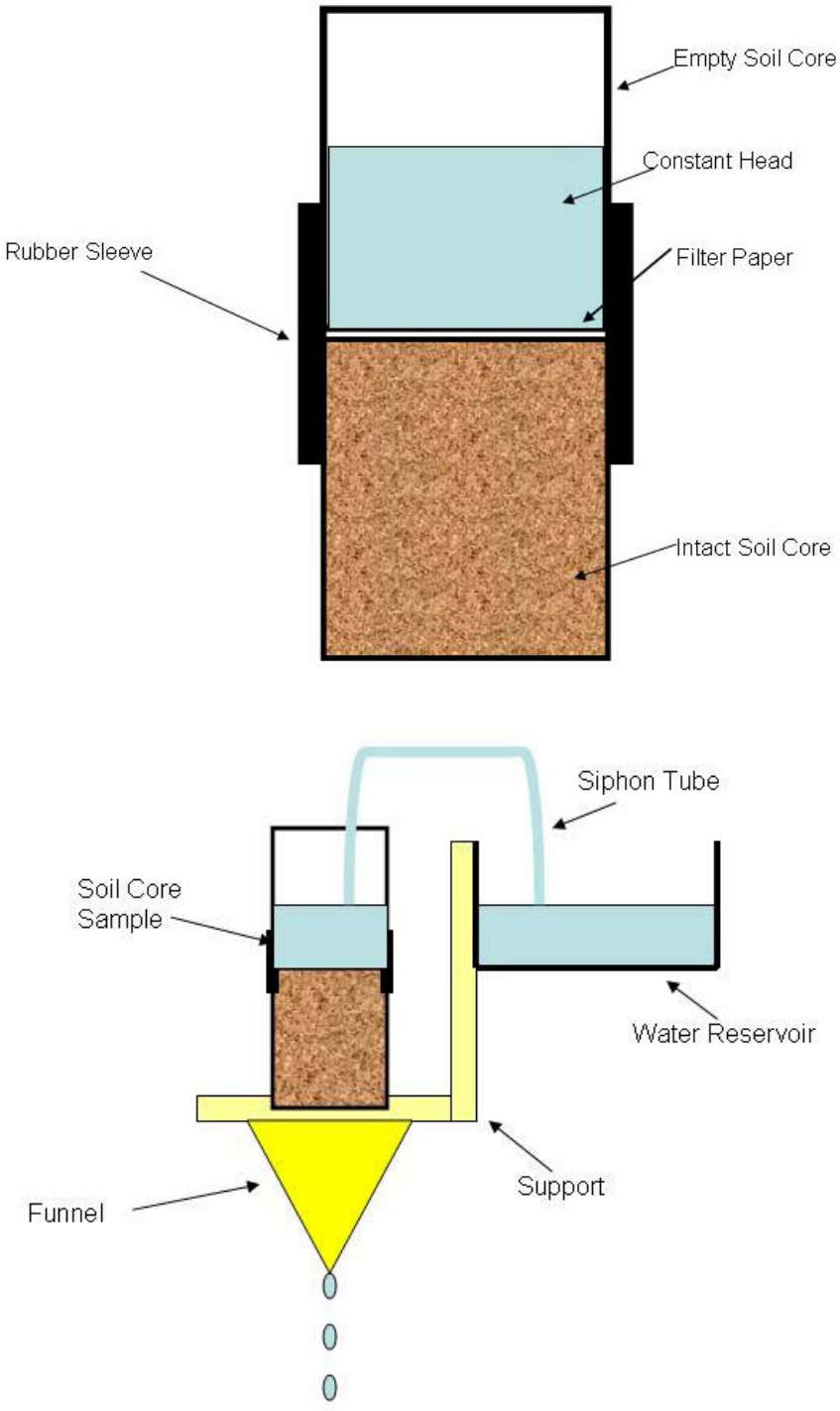

Fig. 3.2. Top: Core setup for the traditional laboratory measurement of saturated hydraulic conductivity. An empty core is placed on top of the soil filled core to maintain a constant head. Bottom: Schematic of the laboratory bench apparatus for measuring saturated hydraulic conductivity. A constant head is maintained from a pump filled reservoir.

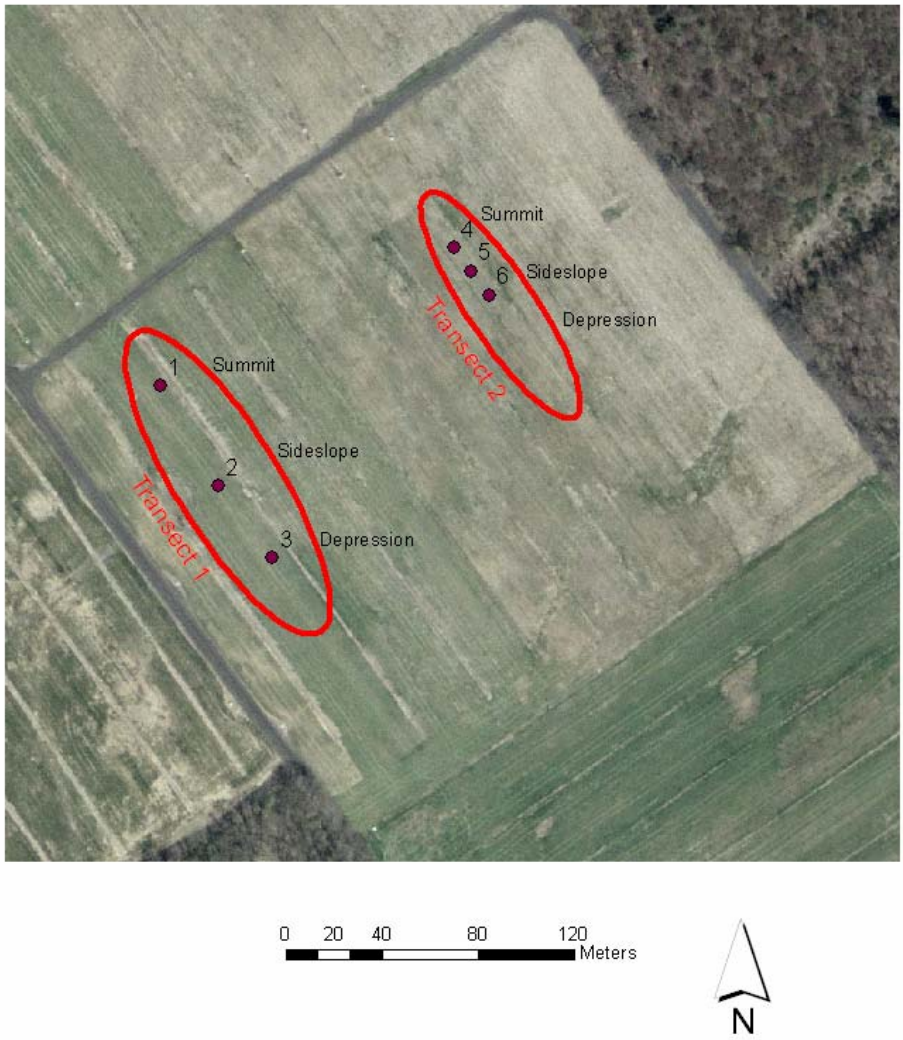

Fig. 3.3. Sample site location for the double ring infiltrometer, tension infiltrometer, and subsurface and surface soil core samples. Each transect has three landscape positions: summit, side-slope, and depression.

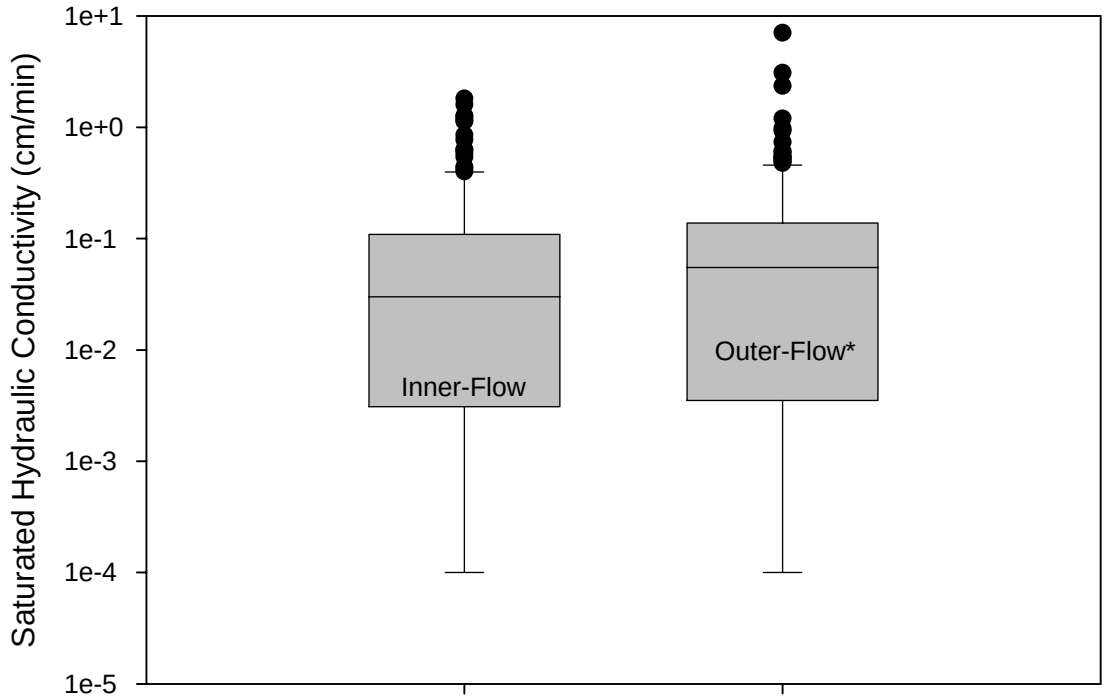

Fig. 3.4. Overall average saturated hydraulic conductivity values for 153 Core samples. There is a statistically significant higher flow ($p < 0.05$*) between the soil and core wall boundary (outer-flow). The error bars represent the 10^{th} and the 90^{th} percentile data. The bottom line on the box represents the 25^{th} percentile, the line within the box represents the median, and the top line on the box represents the 75^{th} percentile data. The dots represent samples outside the 10 to 90^{th} percentile range.

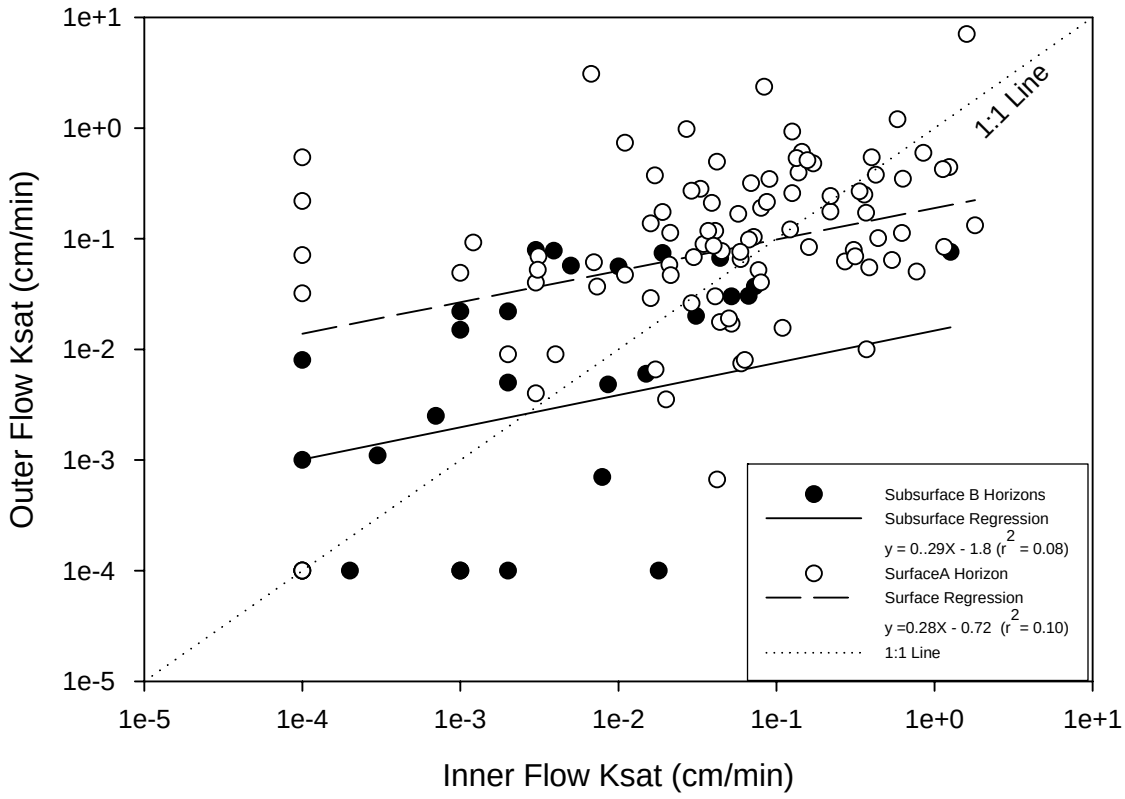

Fig. 3.5. Comparison of the inner ring saturated hydraulic conductivity versus the outer ring saturated hydraulic conductivity for vertical cores (perpendicular to the surface). The hollow circles represent surface soil cores and the solid circles represent subsurface soil cores.

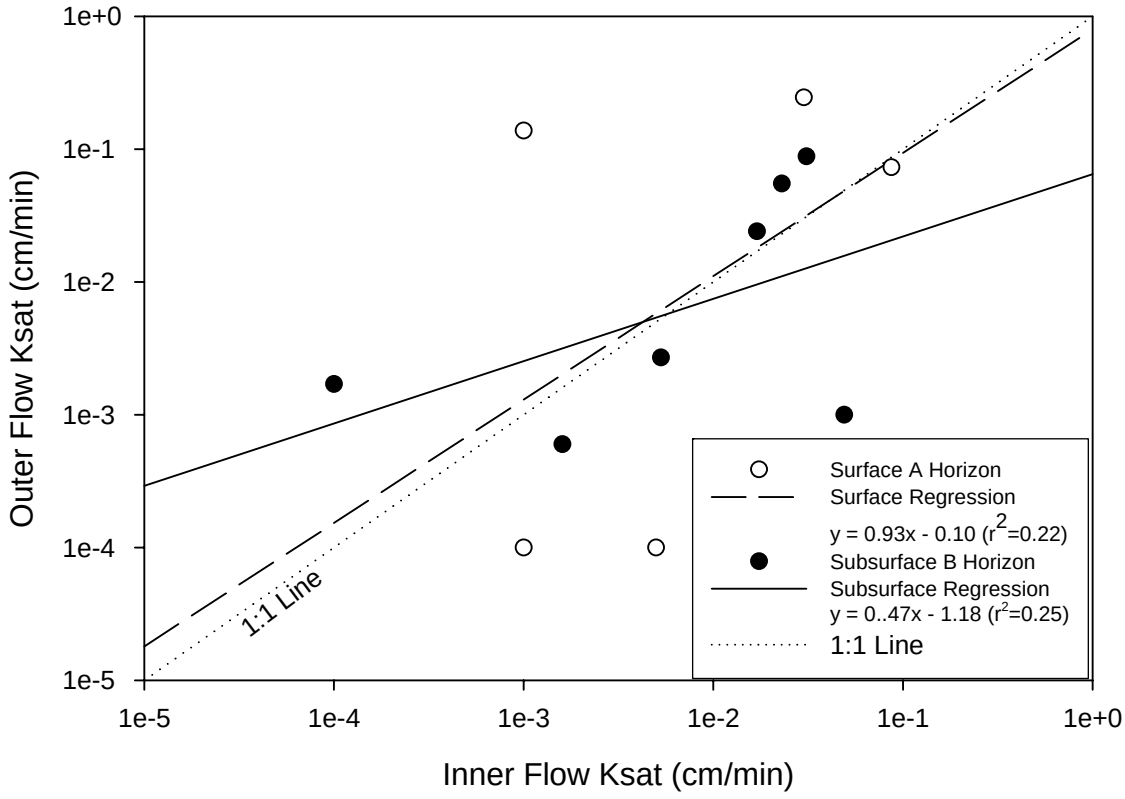

Fig. 3.6 Comparison of the inner ring saturated hydraulic conductivity versus the outer ring saturated hydraulic conductivity for horizontal cores. The hollow circles represent surface soil cores and the solid circles represent subsurface soil cores.

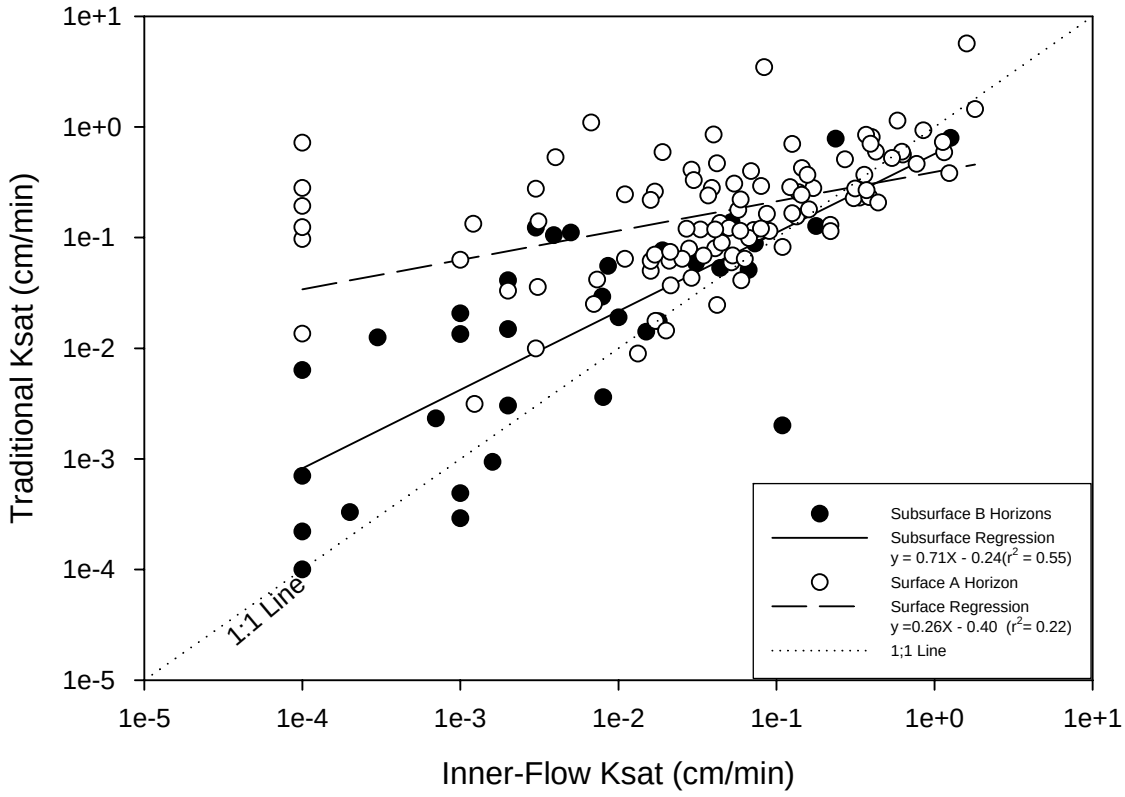

Fig. 3.7. Comparison of the inner flow Ksat versus the traditional Ksat measurements for vertical cores. The hollow circles represent surface soil cores and the solid circles represent subsurface soil cores.

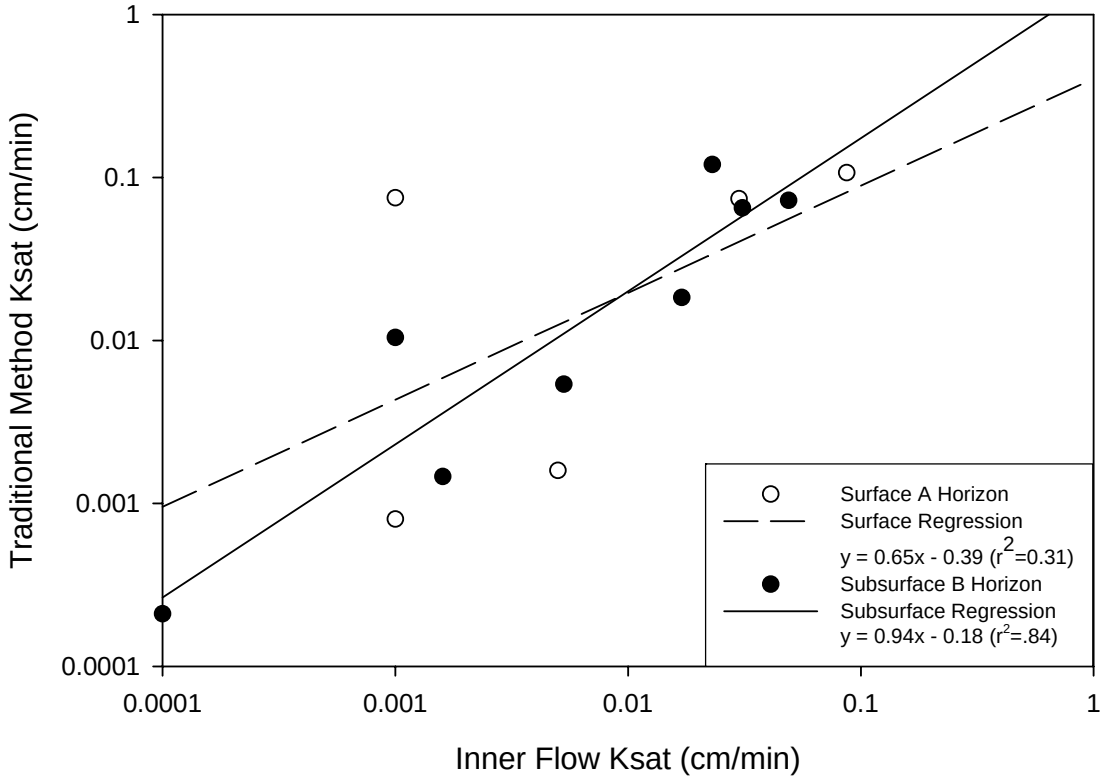

Fig. 3.8. Comparison of the inner flow Ksat versus the traditional Ksat measurements for horizontal cores. The hollow circles represent surface soil cores and the solid circles represent subsurface soil cores.

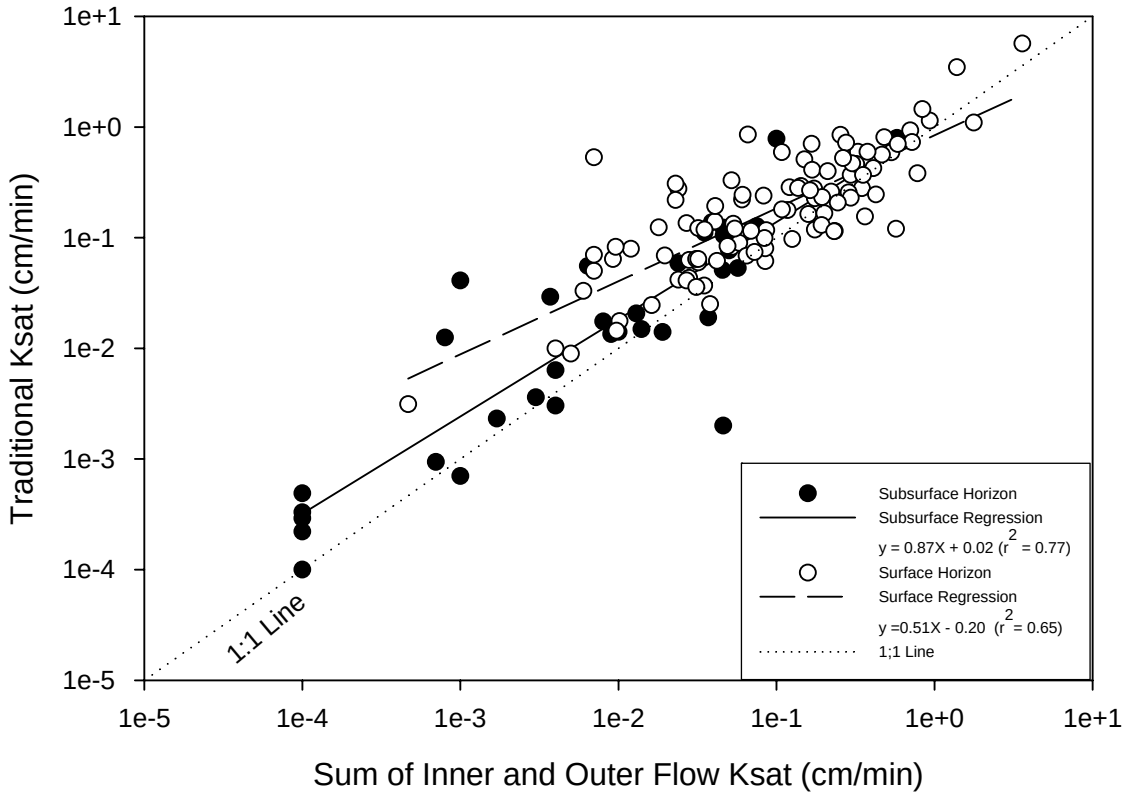

Fig. 3.9 Comparison of the new method hydraulic conductivities (sum of inner flow and outer flow) versus the traditional Ksat method, using the same soil cores.

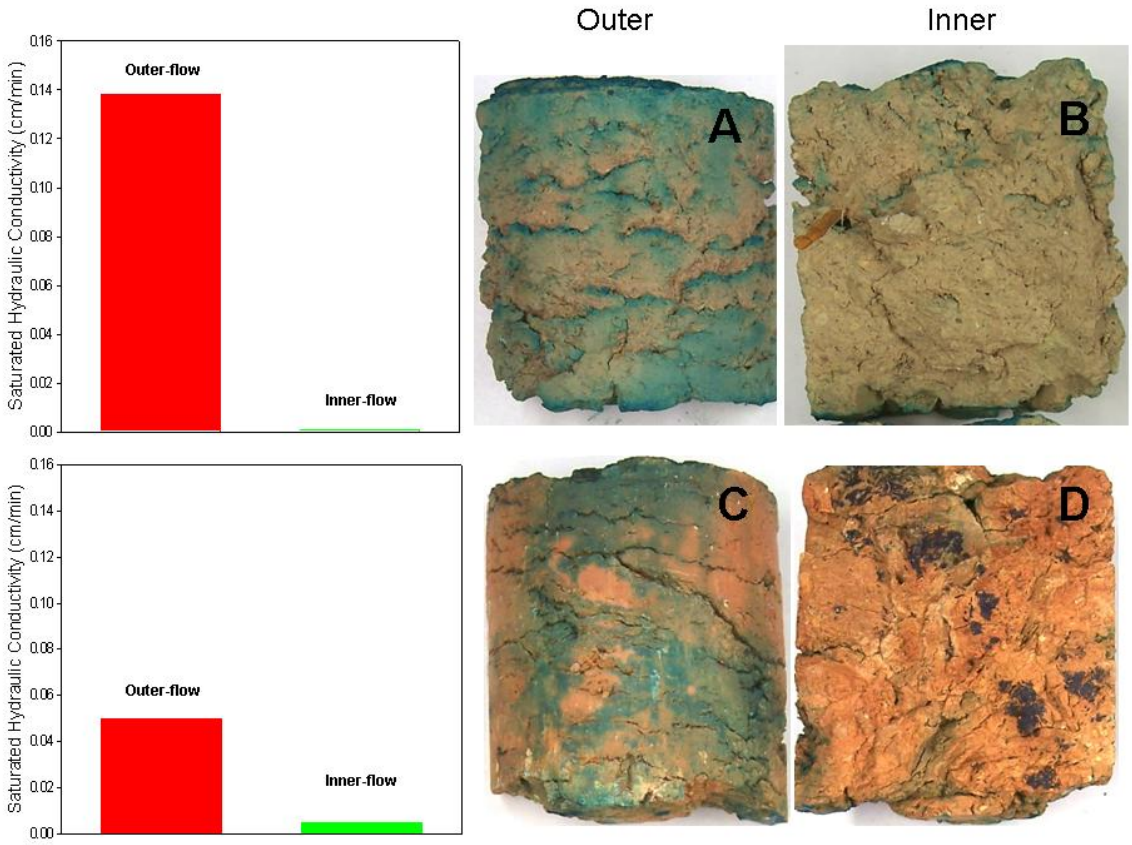

Fig. 3.10. Quantitative and qualitative results depicting individual cores that experienced high edge flow. A and C are photographs of the outside of cores that had high edge-flow and low inner-flow represented by B and D.

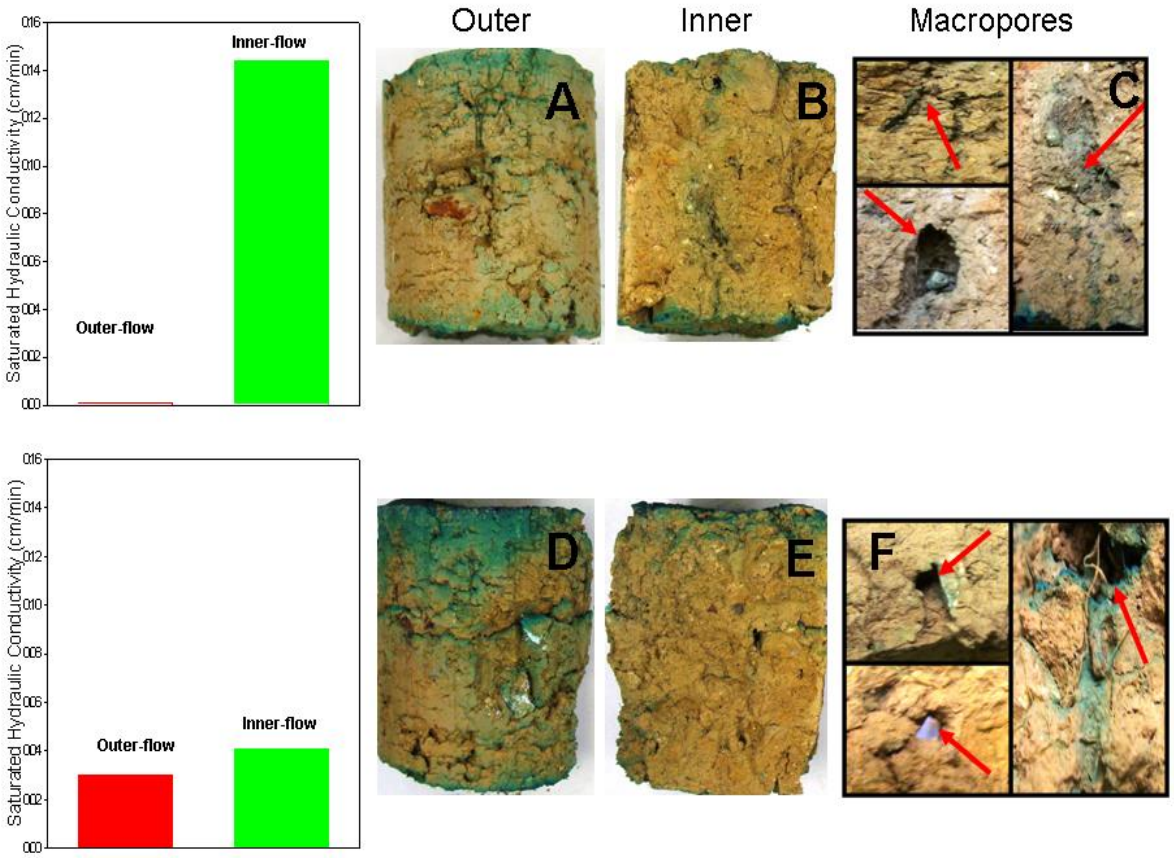

Figure 3.11. Quantitative and qualitative results depicting individual cores that experienced high edge flow Pictures A and B represent the outside and inside of a core that had low edge-flow and high inner flow. Picture C displays the macropores found within that core that could have caused the high inner flow. Picture D and E represent a core that had nearly equal inner and outer flow. Picture F shows macropores within the last core that led to a higher flow through the inner portion without much staining.

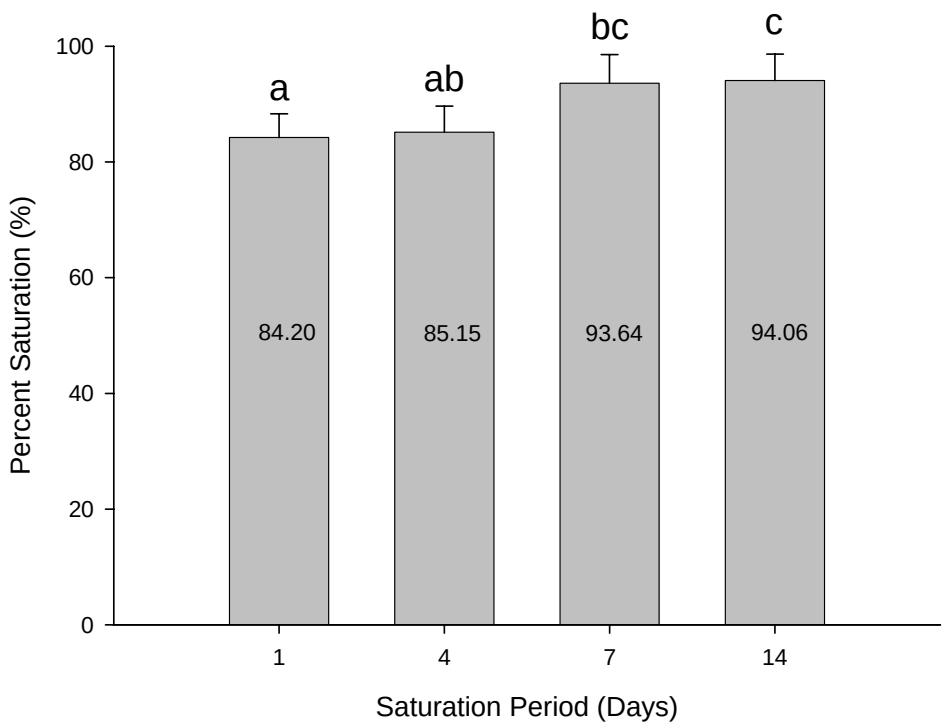

Fig. 3.12. Percent saturation based on the number of days the triplicate samples were saturated. The error bars represent the standard deviation of the mean. Identical letters indicate no significant difference ($p = 0.049$).

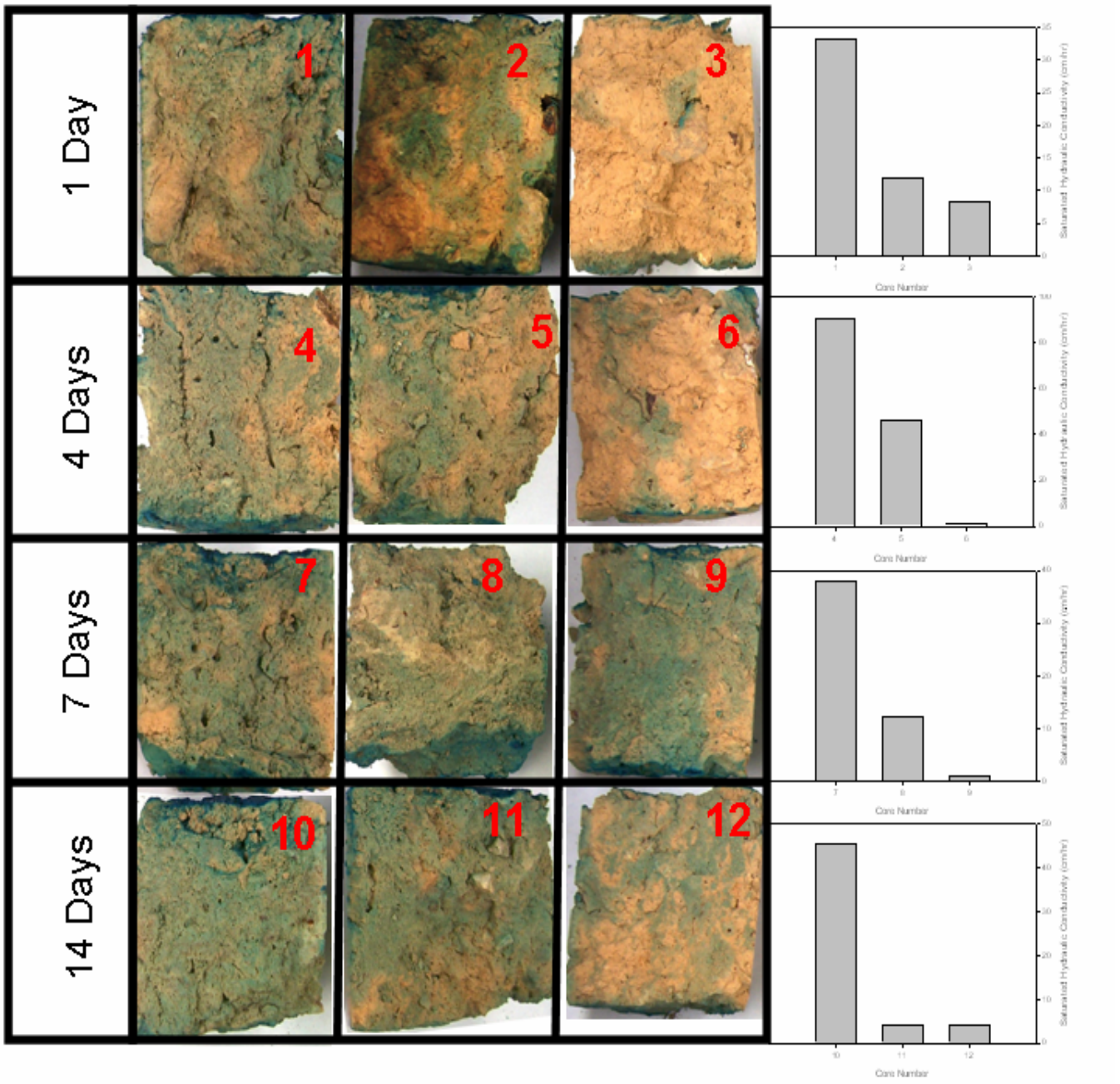

Fig. 3.13. Results from the saturation experiment. The cores were saturated for different periods of time, followed by conducting the traditional constant head saturated hydraulic conductivity measurement with brilliant blue dyed water. The graphs on the right represent the individual saturated hydraulic conductivity values for the respective core (cm/hr).

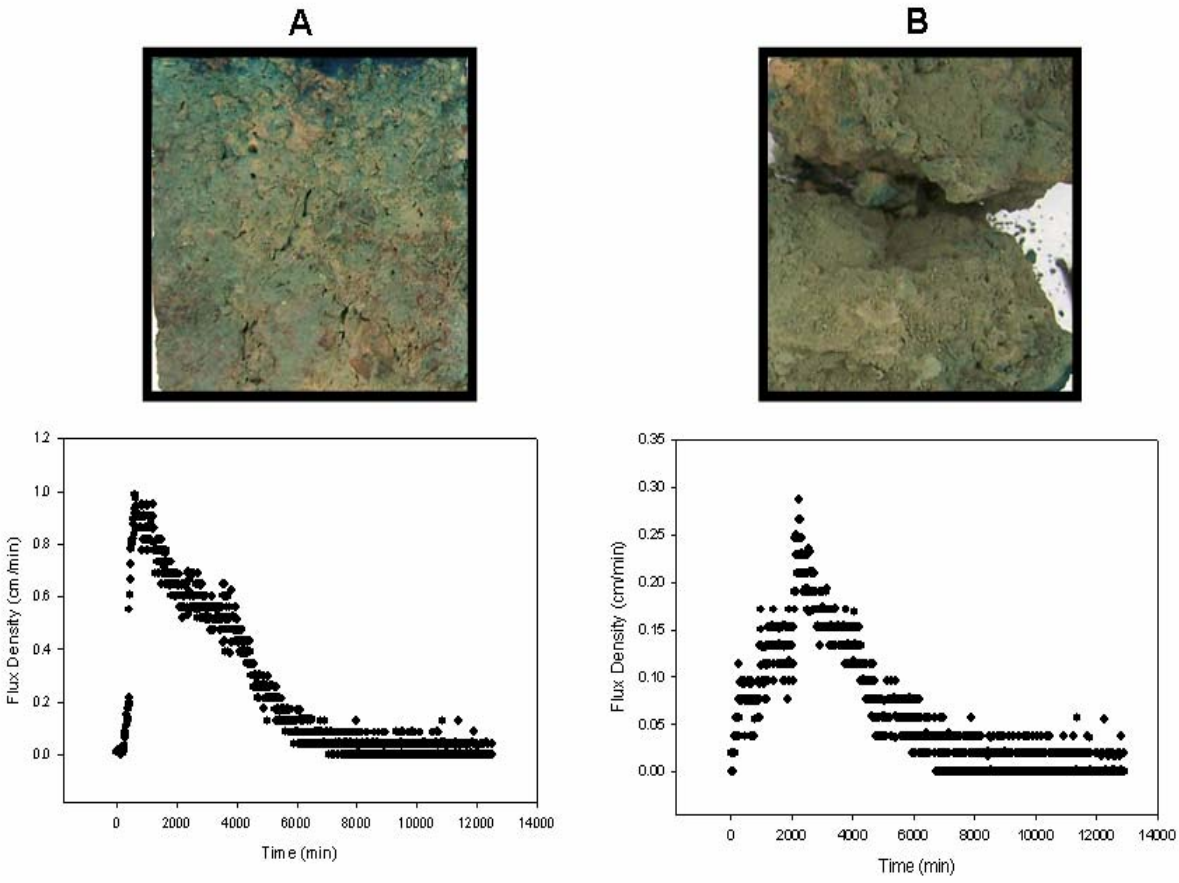

Fig. 3.14. Data from a 8-day Ksat experiment. Cores were subjected to a constant head of brilliant blue dye solution for eight days. The graphs depict the flux density flowing through the cores.

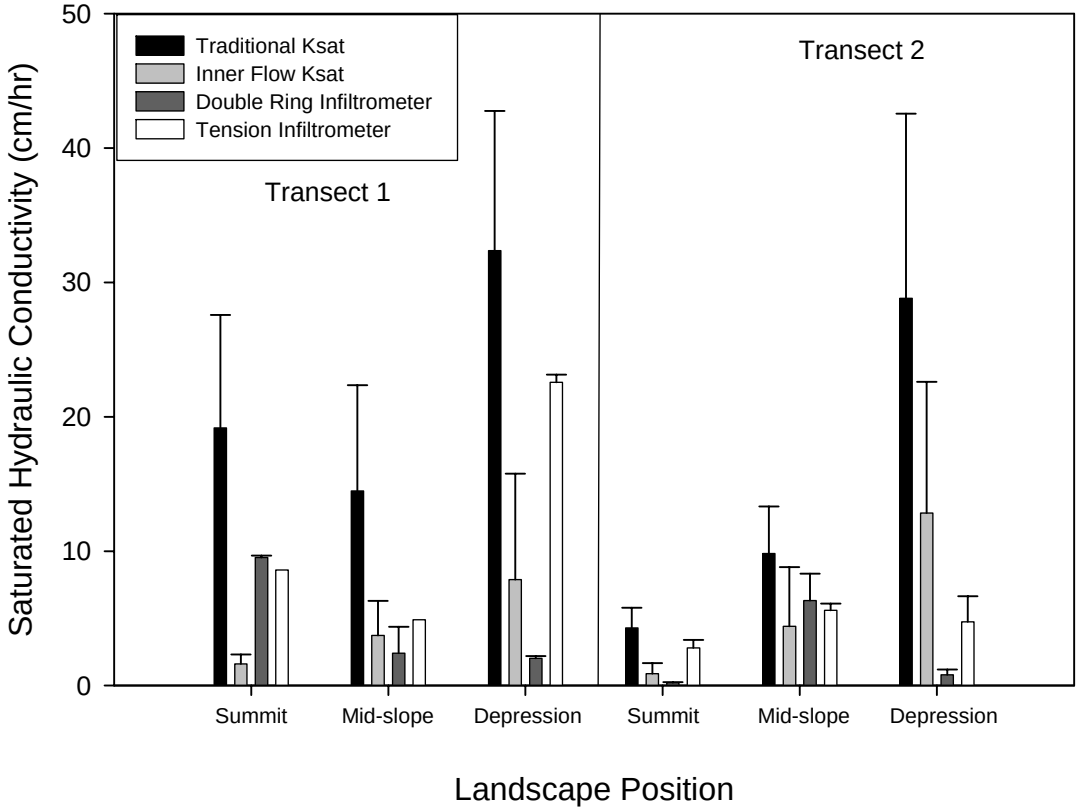

Fig. 3.15. Comparison of the traditional laboratory method, the new laboratory method using only the inner portion of flow, the double ring infiltrometer field method, and the tension infiltrometer field method for determining saturated hydraulic conductivity at six field sites. Laboratory measurements were conducted in replicates of three as was the tension infiltrometer measurements, whereas the double ring infiltrometer measurements were conducted in replicates of two.

CHAPTER 4

SOIL PROPERTIES CHANGES AFTER DECADES OF WASTEWATER IRRIGATION

ABSTRACT

For over 40 years, The Pennsylvania State University (PSU) has irrigated its wastewater onto both cropped and forested lands. While this method of wastewater disposal has gained popularity in water-deficit regions, it is not widely used in areas that have a surplus of water. Despite local weather conditions, PSU sprays two inches of wastewater a week. This irrigation, combined with the natural precipitation, amount to approximately 140 inches of water per year, which is equivalent to tropical rainfall. The objective of this study was to investigate the morphological and functional changes in soils as a result of this significant increased water load.

The research area has a karst geology and is dominated by rolling hills with many small depressions that act as sinks for runoff. Along with six soil trenches, 47 soil cores were taken within the 16-acre field. The field was cropped with a corn and winter wheat rotation, using a no-till farming practice. The predominant soil in the study is the Hagerstown soil series (*Typic Hapludalf*). The Hagerstown soil is generally very deep, well drained, and is formed from limestone/dolomite residuum.

Previous studies conducted at this site provided an estimate of the original soil properties. Soil morphological parameters, including structure, horizonation, and redoximorphic features, were evaluated from the soil cores and *in situ* soil pits. In addition, soil functional parameters, including saturated hydraulic conductivity, bulk

density, texture, organic matter content, and soil pH, were evaluated to determine the longevity of the system.

Results indicate that the soils are experiencing periods of saturation and local erosion, which are explained by redoximorphic features and over thickened A-horizons found on the site. Redoximorphic features were found at sixteen sites throughout the study area. The sites that experienced the periods of saturation, denoted by the redoximorphic features, were primarily found in depressional areas. It was evident that these areas experienced high volumes of run-on, not only by the presence of redoximorphic features, but also from the large accumulation of A-horizon material. Three different landscape positions, summit, midslope and depression, were found to be statistically significant when describing morphological features (i.e. manganese coating percentage, A-horizon depth, soil structure) and physical features (i.e. bulk density).

As a result of prolonged irrigation, soil functionality has also changed. Visual observations of increased runoff amounts are supported by laboratory findings of reduced saturated hydraulic conductivity in the select regions of the study area. In the area that has received irrigation for 22 years, the surface saturated hydraulic conductivity values have decreased from 14.23 to 1.2 cm/hr. The area that has received irrigation for over 40 years, the surface saturated hydraulic conductivity values have decreased from 9.06 to 7.2 cm/hr, since last measured in 1978.

Collectively, these findings indicate, in certain areas, the soils are experiencing some adverse effects from receiving an additional 100 inches of rainfall per year. By evaluating the areas based on landscape positions, remediation could be implemented in select areas, rather than the entire field.

INTRODUCTION

Wastewater irrigation, considered tertiary treatment, has been in practice around the world for many years and has recently grown in popularity (Tamminga, 1995). Municipalities treat the wastewater to secondary standards and then irrigate the effluent onto the land through a variety of methods. Land uses, such as agriculture, forests and golf courses, can all benefit from receiving treated wastewater. The soil organisms and plants utilize the water to help build biomass and remove nutrients that can harmfully affect the groundwater supply.

Using large scale wastewater irrigation on agricultural lands can be a synergistic management practice. The wastewater will have a different fate than being pumped into a river and the agricultural crops can make use of the extra water and nutrients (Toze, 2006). Since agriculture is the world's foremost user of the limited supply of freshwater (Bazzaz and Sombroek, 1996), any means of reducing the demand for freshwater, such as switching from freshwater to wastewater irrigation, will help prolong the limited life of aquifers.

Wastewater irrigation systems are also being implemented on a smaller scale. For instance, Pennsylvania has approved the Individual Residential Spray Irrigation System (IRSIS) as a conventional method of on-lot sewage disposal (Jarrett and Regan, 2002). It was developed for soils with a shallow depth to bedrock or high water tables. This system does have some drawbacks; homeowners are required to spray the irrigation over a large land area during dry weather. Even on the small scale, a system such as this helps to mitigate wastewaters, as well as prevent groundwater and surface water pollution.

Irrigation systems are not common in Pennsylvania because of its udic soil moisture regime (Waltman et al., 1997). Soils in the udic soil moisture regime typically can provide enough moisture to sustain most agricultural crops (Buol et al., 1997). Most of Pennsylvania currently experiences a water deficit in the months of June, July, and August; however, irrigation expenses, such as pumping costs, are not offset by the increase in yield for a particular crop. Therefore, in a climate that typically receives 40 inches of precipitation a year, wastewater irrigation systems have many uncertainties with respect to the capabilities of soils to handle the increased load of water. Understanding how excess wastewater reacts with the soils may also provide some insight as to how the soils may react to global climate change.

Previous research indicates that wastewater irrigation has the potential to alter soil properties (Coppola, 2004; Filip et al., 1999; Magesan et al., 2000; Tarchitzky et al., 1999; Toze, 2006; Vinten et al., 1983; Wallach et al., 2005; Wang et al., 2003). However, few studies have investigated wastewater irrigated soils by taking a landscape approach. A landscape approach would not only evaluate how soils are reacting at a particular point, but would link point descriptions to their landscape position. In turn, management decisions for sustainability could be based on an area's landscape position. Everything from the method of irrigation, composition of effluent, land use, soil type, local climate, and irrigation frequency could have potential impacts on how well the soil can handle excess water in a sustainable manner. Many of these issues can be troublesome to soil quality on an individual basis, but with wastewater irrigation's increased content of salts and suspended solids, there is a potential to produce compounding negative effects on soil quality.

Throughout history, irrigation in arid and semi-arid regions has been associated with an increasing concentration of salts in the soil (Bagarello et al., 2006). High sodium contents in irrigated soils can occur while using fresh water for irrigation, in addition to using wastewater that typically has elevated levels of sodium present. Excess sodium in soil can cause a variety of problems in agriculture, most notably the destruction of soil structure and harm to plants and dispersion of clays. Soil structure degradation is caused by clay dispersion and leads to reduced infiltration and hydraulic conductivity capacities of soils (Bagarello et al., 2006; Tarchitzky et al., 1999). The reductions in conductivity not only affect one area of the soil profile, but can affect water movement over the entire soil profile (Coppola, 2004).

The reduction of the soil's hydraulic conductivity and infiltration capacity in wastewater irrigation areas can also be attributed to the irrigation method. Even without extra sodium in the water, sprinkler irrigation systems reduce the soils ability to receive water (Santos et al., 2003; Tarchitzky et al., 1984). This reduction in infiltration is caused by the pure kinetic energy from the fall of rain drops. The rain drop's impact detaches soil particles from the existing structure, which can compact soil and clog pores (Santos et al., 2003). This process is fully capable of forming an impermeable crust at the surface of the soil, and extra chemicals or suspensions in wastewater could make things worse.

Many studies have also investigated various soil physical and chemical parameters in wastewater irrigation areas. Wang et al., (2003) studied the effects of wastewater irrigation by characterizing physical, chemical, and biological properties from soil samples taken of irrigated and non-irrigated California cropland. They determined

bulk density, total porosity, clay content, saturated hydraulic conductivity, and others in the hope of determining the attributes that would best describe soil quality. Total porosity and magnesium content were the only two attributes found to be significantly different between the irrigated and non-irrigated cropland. Pollice et al. (2004) investigated the effects of tertiary filtered wastewater drip irrigation on soils and found no change in soil chemical properties after two years of irrigation.

Other research has investigated the roles that wastewater irrigation plays on soil water repellency. Wallach et al., (2005) describes soils that have developed water repellency after being irrigated for over twenty years. The repellency was variable throughout the landscape and with depth. Resulting flow patterns showed "repellency" tongues that had developed within the area. This phenomenon could also cause excess runoff and affect agricultural production.

Microbiological investigations have also been performed in wastewater irrigation areas. Filip et al., (1999) investigated microbiological characteristics of soils in Germany and found significant increases in microbial populations in soils that had been irrigated with wastewater for up to 100 years. Friedel et al., (2000) found similar results in that the irrigation did not negatively affect the microbial biomass and its activities, which may have been due to the increased organic matter content of the area.

Soil quality measurements have received a lot of attention over the last ten years, with many researchers developing soil quality indices (Brejda and Moorman, 2001; Bucher, 2002; Cambardella, 2004; Diack and Stott, 2001; Filip et al., 1999; Grossman et al., 2001; Seybold et al., 2004). The quality rating of the soil is normally based on the soil's designated use. A sandy soil may be good for one type of crop, whereas a clayey

soil may be better for a different crop. It is therefore necessary to have clear goals and objectives before choosing or developing a soil quality rating system. By taking into account the variability of different soil quality measuring schemes, this study attempts to use a soil quality assessment based on soil morphology for the purpose of sustaining wastewater spray irrigation.

In 1978, Simpson and Cunningham studied the soils' ability to handle increased application of irrigation. They developed a morphological rating scale to "accentuate changes in subsoil morphology which might relate to changes in soil water properties." Common pedological descriptors such as soil structure, color, redoximorphic features, manganese coatings, and consistency were factored into their rating system. They assigned point values to each characteristic soil morphological feature based on their knowledge of that feature's relationship to dry or wet conditions. Simpson and Cunningham (1978) applied and tallied their scores from soil pit descriptions and suggested that the area under this study would only last for an additional 15 years for wastewater irrigation.

The Pennsylvania State University has used a spray irrigation system for tertiary wastewater treatment for over 40 years now. The system was designed as a research system in 1962 and was expanded in 1984 to become a full-scale operation. At that time the university stopped discharging water into the Spring Creek, a class one trout stream in the area (Tamminga, 1995). Instead, wastewater is irrigated throughout the year on both agricultural and forested lands, each having a number of different soil types.

The original goal for the irrigation system was to reduce nitrogen and phosphorous from the secondary treated wastewater, while providing extra nutrients and

water to the crops or forests. However, with the continuous advancements made at the university's wastewater treatment plant, the nitrogen and phosphorous levels had significantly decreased in the irrigation effluent. With the lowering of the eutrophication-causing nutrients at the treatment facility, the role of the irrigation onto the soils has changed.

The university currently uses the system to help with groundwater recharge, while still performing some tertiary and possibly quaternary treatment. Along with the focus of the irrigation system being changed, the management practices are also evolving. The concept of ecosystem management, adopted in the 1990's, provides a better distribution of the irrigation with respect to agricultural vs. environmental concerns. The idea of managing individual landscapes within the system also surfaced with the goal of providing a sustainable system to grow crops, treat wastewater, and recharge the local aquifers. However, even with intense management practices, problems arise from spraying over two million gallons of water a day on approximately 209 hectares of the land (Tamminga, 1995).

The Pennsylvania State University is now concerned with an apparent decrease in infiltration rate in the irrigation area. The reduced rate of infiltration increases the amount of runoff and decreases groundwater recharge. This study was commissioned to determine if there is an actual decrease in infiltration rates and determine what soil properties are causing the reduction. In addition to the infiltration measurements, a wide array of morphological, physical, and chemical properties of the soils were studied to determine soil changes after decades of wastewater irrigation. This study will help determine the current state of the soils in the area and provide insights into the system

sustainability. We used historic data from previous years in the 1970's to determine if the quality of soil has decreased during the period of operation. The historic data was compared with our results to determine to what degree the soils have changed.

MATERIALS AND METHODS

Study Site

The Pennsylvania State University's (PSU) Spray Irrigation Facility is located off of Fox Hollow Road in Centre County, PA (Figure 4.1). The irrigation area is divided into two parcels of land, known as the Gamelands and the Astronomy Site, bringing the total land area to 209 hectares (PSU, 1983). This area is located in the Ridge and Valley Physiographic Province, and is primarily underlain by several hundred to several thousand feet thick dolomite and limestone bedrock with some inter-bedded sandstone (Parizek, 1967). The soils from the Hagerstown and Hublersburg series are primarily found in the limestone bedrock region, whereas Morrison soils are found in the sandstone regions.

This study is primarily concerned with the Astronomy Site (Fig. 4.1). The Astronomy Site is part of the initial irrigation area, which has received wastewater irrigation for over 40 years (Cornfield site in Fig. 4.1). The site also includes an area that has been irrigated for 20 years (Cornfield control site in Fig. 4.1). The land has been continuously cropped with a corn and wheat rotation since irrigation was initiated. Currently, no-till farming practices are in place. The Pennsylvania Department of Environmental Protection allows the study area to receive two inches of irrigation a week, for the entire year. There are two phases of the Hagerstown soil series that were mapped in the study area, Hagerstown Silt Loam and Hagerstown Silty Clay Loam (Fig. 4.1). The Hublersburg soil series was also mapped in the study area, but did not appear to be present upon field observations.

The Hagerstown soil series (*Typic Hapludalf*) is a limestone derived residual soil that is deep and well drained with a moderate permeability. Morphological and physical characteristics of the soils used for this analysis can be found in Table 4.1. The texture of the surface soils ranged from loam to silt loam and the surface structure was granular. The subsurface samples had silty clay loam, clay loam, silty clay, and clay textures. The structure of the subsurface samples was subangular blocky. Iron and manganese stains were also common within the pedon.

Sampling Scheme

To determine soil physical, morphological, and chemical properties of the irrigation area, samples were taken from soil trenches and soil corings (Fig 4.2). The locations of the sample points were chosen based on landscape position and previous research performed in the area. Three major landscape positions were utilized for sampling purposes: summit, midslope, and depression (Table 4.2). Figure 4.3 displays the relative relief of the two transected depressions. Previous research from Simpson and Cunningham (1978) also provided a map to help guide soil sampling in this study (Fig 4.4). A total of 47 soil cores (120 cm in length and 5 cm in diameter) were taken from the study area using a hydraulic Gidding's probe mounted on a tractor. The soil cores represented samples from each of the 11 depressional areas and various midslope and summit positions. The cores were sealed in plastic tubes until they were morphologically described and sub-sampled for chemical analyses. Six soil trenches were also excavated, described, and sampled to determine a full suite of soil morphological, physical, and chemical properties. We located the soil pits in the general

area of the prior soil pits excavated by Simpson and Cunningham (1978). Two of the soil trenches were in the original control (Fig. 4.2) area, which has now been irrigated for 22 years. The remaining four soil trenches were located in the original irrigated area, which has received wastewater effluent for over 40 years. All sample locations were determined using a Trimble GPS Unit, followed by data post-processing with a base station located at University Park, PA, to increase accuracy of the measurements.

Soil Morphological Analyses

The soil trenches were described according to the USDA-NRCS field book. Each pit had a single description if the pit was homogeneous; however, two descriptions were given if the trenches were not homogeneous. The soil cores, taken with the Gidding's probe, were also described according to the USDA-NRCS field book. Information collected for each description included the following: horizonation, hand field texture, rock fragments, rupture resistance, color, roots, pores, structure grade, structure size, structure type, boundary, manganese size, manganese percentage, redoximorphic feature size, and contrast. Intact core samples were also taken from the soil trenches in both the vertical and horizontal positions for laboratory saturated hydraulic conductivity measurements and for bulk density measurements. The vertical cores were taken perpendicular to the landscape of the trench to capture the ability of the soil to move water vertically, whereas the horizontal cores were taken parallel to the landscape of the trench to better understand the potential for horizontal water flow.

Quantification of Morphological Features

Simpson and Cunningham (1978) developed a quantification system to measure the soil's ability to handle irrigation for the Penn State spray irrigation area, based on morphological features. This system was repeated in the present study to determine how the soils have changed since 1978. This profile rating system considers morphological properties such as color, structure, redoximorphic features, manganese concretions, and consistency (Table 4.2). Soil morphologic properties usually associated with wetter soil conditions receive lower values, whereas soil properties that are associated with drier conditions receive higher values

Since redoximorphic features (RF) indicate a prolonged period of saturation, their presence is heavily weighted in this quantification system. The depth to RF indicates the depth to saturation, which results in a lower score. If there are no RF present, the highest score of 50 is assigned. The size, abundance, and contrast of the RF are also incorporated into the score. The larger, brighter, and more frequent the RF are, the lower the score that site receives. If there are no RF present, a score of 32 points is assigned for each of the different RF feature properties.

Structure of the B Horizon is a key component of a soils ability to transport water. This quantification system subdivides soil structure into the three common attributes, which are averaged together for each subsurface horizon within the profile. The first attribute is structure size, which can be critical to water flow. When structural units are fine, there are more pathways for water to transmit. However, when structural units are

coarse, there are few boundaries to permit flow. Therefore, in this rating system, fine structural units receive a value of 18, whereas, coarse structural units receive a value of 6. Structure type and grade was also considered in this rating system. Prismatic and platy structures are considered to have less ability to handle water so they have lower values, while blocky structures receive higher values. Soils with a strong grade of structure, received the highest points, whereas soils with weak structure received the fewest points.

Color of the B horizon can also be an important indicator of how well a soil transmits water. Normally, with Hagerstown soils, the hue approaches the 5 YR to 2.5 YR range. However, when the soil is subjected to more water, the hue of the soil tends to be in the 7.5 YR to 10 YR range. This has resulted in giving the soils with a hue of 2.5 YR the highest score and the soils with a hue of 10 YR and 2.5 Y the lowest scores. The soil's value and chroma follow the same pattern. Soils that have a low intensity color receive the lower scores, whereas the vivid soils get higher scores.

The percentage of manganese concretions and the soil's consistency were also taken into consideration. Manganese can indicate a presence of water in the soil, but not totally saturated conditions, which are needed for the formation of RF (Vepraskas and Bouma, 1976). The soil's B-horizon consistency can also be quantified for water transportation. A firm soil was given the lowest value of zero, whereas, a friable soil was given a value of six.

After the field descriptions had been performed, each soil property for each subsurface horizon was given the relevant rating. The individual horizon scores were then averaged for the respective soil property. To determine significance between the initial research by Simpson and Cunningham (1978, Table 4.3) and the current soil

condition, non-parametric analyses were performed on the morphologic scores that each profile received. Non-parametric analyses were chosen because the data was not normally distributed. The Mann-Whitney pair-wise comparison was used to calculated differences between the 2006 and 1978 data, and the Kruskal-Wallis (non-parametric 1 way ANOVA) was used to calculated differences in landscape position (Minitab 13, State College, PA). Interpolated maps were made using the cokriging interpolation method in ArcView 9.1 (Redlands California), with a sample size of 43 points within the study site.

Soil Physical Analyses

The methodology used to determine the saturated hydraulic conductivity (Ksat) followed that prescribed by Klute (1986), which was modified in Chapter 3. Core samples (60 mm in height with an inner diameter of 54 mm) were saturated for at least 24 h prior to Ksat measurement, with care taken to saturate slowly from the bottom of the sample to the top. The water used was de-aired and treated with 0.005 M $CaSO_4$ to help reduce clay dispersal. After saturation, a piece of filter paper was placed on top of the sample, followed by an empty ring to allow for ponding (see Fig. 3.1). The sample was moved to a constant head apparatus that was constructed to maintain a constant head on samples at all times. Flow was recorded by collecting the effluent and weighing it every 10 to 20 minutes, depending on flow rate. The core remained ponded until reaching steady-state conditions. The saturated hydraulic conductivity was calculated based the flow measured from the inner part of the core and on Darcy's Law (Eq 3.1). After the saturated hydraulic conductivity measurement was completed, the cores were placed in a

105^{o}C oven and dried until a constant weight to provide the bulk density of the soil. All samples were analyzed in triplicate.

In situ saturated and unsaturated hydraulic conductivity tests were performed adjacent to each of the soil pit sites using the tension infiltrometer (Ankeny et al., 1991; Lin and McInnes, 1995; Lin et al., 1997). Three modified tension infiltrometers were set up with pressure transducers to measure both the height of water and the tension in the infiltrometer disc, as described in the previous chapter. Site preparation was kept to a minimum and followed the protocol of Lin et al. (1997). Sequential tensions of 12, 6, 3, 2, and 1 cm were utilized to determine unsaturated flow characteristics of the site along with a zero tension measurement that was used to determine the saturated hydraulic conductivity (Table 4.5). Calculations were made using two supply tensions to calculate the alpha value described in the Wooding's Equation (Lin et al., 1997).

The use of different tensions on the tension infiltrometer provides for the determination of various pore size contributions to water flow in the irrigation area. The pore size information from these instruments is based on the capillary rise equation (Eq. 2), which describes a relationship between pore size and water tension. The soil pore size that contributes to water flow is inversely proportional to the tension of the water:

$$r = \frac{2\sigma\cos\theta}{\rho g h} \qquad \text{[Eq. 2]}$$

Where: σ = surface tension of water (kg s^{-2})
θ = contact angle between water and pore wall (assumed to be 0)
ρ = density of water (kg m^{-3})
g = acceleration due to gravity (m s^{-2})
h = tension (m)
r = pore radius (m)

Table 4.4 relates the tensions to the maximum pore size radius, along with the pore size classification (SSSA, 2004).

Soil texture was analyzed in the laboratory using a rapid method (Kettler et al., 2001). Fifteen grams of < 2 mm sieved soil and 90 mL of 3% hexametaphosphate were added to a 300 mL fleaker. The fleaker was placed on a reciprocating shaker (120 reciprocations per minute) for 2.5 hours. The soil solution was rinsed through a 0.053 mm sieve and collected in a 600 mL beaker. The > 0.053 mm fraction (sand) was rinsed into a separate beaker and dried to a constant weight at 105^{o}C. The soil solution was allowed to settle for 2.5 hours. The liquid (clay) was then decanted from the beaker and discarded. The silt was dried at 105^{o}C until it reached a constant weight. Since this method is relatively new, soils with a known texture, determined by the pipette method, were analyzed along with the unknown samples.

Soil Chemical Analyses

Soil pH was measured using a 1:1 ratio by mass of distilled water and soil. The samples were stirred every five minutes until the saturation period reach 0.5 hours. The pH was then determined by a temperature compensated pH electrode (VWR International, West Chester, PA). Organic matter content was determined by the loss of ignition method (Storer, 1984). A five gram soil sample was dried at 105^{o}C until it reached a constant weight. The soil was placed in a 360^{o}C oven for two hours, which was followed by cooling to 150^{o}C and weighing using a draft-free scale. The weight change due to loss of ignition was then converted to organic matter content by using the following equation:

$$\text{Organic Matter (\%)} = -0.23 + (0.80 \times \text{LOI (\%)}) \qquad \text{[Eq. 3]}$$

This equation was developed by a regression analysis comparing the Walkley-Black method with the loss of ignition, for Pennsylvania mineral soils (Penn State Agricultural Analytical Services).

RESULTS AND DISCUSSION

Morphological Properties Change

Although redoximorphic features, which indicate a period of saturation within the soil, are not typically found in the well-drained Hagerstown soils, five out of the six soil trenches and 11 out of 47 soil cores displayed these features within the profile. Sites three (depression), five (back slope), and six (depression) had redoximorphic features present throughout the whole trench. However, the redoximorphic features found at sites one (summit) and two (back slope) were not consistent within the entire soil trench. Site 4 (summit) did not display any redoximorphic features. We found the size of the redoximorphic features to be "coarse" at all trenches except for one, which had a "fine" size designation (Table 4.1) The horizons that displayed redoximorphic features had a texture of either clay, silty clay, or silty clay loam (Table 4.1). These horizons frequently exhibited coarse subangular blocky structure, or were overlying a horizon with coarse subangular blocky structure (Table 4.1).

Lin et al.(1999) found a negative relationship between structure size and the ability to transmit water vertically. As structure size increases there are fewer vertical ped-face boundaries for water to move. In the present study, structure size was shown to increase over the years of irrigation, which may be a result of increased levels of organic matter within the soil profile (Table 4.1, Figure 4.21). Jastrow (1996) indicated that as aggregates become larger, there is a greater amount of recently incorporated organic matter. Likewise, Six et al. (2000) found decreasing soil aggregate size with decreasing soil carbon. The increase in structure size found in the study area may lead to longer

periods of saturation and result in larger, more distinct redoximorphic features observed in the soil trenches.

The soil cores that displayed redoximorphic features were also from each of the three different landscape positions: depression, midslope, and summit. The depressional areas (n=5) that displayed redoximorphic features appeared to receive runon from adjacent summit and midslope areas. These depressions also exhibited a buildup of A-horizon material (Figure 4.5). In contrast, most of the midslope points (n = 5) and the summit area (n =1) that had signs of RF were located on the down slope side of a depression, which would indicate the lateral movement of water from the depression to adjacent down slope areas.

Based upon Simpson and Cunningham's (1978) rating scale, the soil trenches exhibited a significant increase in redoximorphic feature size ($p = 0.03$) compared to their observations in 1978 (Fig. 4.6). This increase in RF size resulted in lower scores on the rating scale (13.9 for 2006 vs. 17.2 for 1978). The contrast of the RF also appeared to become more distinct, although not statistically significant ($p = 0.27$). Neither the depth to RF nor the abundance of RF appeared to change significantly since the last soil pit descriptions in 1978. The control area (22 years of irrigation) did not experience any statistically significant changes in RF (Figure 4.7). Over the entire landscape, the core samples displayed fewer redoximorphic features than did the soil pits, hence the larger values for the rating scale (Fig 4.8 and 4.9).

Although we originally hypothesized there to be a significant increase in the number of sites with redoximorphic features in the study area, there was not enough evidence to accept this hypothesis. While perched water tables were commonly found

during field observations, redoximorphic features were less prevalent. Typically, there are five conditions that need to be present for redoximorphic features to form: lack of oxygen, presence of organic carbon, moderate temperatures, time, and a microbial population (Dobos et al., 1990). Upon initial considerations of the site, it appeared to be well suited for the formation of redoximorphic features. However, several possibilities may be responsible as to why the occurrence of these features did not change, such as lack of soil microbes, initial soil color and temperature.

Soil microbes also play an important role in the reduction and oxidation of iron, which causes mottling (Ciolkosz and Dobos, 1990). These microbes need an energy source, such as carbon, which normally is present in wastewater. When microorganisms digest soil organic material, they need an electron accepter, such as oxygen, in aerobic conditions, or iron and manganese during anaerobic conditions. If the iron accepts the electron, it becomes soluble and can leave the soil matrix, causing the redoximorphic features that are used to determine areas of periodic saturation (He et al., 2003). Some areas that have been treated with primary wastewater irrigation have experienced increases in the microbial population (Filip et al., 1999). The irrigation at our site has already been treated to the secondary standards and chlorinated, which may have altered the bacterial population in the receiving soils.

Initial soil color may also play a role in the absence of redoximorphic features. In selected areas, there have been documented cases of observing seasonal high water tables in areas that did not have redoximorphic features, with soils that had a reddish hue being especially problematic (Rabenhorst and Parikh, 2000). The Hagerstown soil series does

normally have reddish subsurface hues, which may be more resistant to the formation of visible redoximorphic features than other soils with yellowish hues.

Another possible explanation for the lack of redoximorphic features observed involves temperature. The mean annual air temperature for Pennsylvania is 9.3^{o}C (Waltman et al., 1997). Although the study site is irrigated year round, when temperature conditions are most favorable for the microorganisms that cause the redoximorphic features, the soil may not be saturated due to the evapotranspiration (ET) from either the wheat or corn crop. After the crop is harvested, reducing ET and favoring saturation, the temperature drops and slows the formation of redox features (Dobos et al., 1990).

Another morphological indicator of water and water movement within the soil profile is the presence of manganese coatings. Elemental manganese (Mn) exists in a number of different valence states (+1 to +7), but the most soluble form is the +2 form. Manganese is released during the weathering process, which is followed by soil water transport. As with the movement of iron, Mn is highly dependent of the Eh and pH of the local soil environment, however, the oxidation and reduction of Mn commonly occurs at less saturated, higher Eh values than iron does (McDaniel and Buol, 1991). These chemical properties allow Mn to be a good tracer for determining water movement through a well drained soil (McDaniel et al., 1992).

Five out of six soil trenches had manganese coatings present, and 40 out of the 47 sites displayed areas with manganese coatings. Maximum profile manganese percentage was statistically different ($p = 0.035$) between the three landscape positions (Fig. 4.10). The side slope position had the highest median percentage of manganese (15%), the depression bottoms had the lowest median percentage (2%), and the summits had a

median percentage of 8%. McDaniel et al. (1992) found similar distributions of Mn while comparing between landscape positions. Therefore, the morphology of the soils suggests there is a potential of lateral movement of water from the summit areas to the depressional areas, despite the relatively low change in relief between the two landscape positions.

. The second B- horizon was the most common place to detect manganese coatings with 32 sites having a concentration ranging from 1 to 50 percent. Seventeen sites had manganese coatings in the first Bt horizon, with concentrations ranging from 0.5 to 30 percent. The lower Bt horizons displayed some of the highest concentrations of manganese coatings with concentrations exceeding 50%. The sizes of the manganese coatings were predominately medium to coarse. Most of the water movement appeared to be occurring in the upper portion of the soil profile.

Along with subsurface flow of water, the study area appears to be experiencing an elevated amount of surface flow, which has resulted in accelerated erosion, measured by depth of A-horizon. Hagerstown soils typically have an A-horizon thickness between 20 and 30 cm deep (Soil Survey Staff, 2006). Figure 4.11 depicts the frequency of observed A-horizon depths, in which 20 sites had A-horizon depths over 30 cm. Landscape position had a statistically significant effect on horizon depth, with depression and summit areas having median depths of 65 and 19 cm, respectively (Fig. 4.12). Four of the cores had A-horizon thicknesses of over 100 cm, which were all located in depressions. There were also eight buried A-horizons found at the site, all located in depressions. Figure 4.5 shows a map of the A-horizon depth over the surface of the study site.

The A-horizons in the soil trenches typically displayed a strong granular soil structure, except when there were multiple A-horizons present, in which a sub-angular blocky structure was found (Table 4.1). We found the subsurface horizons in the trenches to have a moderate to weak subangular blocky structure. The sizes of the structural units were primarily medium to coarse. However, upon examination of the soil cores, many of the surface and subsurface horizons showed signs of a weak to moderate platy structure along with subangular blocky structure. Simpson and Cunningham's (1978) scale was able to statistically show differences between landscape position and structure type ($p = 0.029$) as well as between landscape position and structure grade ($p = 0.003$) for the 47 core samples. The depressional areas had the lowest (wettest) median score for both structure grade (6) and structure type (6), whereas the summit position had the highest (driest) median score for structure grade (10) and for structure type (9.33).

While investigating the soil texture of the trench samples (Table 4.1), we found that most of the surface horizons had a silt loam or loam texture, which is normal for the Hagerstown soil series. The first subsurface horizon also had low clay and high silt levels. This suggests a rapid downward movement of clay occurring as a result of the large volume of water the soil receives (Presley et al., 2004). The sites that had large amounts of silt in the first subsurface horizon were also the sites that displayed redoximorphic features lower in the subsurface horizons, which again is indicative of areas receiving large volumes of water.

Soil color was consistent throughout the surface horizons, whereas the subsoil's color varied widely throughout the study area. Hues ranged from 2.5 YR to 2.5 Y, in the

subsurface horizons. The Munsell values and chromas were consistent throughout the soil trench profiles, with values ranging from three to five for the surface horizons, and from four to six for the subsurface horizons. The chromas ranged from three to six on the surface, and from three to eight on the subsurface horizons. Investigating the soil colors over the landscape using Simpson and Cunningham's (1978) scale yielded statistically different hue ($p < 0.001$) and chroma ($p < 0.01$) values for the various landscape positions. The depressional areas had the lowest median values for hue and chroma (2 and 8, respectively), whereas the summit had the highest median value for the hue (10) and the same value as the side slope position for chroma (10). There was also a strong negative correlation between the hue of the soil and the amount of clay in the soil. As the hue decreased, more red pigments were visible in the soil, and the clay content increased (Fig 4.13). Likewise, there was a positive correlation between the hue of the soil and the amount of silt present in the soil (Fig. 4.14).

Although there were no statistical differences in soil color since the 1978 study for the trench samples (Figs. 4.6, 4.7), the irrigated core samples (Figs. 4.8, 4.9) did show a significantly "wetter" soil color. The soils receiving the most water, primarily due to landscape position, had a more yellowish color. In many subsurface horizons found in Pennsylvania, colors normally range from 2.5 YR (red hues) to 10 YR (yellowish brown) hues (Ciolkosz and Dobos, 1990). The soils in our study area had hues ranging from 2.5 YR to 2.5 Y. The red hues were due to a high concentration of hematite (Fe_2O_3), whereas yellowish brown colors were due to goethite (FeOOH) (Schwertmann and Taylor, 1989). The mineral goethite occurs in soils that experience short term saturation and may actually develop from the mineral hematite (Buol et al., 1997). This suggests that the

rating scale developed by Simpson and Cunningham (1978) is correct in giving fewer points to soils that have a yellowish brown hue.

While comparing the current control area descriptions (22 years of irrigation) with the current irrigated area descriptions (40+ years of irrigation), there are no statistical differences at ($p > 0.05$). However, throughout the different morphologic properties, the irrigated area has lower scores than the control area, except for structure grade (Fig. 4.15). The irrigated area did show signs of more redoximorphic features than did the control area, which is expected since it has been irrigated nearly twice as long as the control area.

Physical Properties Change

Vertical saturated hydraulic conductivity in the surface was significantly greater than that of subsurface soils. The average surface hydraulic conductivity values were also lower than the values measured for the same area in 1978. Sopper and Richendorfer (1978) reported average saturated hydraulic conductivity values for the control and irrigated areas to be 14.23 and 9.06 cm/hr, respectively. Currently, the mean values for hydraulic conductivity are 1.2 cm/hr and 7.2 cm/hr for the control and irrigated areas, respectively. The area that has been irrigated for 22 years experienced a much greater decrease in conductivity than did the area that has been irrigated for over 40 years. Since the 22 year area, had not received effluent prior to its measurements, there may be indications that the greatest decrease in conductivity occurs within the first years of irrigation. Although there were no significant relationships between landscape position and saturated hydraulic conductivity values (Fig. 4.16, $n = 29$), the depression bottom did

have the highest mean surface saturated conductivity (15 cm/hr) and the summit position had the lowest mean surface saturated hydraulic conductivity value (6.95 cm/hr). Fig 4.17 depicts saturated hydraulic conductivity values as a function of depth for all of the soil trench samples. Mean saturated hydraulic conductivity values were calculated for the Ap, Bt1, Bt2 and Bt3 horizons for the entire field, and yielded an exponential decrease for each subsequent horizon (Fig. 4.17).

As explained earlier, surface saturated hydraulic conductivity has been shown to decrease since last measured in 1978 (Sopper and Richenderfer). Although there is no historical information for the subsurface saturated hydraulic conductivity, there appears to be an exponential decrease in saturated hydraulic conductivity from the surface to each subsequent horizon. Reductions in hydraulic conductivity in both fresh water and wastewater irrigation systems are common (Coppola, 2004; Santos et al., 2003; Tarchitzky et al., 1984; Vinten et al., 1983). However, in trenches one, two, four, and six, the saturated hydraulic conductivity does start to increase below the first subsurface soil horizon, possibly indicating that the first subsurface horizon is the most restrictive within the profile. Although the presence of a restrictive layer (i.e. pores filled with suspended solids) is common in wastewater irrigation systems (Coppola, 2004), the organic matter content of the soil does not show any increase in the first subsurface horizon.

Reduction of saturated hydraulic conductivity was observed when comparing the surface to the subsurface horizons. Taken together with the loss of A-horizon in some areas, these results may provide some insight as to why there appears to be an increasing amount of run-off and more heavily saturated areas. The other phenomenon that can be

interpreted from the hydraulic conductivity data is the capability of the depression to handle more water than the other sites. The fact that the depressional areas appear to be wet most of the time is not due to reductions in conductivity, but because they are experiencing high amounts of run-on. The run-off phenomenon is most likely being caused by the reduction of hydraulic conductivity in the surface layers of areas that have experienced moderate to severe erosion.

The tension infiltrometer conductivity values were similar at higher tensions (Fig. 4.18, 12 and 6 cm), whereas deviations in the conductivity started to occur at the lower tensions (3, 2, 1, and 0 cm) (Figure 4.18). The low unsaturated conductivity during higher tensions indicated that pores smaller than 0.25 mm provide a small contribution to the entire flow regime. Site three had the highest conductivity values, with the 0 cm tension value yielding an average value of 22.6 cm/hr (n=3). The results from site three are consistent with our Ksat laboratory measurements, where the depressional areas had the highest rate of infiltration. The lowest infiltrometer values were found at site four. These results are also consistent with the laboratory results.

Previous studies have also demonstrated correlations between tillage practices and infiltration rates. Researchers indicate that conservation tillage practices are beneficial because of the potential network of long-continuous macropores that it can sustain (Hangen et al., 2002). Other studies have found that minimum tillage systems have the highest infiltration rates, and no-till systems have the lowest infiltration rates (Akinyemi, 2004). Our study area has been in a no-till practice for at least fifteen years. The combination of the long period of no-till with the constant rain drop impact could result in reduced infiltration rates. The data from the tension infiltrometer does support the idea

that most of the infiltration is occurring through macropores, which are associated with conservation and no-till practices.

Unlike the saturated hydraulic conductivity measurements, there were no significant differences between surface and subsurface bulk density. The surface bulk density of the soils in 1974 was 1.27 gm/cm^3 and 1.41 gm/cm^3 for the control and irrigated areas, respectively. Over the landscape, there was a significant difference in bulk density values ($p > 0.05$). The summit position had the highest average bulk density value, 1.51 gm/cm^3, whereas both the depression and side slope positions had mean values of 1.42 gm/cm^3 (Fig. 4.19).

Another possible explanation for the decreased infiltration may be the increase in bulk density on the surface layers. The overall increase in bulk density of the surface soil layers, which signifies compaction and reduced porosity, has been a common finding in wastewater irrigated areas (Coppola, 2004; Wang et al., 2003). The increase in bulk density was also observed in the initial research performed at the same area (Sopper and Richenderfer, 1978). Although the increase in bulk density is common for wastewater irrigation systems, it may also occur in regular farming systems that utilize heavy machinery for planting, fertilizing, and harvesting (Lipiec, 2003; Trautner and Arvidsson, 2003).

Chemical Properties Change:

While investigating the pH of the soil, we found an increase throughout the profile, when comparing the current information with that of Hook (1971) (Figure 4.20). The soils have increased in pH even though there has been no application of lime. This is

a common finding for soils receiving wastewater irrigation and for those receiving plain irrigation waters (Filip et al., 1999; Hu et al., 2006; Presley et al., 2004). The elevated pH in the soils may reduce the ability of iron to mobilize, resulting in fewer redoximorphic features. In some situations, the soil's pH profile was indicative of its hydraulic conductivity values. For instance, sites two and four had sharp decreases in their pH values directly below the surface, corresponding to low conductivity values found both in the laboratory and the field. There were also sharp decreases in pH levels associated with redoximorphic features. The pH normally decreased in and below horizons that displayed redoximorphic features, further signifying a reduction in water movement. The pH of the soil is close to being at equilibrium with the pH of the wastewater (Parizek et al., 2006).

Soil organic matter (OM), measured by loss of ignition, displayed similar trends to the soil pH (Figure 4.21). Comparing the 2006 content to that of Hook (1971), the soils have experienced a slight increase in the surface horizons and a sharp increase in subsurface horizons. The highest organic matter percentage was found on the surface of trench three, which was 3.72 percent. The lowest percentage was located at trench two, with a value of 1.02 percent. Although organic matter and carbon are generally considered beneficial, some problems may arise from elevated levels, such as soil hydrophobicity and reduced hydraulic conductivity (Magesan et al., 2000; Wallach et al., 2005). The elevated level of organic matter throughout the entire profile indicates that, although the conductivity has been reduced, there is still water moving through the profile to transport the organic matter.

CONCLUSIONS:

The goal of this research was to comprehensively evaluate the soils that have received wastewater irrigation for over 40 years. In order to fulfill our goals, sample sites were chosen based on landscape position and from previous research. Each of the three landscape positions (summit, midslope, and depression) have reacted differently to the 100 inches of additional wastewater irrigation, despite their close proximity to each other and relatively small elevation changes. These differences can be seen from the morphological analyses and the physical analyses, which are linked to each other.

Throughout the landscape, the morphological and physical features for the summit positions indicated that they were the source of several critical problems throughout the rest of the landscape. Morphologically speaking, the summit areas had the shallowest A-horizons. The loss of A-horizon material suggests that these areas are particularly prone to runoff. The summits also displayed few redoximorphic features and had the lowest percentage of manganese coatings. The subsoils appeared to be less weathered than that of the other landscape positions, exhibiting a reddish soil color. These features suggest that the summit soils are not receiving as much water as what the lower landscape positions are. The morphological results are supported by the results of the physical analyses. The summit areas exhibited the highest bulk density and generally lowest hydraulic conductivity when compared to the other landscape positions. Both the morphological and the physical analyses suggest that the summit areas may be the source of the runoff that is affecting the other landscape positions and the irrigation area as a whole.

The midslope landscape position showed signs of being the hydraulic link between the summits and depressions. These regions had the highest percentage of manganese coatings as compared to summit and depression positions. The manganese coatings act as a tracer and suggest there is lateral flow of water from the summit areas to the depressional areas. Throughout the study area, these landscape positions are the most likely to have subsurface water movement due to their sloping nature, which causes a hydraulic gradient. In addition, midslopes had a higher occurrence of redoximorphic features, than did the summit areas. This also suggests these areas are receiving additional water from the summit positions. The color of the B-horizon in the midslope soils was moving from the reddish color of the summit to a more yellowish color, again an indicator of more weathering. These areas had a deeper A-horizon than the summit position, but did not exhibit the accumulation that was experienced by the depressional areas. The physical attributes of these soils suggest that the midslope landscape positions have hydraulic conductivity values and bulk density values that were similar to the summit positions.

Over the landscape, the depressional areas appear to be receiving the bulk of the irrigation water. These areas have the deepest A-horizons, indicating that they are receiving a high amount of run-on and sedimentation. The high amount of run-on is also causing periods of total saturation, explained by the occurrence of redoximorphic features in these areas. Manganese coatings were not as prevalent in these areas, which may also be a result of being saturated for longer periods of time. Although the depression regions have the wettest morphologic features, their physical properties indicate that they can transmit the greatest amount of water, especially through the thick collection of A-

horizon material. The depressions have low bulk densities and also the highest surface laboratory saturated conductivity values. These results suggest that although the depressional regions are saturated, and sometimes ponded, this occurrence is due primarily to the region receiving the most run-on, rather than an inability to transport water.

Our results indicated that throughout the irrigation area, the total number of redoximorphic features did not appear to increase. However, those features that were observed grew in size and were more distinct, since last observed in 1978. Many of the redoximorphic features observed appeared in small pockets within the soil trenches. Therefore it would be difficult for the core samples to represent the total number of redoximorphic features within the study area. Another limitation of the core samples was the depth in which we could describe the soils. In a number of depressions, the areas most susceptible to redoximorphic features, the entire core was filled with transported A-horizon material. Redoximorphic features may have been present, but we didn't have the ability to observe them.

The soils have also experienced some chemical alterations. Throughout the surface and the upper B-horizons, the pH of the soil has increased by one to two pH units. This increase has occurred without the addition of lime, and despite the influence of acid precipitation. Organic matter has also shown an increase throughout the profile. This may be causing the formation of larger soil structural units that were observed during the trench investigations. The increase in size of the soil structure was also related to the presence of redoximorphic features. These features were located in or directly above horizons that had a coarse structure size.

Despite the morphological, physical and chemical changes experienced in this area after receiving the prolonged period of irrigation, the soils have retained their functionality. By dividing the area into different landscape positions, we have been able to determine the problem areas within the field. Although the depressional areas appear to be the most affected by the irrigation water, the summit areas may be the cause of the problems. Therefore, remediation will be recommended in those affected areas to keep this area sustainable for another forty years.

REFERENCES

Akinyemi, J., A. Adedeji. 2004. Water Infiltration Under No-Tillage, Minimum Tillage and Conventional Tillage Systems on a Sandy Loam Alfisols. 2004 ASAE/CSAE Annual International Meeting.

Ankeny, M., M. Ahmed, T. Kaspar, and R. Horton. 1991. Simple field method for determining unsaturated hydraulic conductivity. Soil Science Society of America Journal 55:467-470.

Bagarello, V., M. Iovino, E. Palazzolo, M. Panno, and W. Reynolds. 2006. Field and laboratory approaches for determining sodicity effects on saturated soil hydraulic conductivity. Geoderma 130:1-13.

Bazzaz, F., and W. Sombroek, (eds.) 1996. Global Climate Change and Agricultural Production. John Wiley & Sons Ltd, West Sussex, England.

Brejda, J., and T. Moorman. 2001. Identification and interpretation of regional soil quality factors for the central high plains of the Midwestern USA, p. 535-540, *In* D. Stott, et al., eds. The Global Farm. Selected papers from the 10th International Soil Conservation Organization Meeting held May 24-29, Purdue University and the USDA-ARS National Soil Erosion Research Laboratory. Purdue University, West Lafayette, IN.

Bucher, A. 2002. Soil Quality Characterization and Remediation in Relation to Soil Management. Ph.D Dissertation, The Pennsylvania State University, University Park, PA.

Buol, S.W., F.D. Hole, R.J. McCracken, and R.J. Southard. 1997. Soil genesis and classification *In* (ed.). Iowa State University Press, Ames, Iowa.

Cambardella, C., T. Moorman, S. Andrews and D. Karlen. 2004. Watershed-scale assessment of soil quality in the loess hills of southwest Iowa. Soil and Tillage Research 78:237-247.

Ciolkosz, E., and R. Dobos. 1990. Color and Mottling in Pennsylvania Soils Agronomy Series Number 108. The Pennsylvania State University, University Park, PA.

Coppola, A., A. Santini, P. Botti, S. Vacca, V. Comegna, G. Severino. 2004. Methodological approach for evaluating the response of soil hydrological behavior to irrigation with treated municipal wastewater. Journal of Hydrology In Press.

Diack, M., and D. Stott. 2001. Development of a soil quality index for the chalmers silty clay loam from the Midwest USA, p. 550-555, *In* D. E. Stott, et al., eds. The Global Farm. Selected papers from the 10th International Soil Conservation Organization Meeting held May 24-29, Purdue University and the USDA-ARS National Soil Erosion Research Laboratory. Purdue University, West Lafayette, IN.

Dobos, R., E. Ciolkosz, and W. Waltman. 1990. The effect of organic carbon, temperature, time, and redox conditions on soil color. Soil Science 150:506-512.

Filip, Z., S. Kanazawa, and J. Berthelin. 1999. Characterization of effects of a long-term wastewater irrigation on soil quality by microbiological and biochemical parameters. Journal of Plant Nutrition and Soil Science 162:409-413.

Friedel, J., T. Langer, C. Siebe, and K. Stahr. 2000. Effects of long-term waste water irrigation on soil organic matter, soil microbial biomass and its activities in central Mexico. Biology and Fertility of Soils 31:414-421.

Grossman, R., D. Harms, C. Seybold, and M. Sucik. 2001. A morphology index for soil quality evaluation of near-surface mineral horizons, p. 637-640, *In* D. Stott, et al., eds. The Global Farm. Selected papers from the 10th International Soil Conservation Organization Meeting held May 24-29, Purdue University and the USDA-ARS National Soil Erosion Research Laboratory. Purdue University, West Lafeyette, IN.

Hangen, E., U. Buczko, O. Bens, J. Brunotte, and E. Huttl. 2002. Infiltration patterns into two soils under conventional and conservation tillage: influence of the spatial distribution of plant root structures and soil animal activity. Soil and Tillage Research 63:181-186.

He, X., M. Vepraskas, D. Lindbo, and R. Skaggs. 2003. A method to predict soil saturation frequency and duration from soil color. Soil Science Society of America Journal 67:961-969.

Hook, J. 1971. Characterization of Phosphorus in Soils Treated with Sewage Effluent. Master of Science, The Pennsylvania State University, University Park, PA.

Hu, C., T. Zhang, D. Kendrick, Y. Huang, M. Dahab, and R. Surampalli. 2006. Muskegon Wastewater Land Treatment System: Fate and transport of phosphorus in soils and life expectancy of the system. Engineerin Life Science 6:17-25.

Jarrett, A., and R. Regan. 2002. Individual Residential Spray Irrigation Systems. Pennsylvania State University Cooperative Extension Fact Sheet 169, University Park, PA.

Jastrow, J.D. 1996. Soil aggregate formation and the accrual of particular and mineral associated organic matter. Soil Biology and Biochemistry 28:656-676.

Kettler, T.A., J.W. Doran, and T.L. Gilbert. 2001. Simplified method for soil particle-size determination to accompany soil-quality analyses. Soil Science Society of America Journal 65:849-852.

Lin, H., and K. McInnes. 1995. Water flow in clay soil beneath a tension infiltrometer. Soil Science 159:375-382.

Lin, H., K. McInnes, L. Wilding, and C. Hallmark. 1997. Low tension water flow in structured soils. Canadian Journal of Soil Science 77:649-654.

Lin, H., K. McInnes, L. Wilding, and C. Hallmark. 1999. Effects of soil morphology on hydraulic properties: I. Quantification of soil morphology. Soil Science Society of America Journal 63:948-954.

Lipiec, J., R. Hatano. 2003. Quantification of compaction effects on soil physical properties and crop growth. Geoderma 116:107-136.

Magesan, G., J. Williamson, G. Yeates, and A. Lloyd-Jones. 2000. Wastewater C:N ratio effects on soil hydraulic conductivity and potential mechanisms for recovery. Bioresource Technology 71:21-27.

McDaniel, P., and S. Buol. 1991. Manganese distributions in acid soils of the North Carolina Piedmont. Soil Science Society of America Journal 55:152-158.

McDaniel, P., G. Bathke, S. Buol, D. Cassel, and A. Falen. 1992. Secondary manganese/iron ratios as pedochemical indicators of field-scale throughflow water movement. Soil Science Society of America Journal 56:1211-1217.

NADP. 2006. National Atmospheric Deposition Program Program Office, Illinois State Water Survey, 2204 Griffith Dr., Champaign, IL 61820.

Parizek, R. 1967. Waste water renovation and conservation. The Pennsylvania State University, University Park, PA.

Parizek, R., J. Nemitz, and G. Moret. 2006. Flow and water quality monitoring data for Toftrees Resort and Country Club. Office of the Physical Plant, The Pennsylvania State University, State College, PA.

Pollice, A., A. Lopez, G. Laera, P. Rubino, and A. Lonigro. 2004. Tertiary filtered municipal wastewater as alternative water source in agriculture: a field investigation in Southern Italy. Science of the Total Environment 324:201-210.

Presley, D.R., M.D. Ransom, G.J. Kluitenberg, and P.R. Finnell. 2004. Effects of thirty years of irrigation on the genesis and morphology of two semiarid soils in Kansas. Soil Science Society of America Journal 68:1916-1926.

Rabenhorst, M., and S. Parikh. 2000. Propensity of soils todevelop redoximorphic color changes. Soil Science Society of America Journal 64:1904-1910.

Santos, F., J. Reis, O. Martins, N. Castanheira, and R. Serralheiro. 2003. Comparative Assessment of Infiltration, Runoff and Erosion of Sprinkler Irrigated Soils. Biosystems Engineering 86:355-364.

Schwertmann, U., and R. Taylor. 1989. Iron Oxides, *In* J. Dixon and S. Weed, eds. Minerals in Soil Environments. Soil Science Society of America, Madison, WI.

Seybold, C., R. Grossman, H. Hoper, G. Muckel, and D. Karlen. 2004. Soil Quality Morphological Index Measured in the 1996 NRI Pilot Study. Soil Survey Horizons 45:86 - 95.

Simpson, T., and R. Cunningham. 1978. Soil Morphologic and Hydraulic Changes Associated with Wastewater Irrigation. Institute for Research on Land and Water Resources, The Pennsylvania State University, University Park, PA.

Six, J., K. Paustian, E. Elliott, and C. Combrink. 2000. Soil structure and organic matter: I. Distribution of aggregate-size classes and aggregate-associated carbon. Soil Science Society of America Journal 64:681-689.

Soil Survey Staff, N.R.C.S. 2006. [Online]. Available by United States Department of Agriculture http://soils.usda.gov/soils/technical/classification/osd/index.html (verified 7 June 2006).

Sopper, W., and J. Richenderfer. 1978. Effects of spray irrigation of municipal wastewater on the physical properties of the soil. Institute for Research on Land and Water Resources, The Pennsylvania State University, University Park, PA.

SSSA. 2004. Soil Science Society of America Online Glossary [Online] http://www.soils.org/sssagloss/table2.html (verified 10 June 2004).

Storer, D. 1984. A simple high sample volume ashing procedure for determining soil organic matter. Communications in Soil Science and Plant Analysis 15:759-772.

Tamminga, K. 1995. Is the "Living Filter" sustainable? Assessing the land application of municipal effluent. The Environmental Professional 17:290-300.

Tarchitzky, J., A. Banin, J. Morin, and Y. Chen. 1984. Nature, formation and effects of soil crusts formed by water drop impact. Geoderma 33:135-155.

Tarchitzky, J., Y. Golobati, R. Keren, and Y. Chen. 1999. Wastewater effects on montmorillonite suspensions and hydraulic properties of sandy soils. Soil Science Society of America Journal 63:554-560.

Toze, S. 2006. Reuse of effluent water--benefits and risks. Agricultural Water Management 80:147-159.

Trautner, A., and J. Arvidsson. 2003. Subsoil compaction caused by machinery traffic on a Swedish Eutric Cambisol at different soil water contents. Soil and Tillage Research 73:107-118.

Vepraskas, M., and J. Bouma. 1976. Model experiments on mottle formations simulating field conditions. Geoderma 15:217-230.

Vinten, A., U. Mingelgrin, and B. Yaron. 1983. The effect of suspended solids in wastewater on soil hydraulic conductivity: II. Vertical distribution of suspended solids. Soil Science Society of America Journal 47:408-412.

Wallach, R., O. Ben-Arie, and E. Graber. 2005. Soil water repellency induced by long-term irrigation with treated sewage effluent. Journal of Environmental Quality 34:1910-1920.

Waltman, W.J., E.J. Ciolkosz, M.J. Mausbach, M.D. Svoboda, D.A. Miller, and P.J. Kolb. 1997. Soil Climate Regimes of Pennsylvania. Bulletin No. 873. Pennsylvania State University Agricultural Experiment Station, University Park, PA.

Wang, Z., A. Chang, L. Wu, and D. Crowley. 2003. Assessing the soil quality of long-term reclaimed wastewater-irrigated cropland. Geoderma 114:261-278.

Table 4.1. Morphological properties each horizon of the 2006 soil trenches, the trench names correspond to Figure 4.2.

Location (LS Position)	Depth	Moist Color	Sand	Silt	Clay	Texture	(---------- Grade	--------Structure--------- Size	----------) Type	MN	(--------Redox---------) Abund.	Size	Contrast	Bulk Density	Ksat	pH	OM
	(cm)		----------%----------							%	%			(gm/cm)	(cm/hr)		
Trench 1 Section 1 (Summit)																	
Ap	0-20	2.5 YR 4/3	33.8	52.7	13.5	Silt Loam	Strong	Medium/Fine	Granular	0	0			1.41	1.60	7.26	2.34
B/Ap	20-28	10 YR 5/6	24.8	48.4	26.8	Loam	Moderate	Medium	SBK	0	0			1.67	*	7.56	1.48
Bt1	28-60	10 YR 5/6	19.8	42.7	37.4	Silty Clay Loam	Moderate	Medium	SBK	0	0			1.58	0.01	7.42	1.57
Bt2	60-112	7.5 YR 5/8	18.7	31.4	49.9	Clay	Moderate	Medium	SBK	10	25	Coarse		1.77	0.01	5.29	1.47
Bt3	112-152+	5 YR 5/8	22.9	15.1	61.9	Clay	Weak	Coarse	SBK	1	< 2	Medium		*	*	5.05	1.66
Trench 1 Section 2 (Summit)																	
Ap	0-34	2.5 YR 4/4	35.6	50.2	14.2	Silt Loam	Strong	Medium/Fine	Granular	0	0			1.66	1.60	7.1	2.20
Bt1	34-52	7.5 YR 5/6	27.4	43.4	29.2	Clay Loam	Moderate	Medium	SBK	0	0			1.70	0.20	7.45	1.12
Bt2	52-80	5 YR 5/8	29.2	18.1	52.7	Clay	Moderate	Medium	SBK	2	0			1.49	1.00	6.04	1.37
Bt3	80-137	5 YR 5/6	34.6	16.5	48.9	Clay	Moderate	Medium	SBK	2	0			1.60	0.58	5.07	1.38
Bt4	137-145+	5 YR 5/8	29.7	11.0	59.4	Clay	Weak	Medium	SBK	0	0			*	*	4.95	1.49
Trench 2 Section 1 (Midslope)																	
Ap	0-20	10 YR 4/4	33.1	45.6	21.3	Loam	Strong	Medium/Fine	Granular	0	0			1.54	1.40	7.23	2.48
Bt1	20-48	10 YR 5/8	18.1	52.7	29.2	Silty Clay Loam	Moderate	Medium	SBK	15	15	Coarse		1.53	0.13	5.64	1.16
Bt2	48-117	7.5 YR 5/8	26.3	36.3	37.4	Clay Loam	Moderate	Coarse	SBK	15	0			1.67	0.40	4.79	1.48
Bt3	117-143+	10 YR 5/8	25.6	32.7	41.7	Clay	Weak	Very Coarse	SBK	2	0			*	*	4.99	1.41
Trench 2 Section 2 (Midslope)																	
Ap	0-21	10 YR 5/6	34.0	46.5	19.5	Loam	Strong	Medium/Fine	Granular	0	0			1.56	3.72	7.27	2.03
Bt1	21-58	7.5 YR 6/8	20.3	26.2	53.5	Clay	Moderate	Coarse/Medium	SBK	30	0			1.60	0.35	6.37	1.99
Bt2	58-90	7.5 YR 6/8	25.9	41.3	32.8	Clay Loam	Moderate	Medium	SBK	2	0			1.70	0.01	5.61	1.31
Bt3	90-104	10 YR 5/8	29.3	41.7	29.0	Clay Loam	Moderate	Medium	SBK	30	0			1.66	0.11	5.14	1.07
Bt4	104-136+	5 YR 5/8	11.4	15.4	73.2	Clay	Weak	Coarse	SBK	2	0			*	*	5.02	2.03
Trench 3 (Depression)																	
Ap1	0-20	2.5 Y 4/4	23.1	63.9	13.0	Silt Loam	Strong	Medium/Fine	Granular	0	0			1.39	7.88	7.4	3.72
Ap2	20-63	2.5 Y 5/4	29.8	59.2	11.0	Silt Loam	Moderate	Medium	SBK	0	0			1.29	5.78	7	2.96
ApB	63-83	2.5 Y 5/3	25.2	61.1	13.7	Silt Loam	Weak	Medium/Fine	SBK	0	0			1.55	0.03	6.86	1.22
Bt1b	83-106	10 YR 5/4	10.2	53.3	36.5	Silty Clay Loam	Moderate	Medium/Fine	SBK	0	0			*	*	6.77	1.12
Bt2b	106-138+	10 YR 5/4	8.3	48.8	43.0	Silty Clay	Moderate	Medium/Fine	SBK	0	30	Coarse		*	*	6.75	1.22
Trench 4 (Summit)																	
Ap	0-20	10 YR 4/4	34.2	45.3	20.5	Loam	Strong	Medium/Fine	SBK	0	0			1.53	0.88	7.11	1.93
Bt1	20-66	5 YR 5/8	24.0	31.5	44.5	Clay	Moderate	Medium	SBK	< 2	0			1.63	0.18	6.48	1.69
Bt2	66-113	7.5 YR 5/6	17.5	37.6	44.9	Clay	Moderate	Coarse/Medium	SBK	15	0			1.59	0.54	6.13	1.69
Bt3	113-140+	7.5 YR 5/6	37.0	27.2	35.8	Clay Loam	Weak	Coarse	SBK	15	0			*	*	5.29	1.17
Trench 5 (Midslope)																	
Ap	0-34	10 YR 4/3	38.2	53.1	8.7	Silt Loam	Strong/Moderate	Fine/Medium	Granular/SBK	0	0			1.52	4.40	6.64	2.20
BE	34-67	10 YR 5/4	12.4	58.3	29.3	Silty Clay Loam	Moderate	Medium/Coarse	SBK	0	0			1.46	3.56	6.7	1.16
Bt1	67-105	7.5 YR 5/6	10.9	48.7	40.4	Silty Clay	Moderate	Coarse	SBK	15	< 2	Coarse		1.34	2.12	6.34	1.44
Bt2	105-144+	5 YR 5/6	20.9	30.4	48.7	Clay	Moderate	Coarse	SBK	25	15	Coarse		*	*	5.47	1.57
Trench 6 (Depression)																	
Ap	0-36	10 YR 3/3	25.5	59.7	14.8	Silt Loam	Strong	Medium/Fine	Granular	0	0			1.27	3.00	6.86	2.45
BE	36-44	10 YR 4/6	24.7	53.1	22.2	Silt Loam	Moderate	Coarse/Medium	SBK	0	0			1.50	0.03	6.98	1.09
Bt1	44-66	7.5 YR 5/6	22.4	47.1	30.5	Clay Loam	Moderate	Coarse/Medium	SBK	< 2	0			1.62	0.52	7.05	*
Bt2	66-105	7.5 YR 5/6	24.6	28.6	46.8	Clay	Moderate	Medium/Fine	SBK	25	0			1.51	0.23	6.86	1.40
Bt3	105-146+	10 YR 5/8	24.3	29.6	46.1	Clay	Moderate/Weak	M/C and M/Thin	SBK/Platy	25	< 2	Fine		*	*	5.03	1.67

Table 4.2. Quantitative scale developed by Simpson and Cunningham (1978) to determine the soil's ability to handle irrigation. Soil morphologic properties usually associated with wetter soil conditions receive lower values, whereas soil properties that are associated with drier conditions receive higher values. (Source Simpson and Cunningham, 1978).

Morphologic Property	Value
Structure (average for subsoil horizons)	
Grade	
Weak	6
Moderate	12
Strong	18
Size	
Coarse	6
Medium	12
Fine	18
Type	
prismatic	0
platy	4
subangular blocky	10
angular blocky	10
Color of B (average for subsoil horizons)	
Hue	
2.5 Y	0
5 Y	0
10 YR	2
7.5 YR	4
5 YR	6
2.5 YR	8
Chroma	
0, 1, 2	0
3, 4	4
5, 6, 8	10
Value	
2,3	4
4,5	10
6,7	3

Morphologic Property	Value
Mottles	
(based on mottled horizons only)	
Depth	
(maximum 50)	(depth from surface)/3
Abundance	
no mottling	32
few	20
common	8
many	0
Size	
no mottling	32
fine	20
medium	8
coarse	0
Contrast	
no mottling	32
faint	20
distinct	8
prominent	0
Manganese Coatings	
(based on horizon with highest % of ped face coatings)	(100-% Mn Coatings/2)
Consistence	
(moist consistence of subsurface horizons)	
friable	6
firm	2
very firm	0

Table 4.3. Side by side comparison of the 1978 morphological properties of soils described by Simpson and Cunningham (1978) and the 2006 morphological properties of soils from the soil trenches. The pit locations follow the map in figure 4.4.

Loc.	Depth	Moist Color	Texture	(---------Structure---------) Grade	Size	Type	MN	Redox
	(cm)						%	
1978 Control Area								
C3								
Ap	0-25	10 YR 4/3	silt loam	weak	fine/medium	granular	0	
A1	25-35	10 YR 4/3	silt loam	weak	fine/medium	sbk/granular	0	
B1t	35-65	10 YR 5/6	light silty clay loam	weak	fine/medium	sbk	<1	
B2t	65-110	10 YR 5/6	light silty clay loam	weak/mod	fine/medium	platy/sbk	5-10	many
B2t	110-180	10 YR 5/6	heavy silty clay loam	weak	fine/medium	sbk	5	
C4								
Ap	0-20	10 YR 4/3	silt loam	weak	fine/medium	granular	0	
A1	20-30	10 YR 4/3	silt loam	weak	fine/medium	sbk/granular	0	
B1	30-40	7.5 YR 5/6	silty clay loam	weak/mod	fine/medium	sbk	3	
B2t	40-50	10 YR 5/8	clay	weak	fine/medium	sbk	7	
B2t	50-65	10YR 5/6	clay	weak/mod	fine/medium	platy/sbk	12	
B3	65-140+	5 YR 5/6	clay	weak	fine/medium	platy/sbk	0	
1978 Irrigated Area								
C1								
Ap	0-36	10YR 4/3	silt loam	weak/moderate	fine/medium	granular	0	
B2t	36-84	10YR 5/6	heavy silt loam	weak	fine/medium	platy/sbk	<2	common
Bx	84-132	7.5 YR 5/4	heavy silt loam	weak	fine/medium	prismatic/platy	5	common
(II)B2t	132-144+	5YR 5/6	clay	weak	fine/medium	sbk	<3	
C2								
Ap	0-30	10 YR 3/2	silt loam	mod/weak	fine/medium	granular	0	
B2t	30-65	7.5YR 5/6	clay	moderate	fine/medium	sbk	4	few
B2t	65-100	10 YR 5/6	clay	weak/mod	med/coarse	platy/sbk	40-50	few
B3t	100-180+	10YR 5/6	silty clay to clay	weak	med	sbk	0	
C5								
Ap	0-14	10YR 4/3	silt loam	weak	fine/medium	granular		
A1	14-24	10 YR 4/3	silt loam	weak	med/coarse	sbk/granular		
A2	24-44	10 YR 4/3	heavy silt loam	weak	medium	sbk		
B1t	44-60	7.5 YR 5/6	heavy silty clay loam	weak/mod	fine/medium	sbk	<2	
B2t	60-96	5YR 5/6	clay	mod/strong	fine/medium	sbk	20-30	
B2t	96-130+	5YR 5/6	clay	weak/mod	fine/medium	sbk	<1	
C6								
Ap	0-20	10YR 4/3	silt loam	weak	fine/medium	granular/platy		
A1	20-32	10YR 4/3	silt loam	weak	fine/medium	granular		
B1	32-60	10YR 6/4	heavy silt loam	weak	fine/medium	sbk		
B2t	60-84	10YR 5/6	heavy silty clay	weak/mod	fine/medium	sbk	1	
B2t	84-156+	5YR 5/6	clay	moderate	fine/medium	platy/sbk	8	common

Loc	Depth	Moist Color	Texture	(---------- Grade	-------Structure-------- Size	----------) Type	MN	Redox
	(cm)						%	%
Control Area (22 Years of Irrigation)								
Trench 1 Section 1								
Ap	0-20	2.5 YR 4/3	Silt Loam	Strong	Medium/Fine	Granular	0	0
B/Ap	20-28	10 YR 5/6	Loam	Moderate	Medium	SBK	0	0
Bt1	28-60	10 YR 5/6	Silty Clay Loam	Moderate	Medium	SBK	0	0
Bt2	60-112	7.5 YR 5/8	Clay	Moderate	Medium	SBK	10	25
Bt3	112-152+	5 YR 5/8	Clay	Weak	Coarse	SBK	1	< 2
Trench 1 Section 2								
Ap	0-34	2.5 YR 4/4	Silt Loam	Strong	Medium/Fine	Granular	0	0
Bt1	34-52	7.5 YR 5/6	Clay Loam	Moderate	Medium	SBK	0	0
Bt2	52-80	5 YR 5/8	Clay	Moderate	Medium	SBK	2	0
Bt3	80-137	5 YR 5/6	Clay	Moderate	Medium	SBK	2	0
Bt4	137-145+	5 YR 5/8	Clay	Weak	Medium	SBK	0	0
Trench 4								
Ap	0-20	10 YR 4/4	Loam	Strong	Medium/Fine	SBK	0	0
Bt1	20-66	5 YR 5/8	Clay	Moderate	Medium	SBK	< 2	0
Bt2	66-113	7.5 YR 5/6	Clay	Moderate	Coarse/Medium	SBK	15	0
Bt3	113-140+	7.5 YR 5/6	Clay Loam	Weak	Coarse	SBK	15	0
rrigated Area (40+ Years of Irrigation)								
Trench 2 Section 2								
Ap	0-21	10 YR 5/6	Loam	Strong	Medium/Fine	Granular	0	0
Bt1	21-58	7.5 YR 6/8	Clay	Moderate	Coarse/Medium	SBK	30	0
Bt2	58-90	7.5 YR 6/8	Clay Loam	Moderate	Medium	SBK	2	0
Bt3	90-104	10 YR 5/8	Clay Loam	Moderate	Medium	SBK	30	0
Bt4	104-136+	5 YR 5/8	Clay	Weak	Coarse	SBK	2	0
Trench 3								
Ap1	0-20	2.5 Y 4/4	Silt Loam	Strong	Medium/Fine	Granular	0	0
Ap2	20-63	2.5 Y 5/4	Silt Loam	Moderate	Medium	SBK	0	0
ApB	63-83	2.5 Y 5/3	Silt Loam	Weak	Medium/Fine	SBK	0	0
Bt1b	83-106	10 YR 5/4	Silty Clay Loam	Moderate	Medium/Fine	SBK	0	0
Bt2b	106-138+	10 YR 5/4	Silty Clay	Moderate	Medium/Fine	SBK	0	30
Trench 4								
Ap	0-20	10 YR 4/4	Loam	Strong	Medium/Fine	SBK	0	0
Bt1	20-66	5 YR 5/8	Clay	Moderate	Medium	SBK	< 2	0
Bt2	66-113	7.5 YR 5/6	Clay	Moderate	Coarse/Medium	SBK	15	0
Bt3	113-140+	7.5 YR 5/6	Clay Loam	Weak	Coarse	SBK	15	0
Trench 5								
Ap	0-34	10 YR 4/3	Silt Loam	Strong/Moderate	Fine/Medium	Granular/SBK	0	0
BE	34-67	10 YR 5/4	Silty Clay Loam	Moderate	Medium/Coarse	SBK	0	0
Bt1	67-105	7.5 YR 5/6	Silty Clay	Moderate	Coarse	SBK	15	< 2
Bt2	105-144+	5 YR 5/6	Clay	Moderate	Coarse	SBK	25	15
Trench 6								
Ap	0-36	10 YR 3/3	Silt Loam	Strong	Medium/Fine	Granular	0	0
BE	36-44	10 YR 4/6	Silt Loam	Moderate	Coarse/Medium	SBK	0	0
Bt1	44-66	7.5 YR 5/6	Clay Loam	Moderate	Coarse/Medium	SBK	< 2	0
Bt2	66-105	7.5 YR 5/6	Clay	Moderate	Medium/Fine	SBK	25	0
Bt3	105-146+	10 YR 5/8	Clay	Moderate/Weak	M/C and M/Thin	SBK/Platy	25	< 2

Table 4.4. Tensions used to determine soil hydraulic properties using tension infiltrometer. The pore size classification was adopted from the SSSA online glossary (SSSA, 2004).

Tension (h) (mm water)	Maximum effective Pore Size Radius (mm)	Pore Size Classification	Approximate measurement time with tension infiltrometer (min)
120	0.125	very fine macropore	60
60	0.25	very fine macropore	60
30	0.5	fine macropore	30
20	0.75	fine macropore	30
10	1.5	medium macropore	15
0	∞	all pores	15

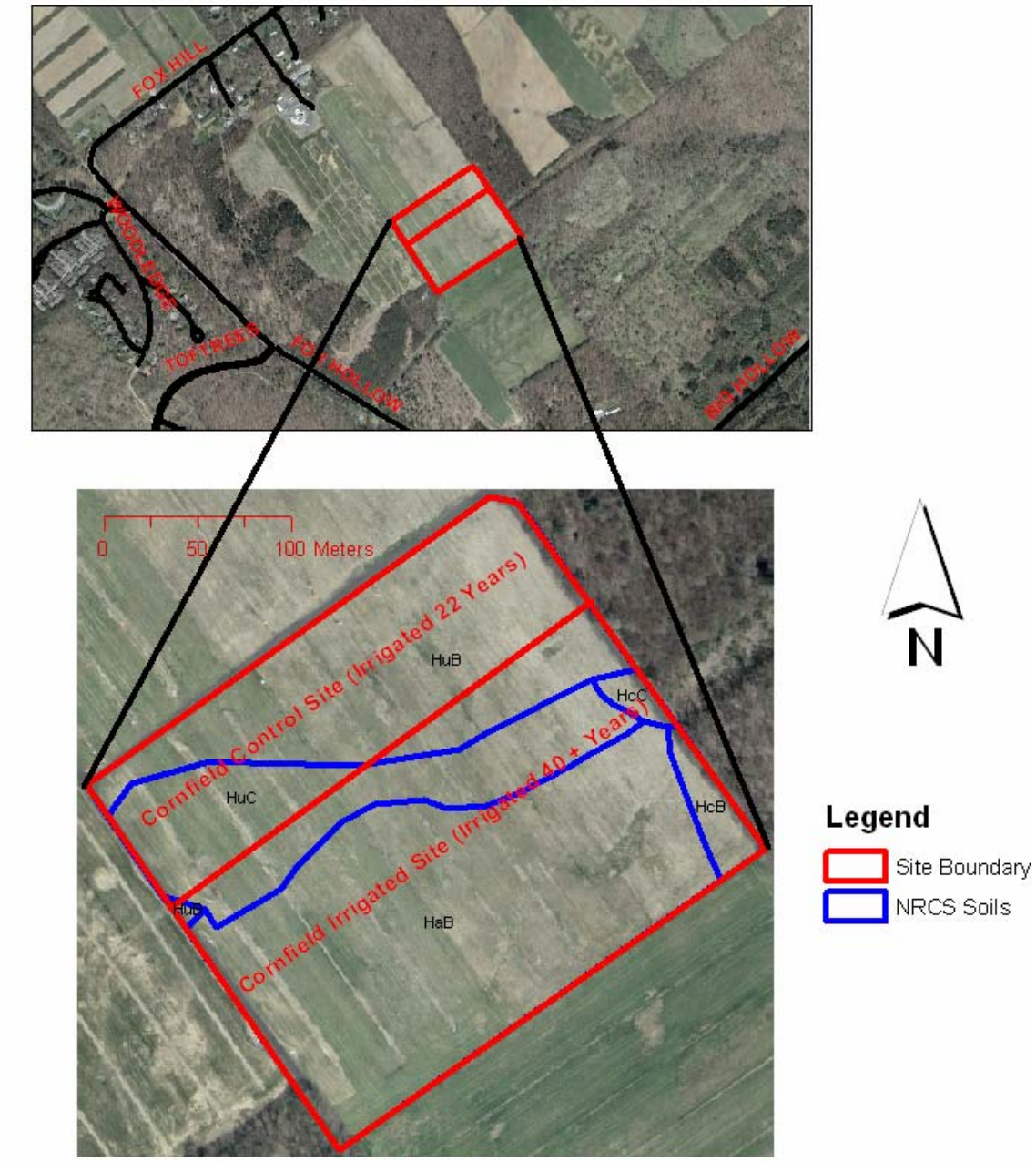

Fig. 4.1. Map of the original control and treatment areas at the Pennsylvania State University's Spray Irrigation, Astronomy Site. The cornfield control site has now been irrigated for 22 years, whereas, the cornfield irrigated site has been irrigated for over 40 years. The soils information is from the 2nd order NRCS soil survey. There are two phases of Hagerstown soils mapped, Hagerstown Silt Loam (Ha) and Hagerstown Silty Clay Loam (Hc). The Hublersburg soil series is also mapped (Hu). The letters B and C represent slope classes of 3-8% and 8-15%, respectively.

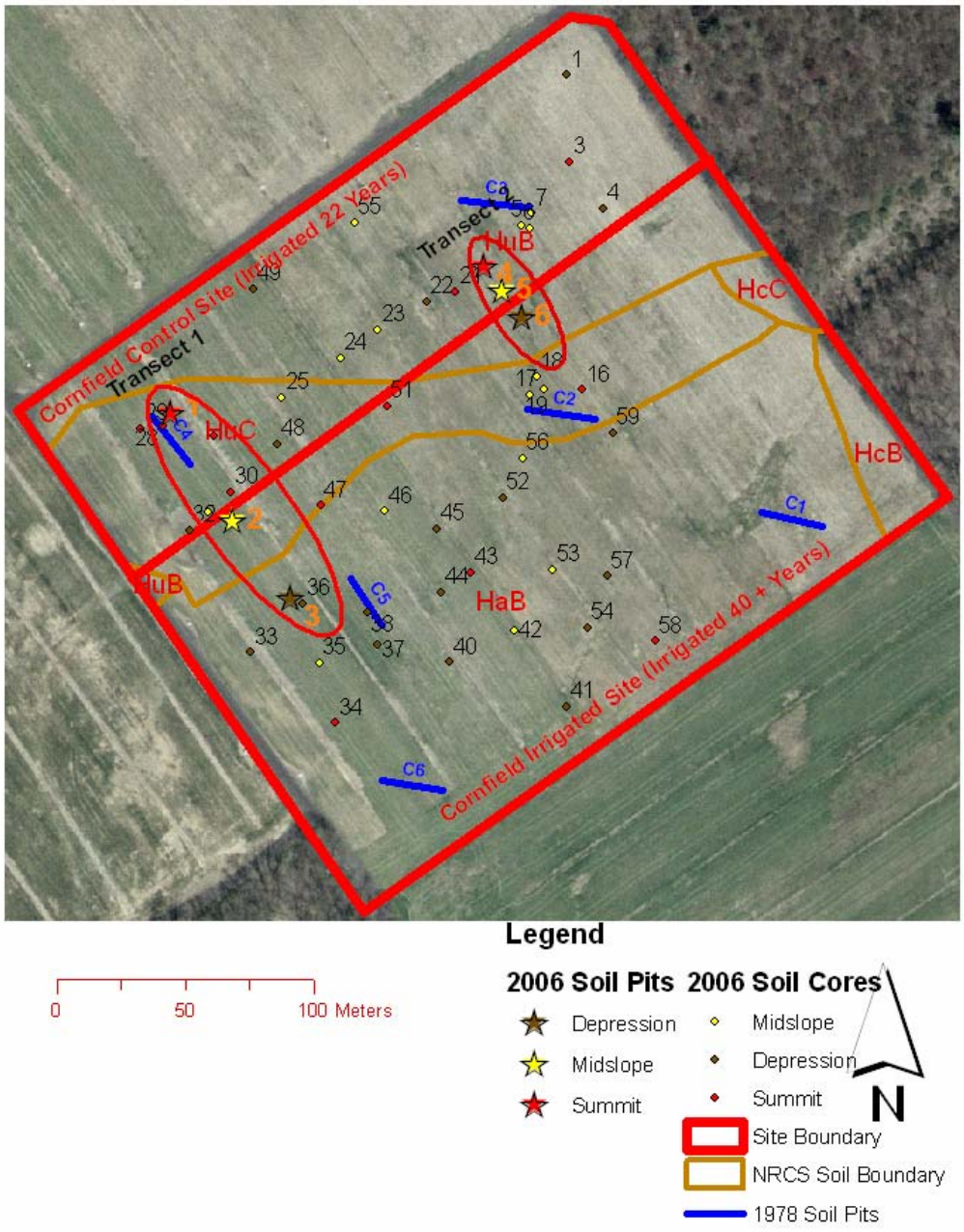

Fig. 4.2. Sampling Scheme used to determine the soil properties of the area. All sample site locations were based on landscape positions (summit, midslope, and depression) The 2006 soil trenches were located in close proximity to the original soil trenches described by Simpson and Cunningham (1978). There were 47 soil cores also described.

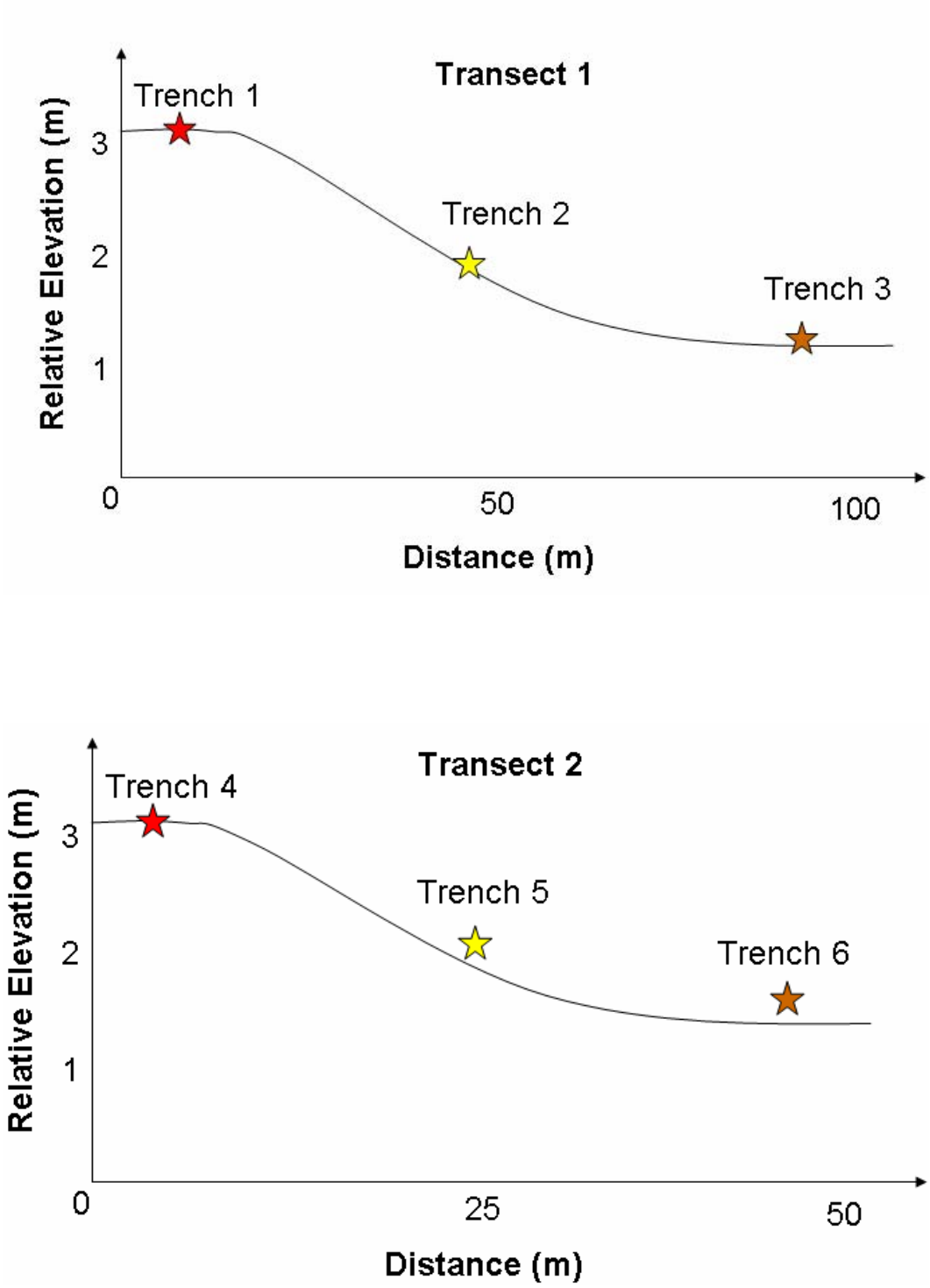

Fig. 4.3 Relative elevation change for the two soil trench transects.

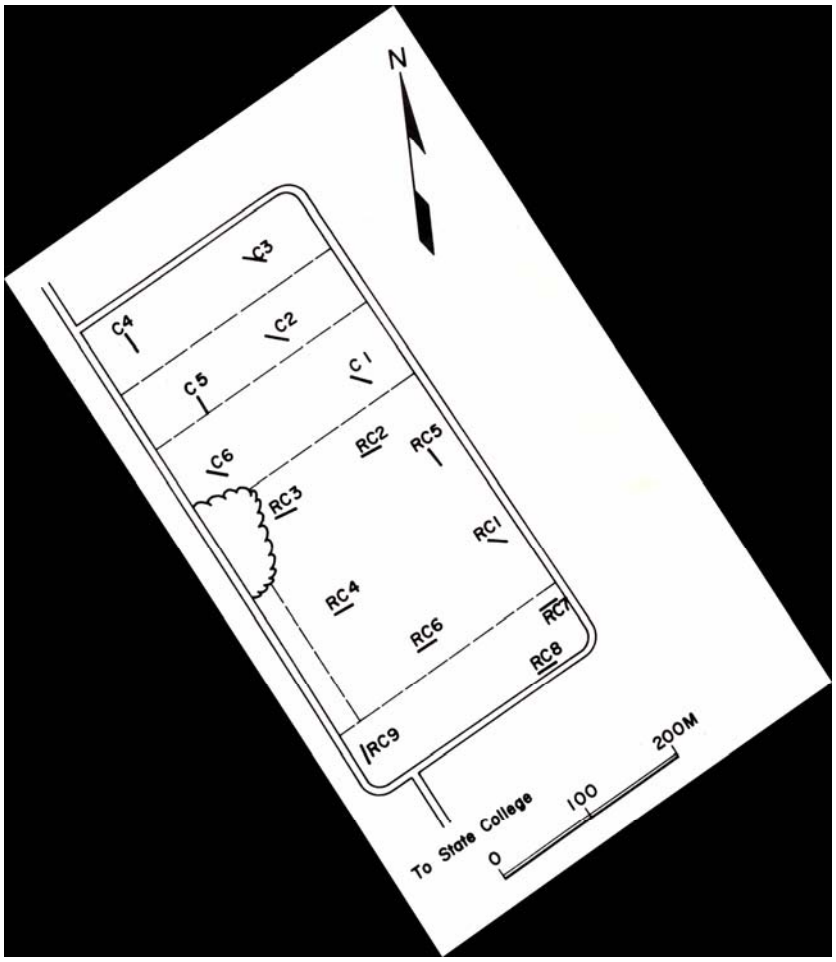

Fig. 4.4. Map of original soil pit locations provided by Simpson and Cunningham (1978). This map was scanned and georeferenced to provide general pit locations and field boundaries for this study. The letter "C" stands for cornfield site and the letters "RC" stand for reed canary grass site. This study uses the cornfield site area, displayed in Figures 4.1 and 4.2.

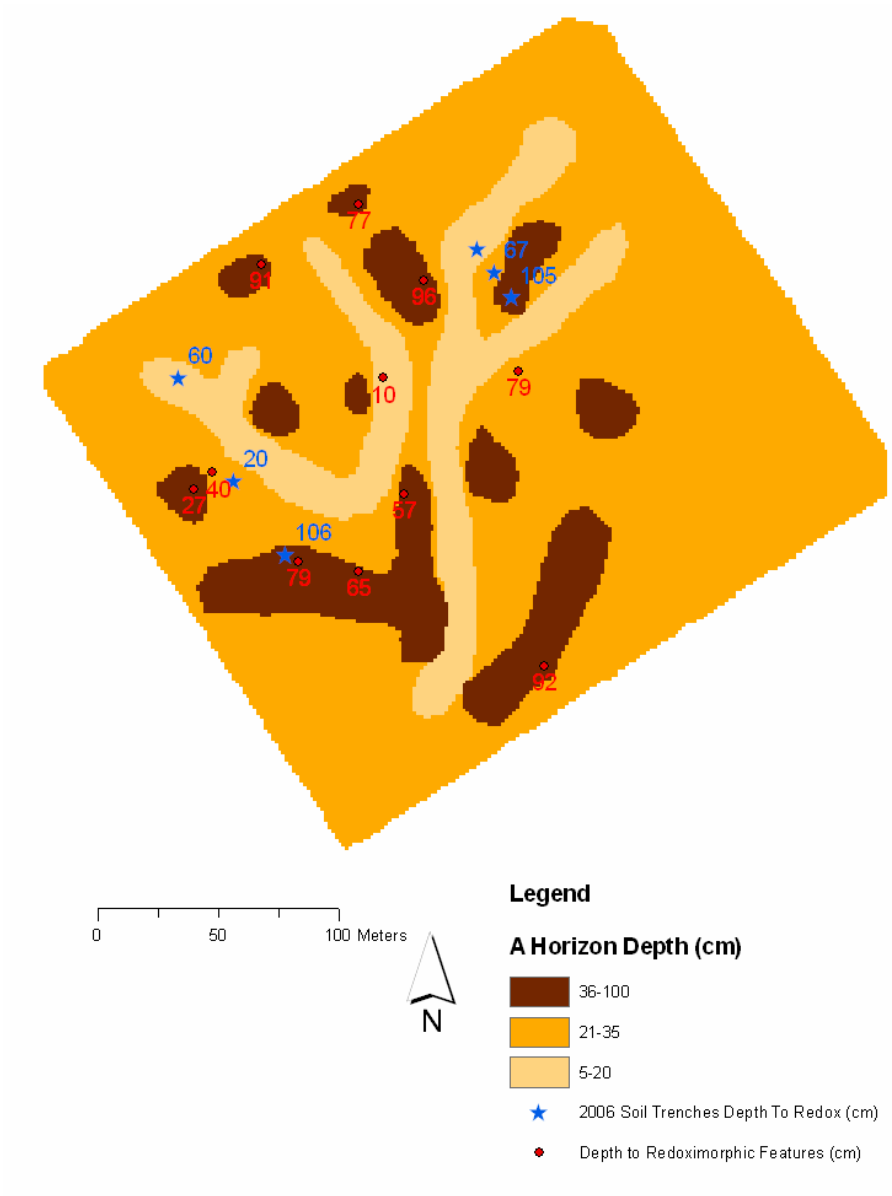

Fig. 4.5. Interpolated depth of A-horizon map combined with sites experiencing redoximorphic features. The red circles indicate sites where redoximorphic features were found within the top 1.1 meter, the labels represent the depth in which redox was determined. This map was made using the cokriging method in ArcView 9.1 (Redlands California), with an A-depth sample size of 53 points within the study site and depression locations.

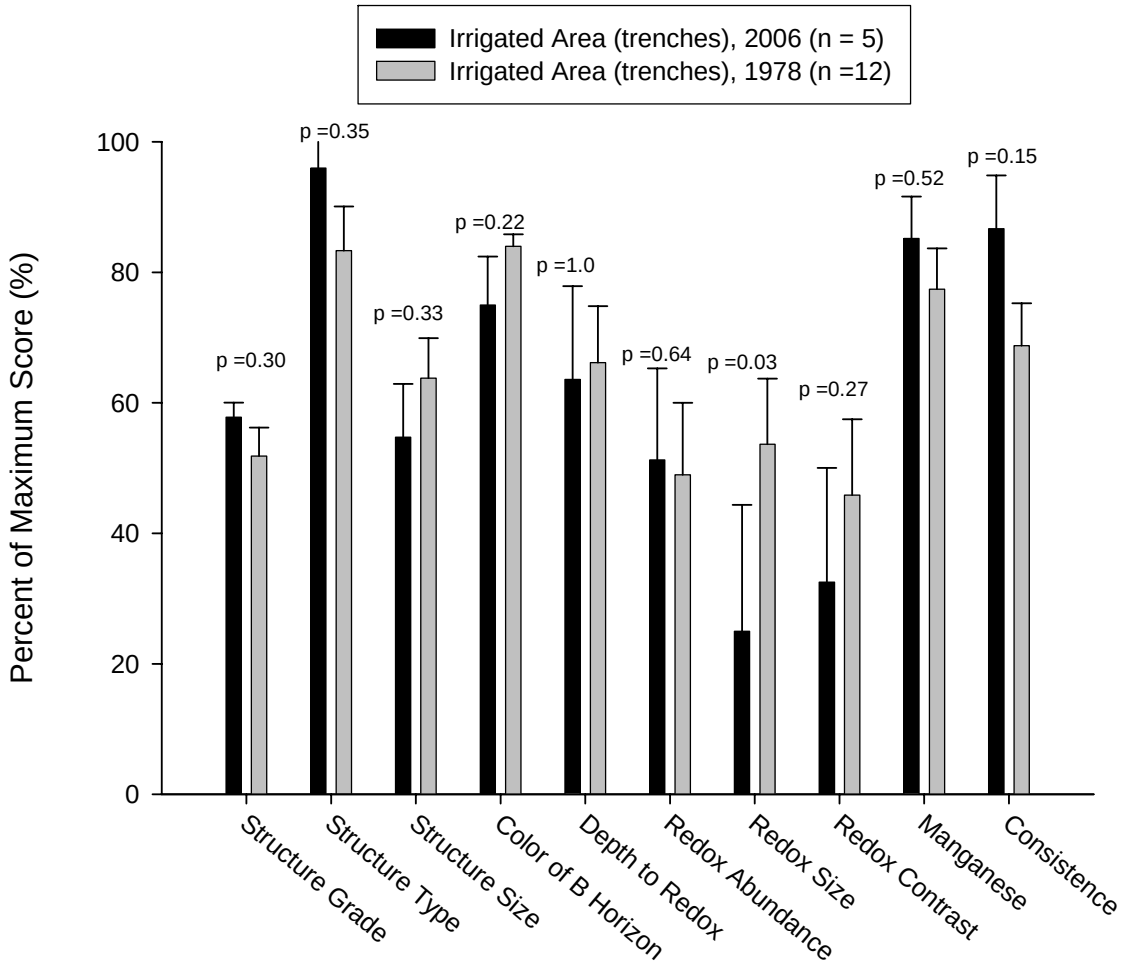

Fig. 4.6. Percent maximum score of morphological features described in the area that has received irrigation for 40 years. The score was based on Simpson and Cunningham's (1978) morphological rating scale. High scores indicate a better capability for transmitting the irrigation water. For example, a score of 100 would mean there were no redoximorphic features present in the redoximorphic feature category. Error bars represent standard error of the mean.

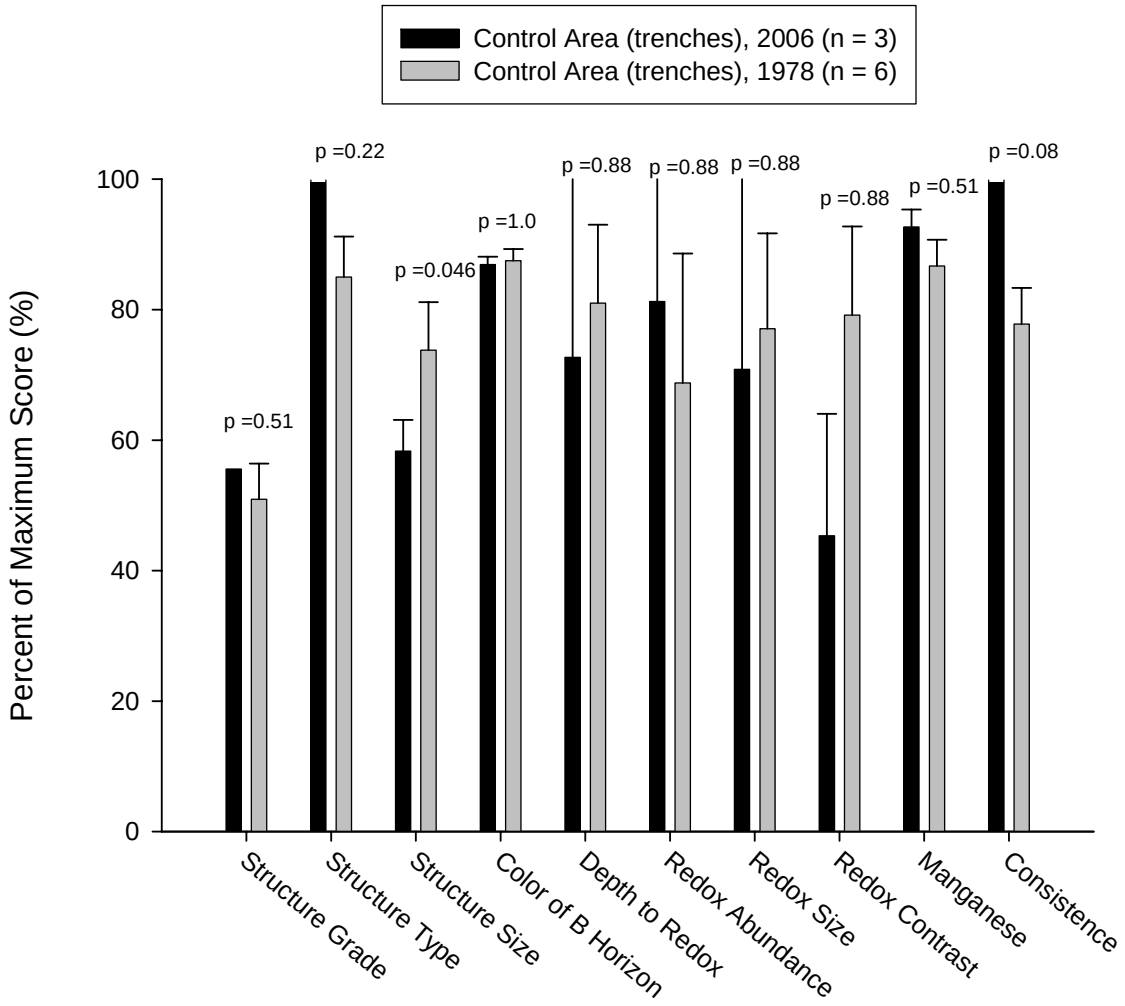

Fig.4.7. Percent maximum score of morphological features described in the area that has received irrigation for 22 years. The score was based on Simpson and Cunningham's (1978) morphological rating scale. High scores indicate a better capability for transmitting the irrigation water. For example, a score of 100 would mean there were no redoximorphic features present in the redoximorphic feature category. Error bars represent standard error of the mean.

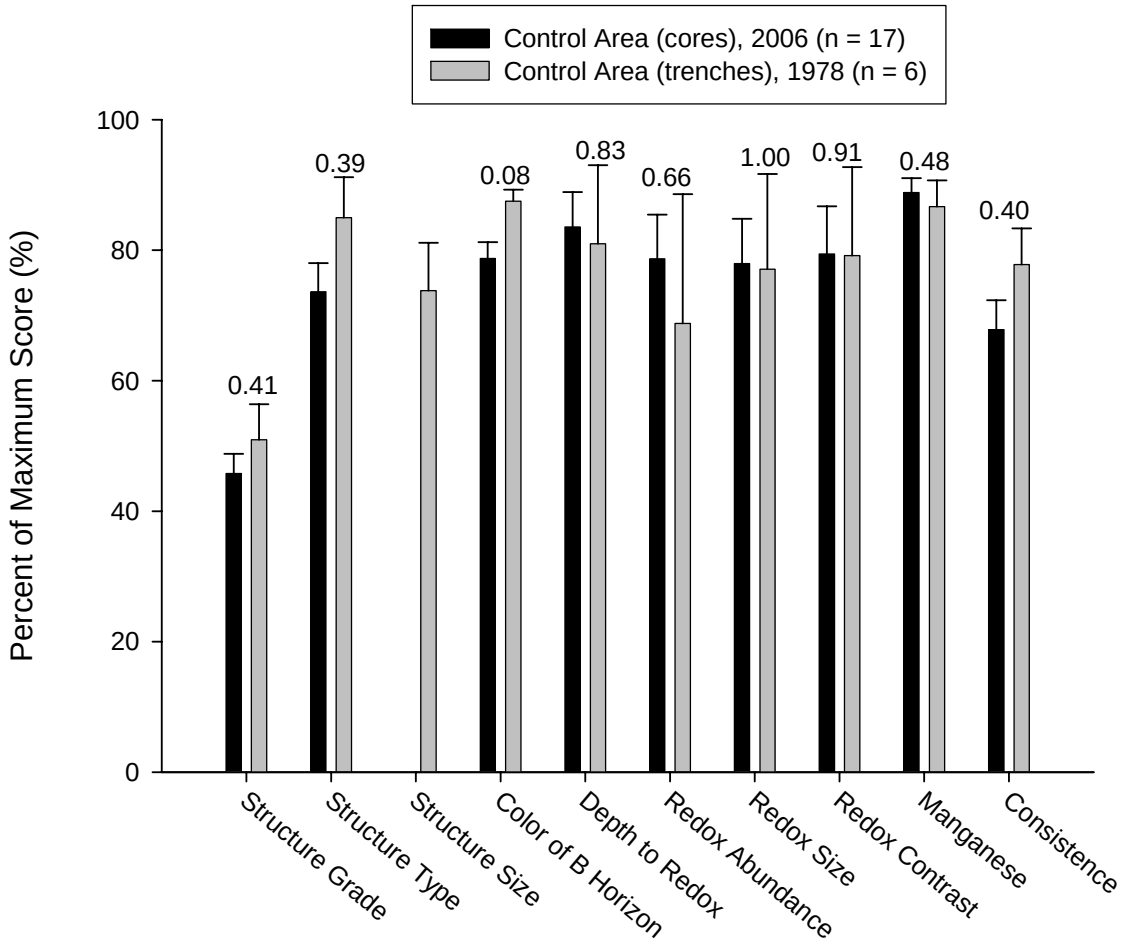

Fig. 4.8 Comparison of 2006 soil trench data and 2006 soil core observations in the area that has received irrigation for 22 years. The score was based on Simpson and Cunningham's (1978) morphological rating scale. High scores indicate a better capability for transmitting the irrigation water. For example, a score of 100 would mean there were no redoximorphic features present in the redoximorphic feature category. Error bars represent standard error of the mean.

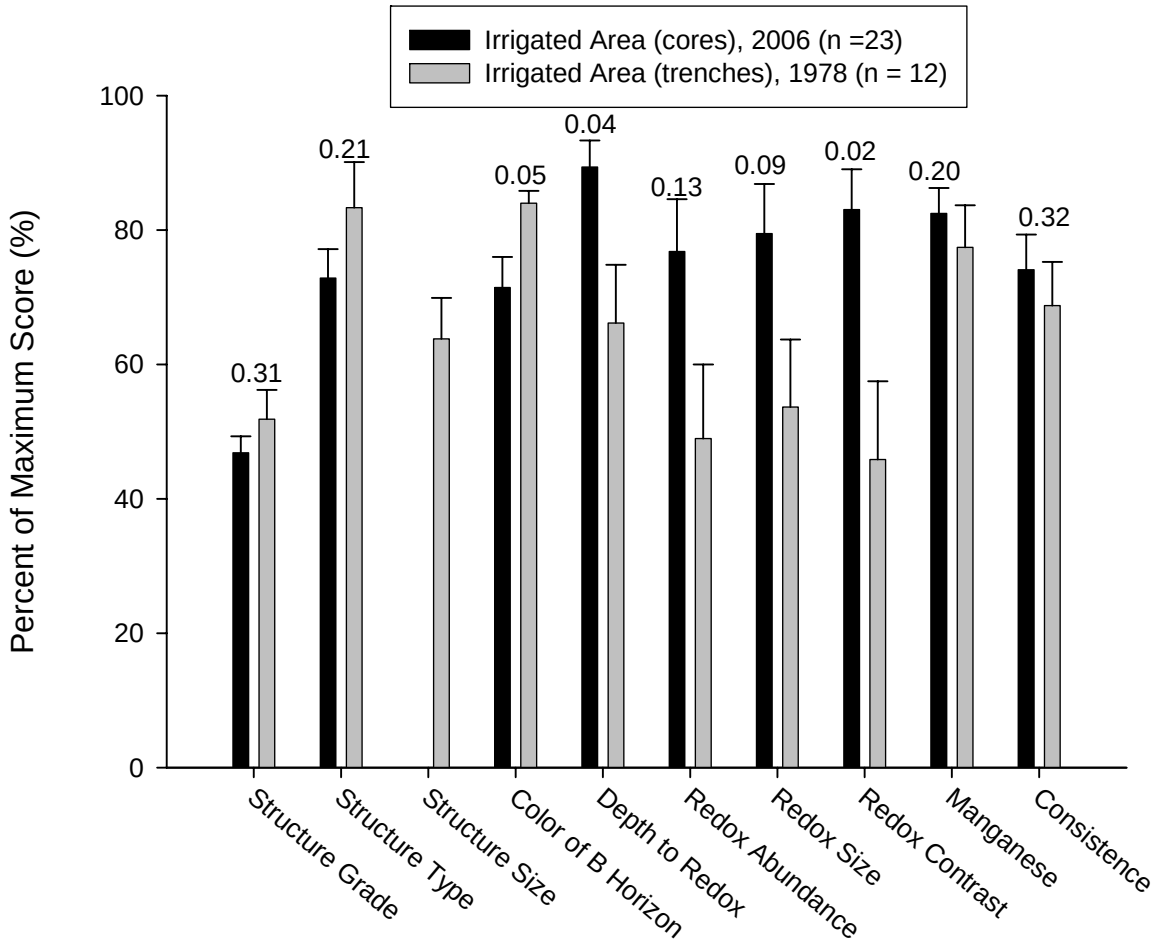

Fig 4.9 Percent maximum score of morphological features described in the area that has received irrigation for 40+ years. The 2006 data is based on soil cores described. The 1978 is based on soil trench descriptions. The score was based on Simpson and Cunningham's (1978) morphological rating scale. High scores indicate a better capability for transmitting the irrigation water. For example, a score of 100 would mean there were no redoximorphic features present in the redoximorphic feature category. Error bars represent standard error of the mean.

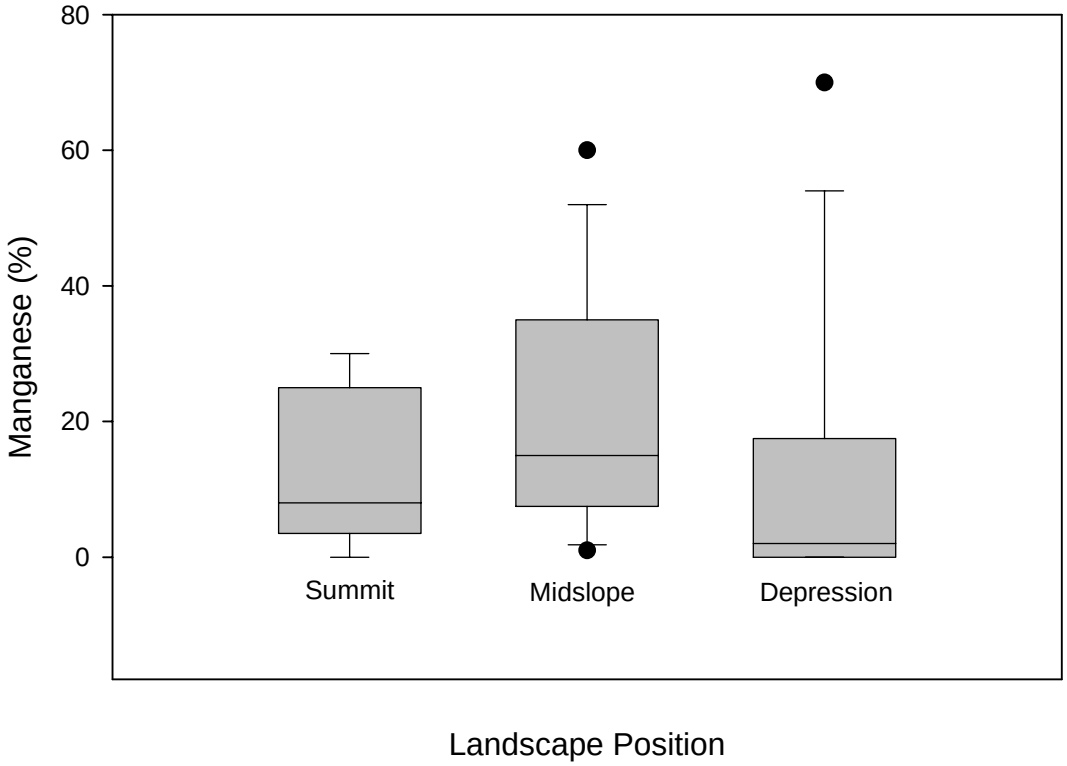

Fig. 4.10. Maximum profile manganese coating percentages (maximum percentage found in the B-horizon) based on landscape position (n = 47). The error bars represent the 10th and 90th percentile data. The box represents the median and 25th through the 75th percentile data. The dots represent data below the 10th percentile and above the 90th percentile.

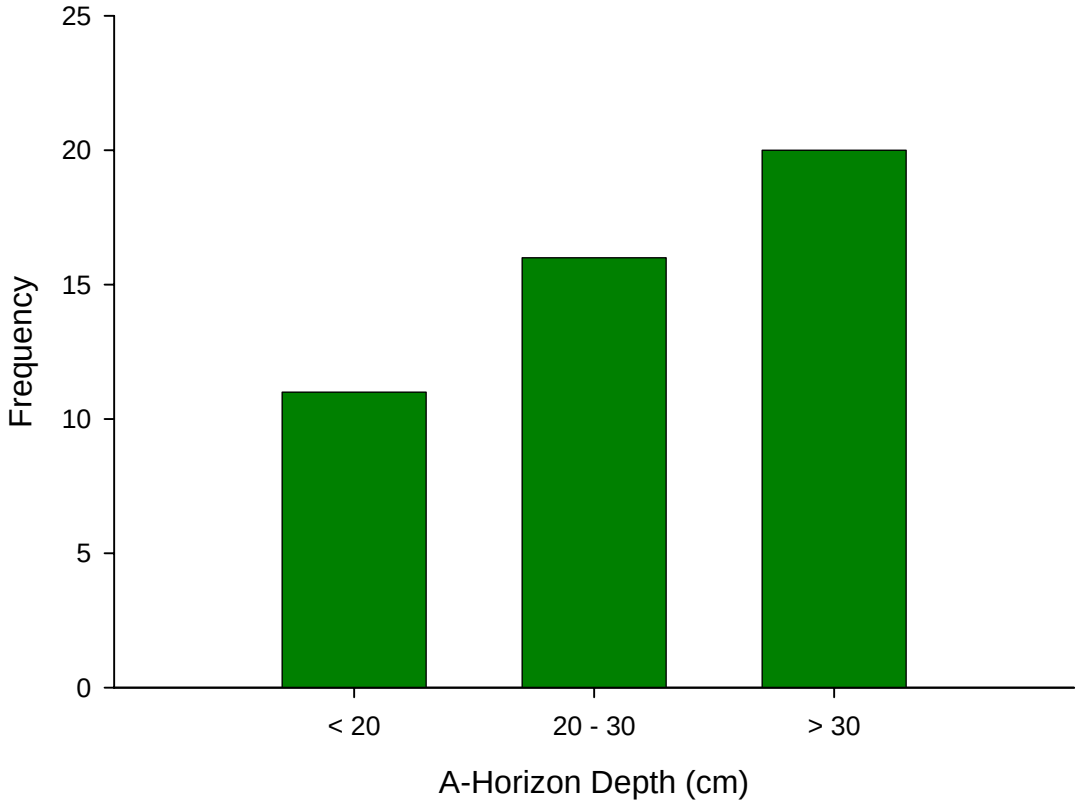

Fig. 4.11. Histogram of A-horizon depths from the 47 core samples. The 20 – 30 cm A-horizon depth designation is the common depth range for an agricultural Hagerstown soil.

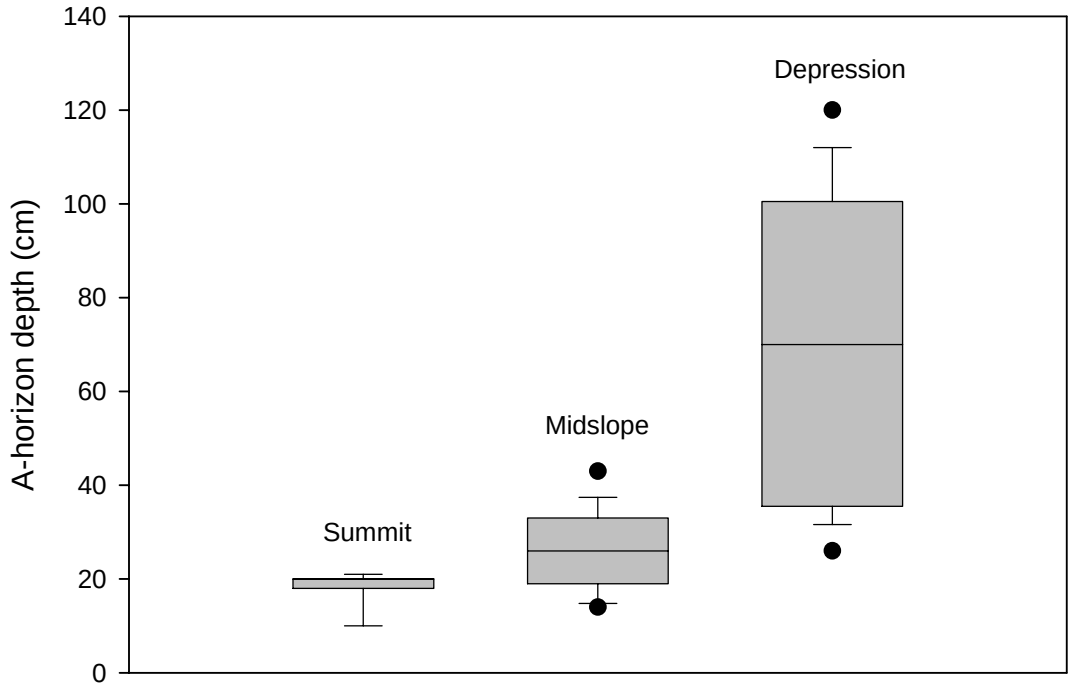

Fig. 4.12. A-horizon depths based on landscape position (n = 47). The error bars represent the 10th and 90th percentile data. The box represents the median and 25th through the 75th percentile data. The dots represent data below the 10th percentile and above the 90th percentile.

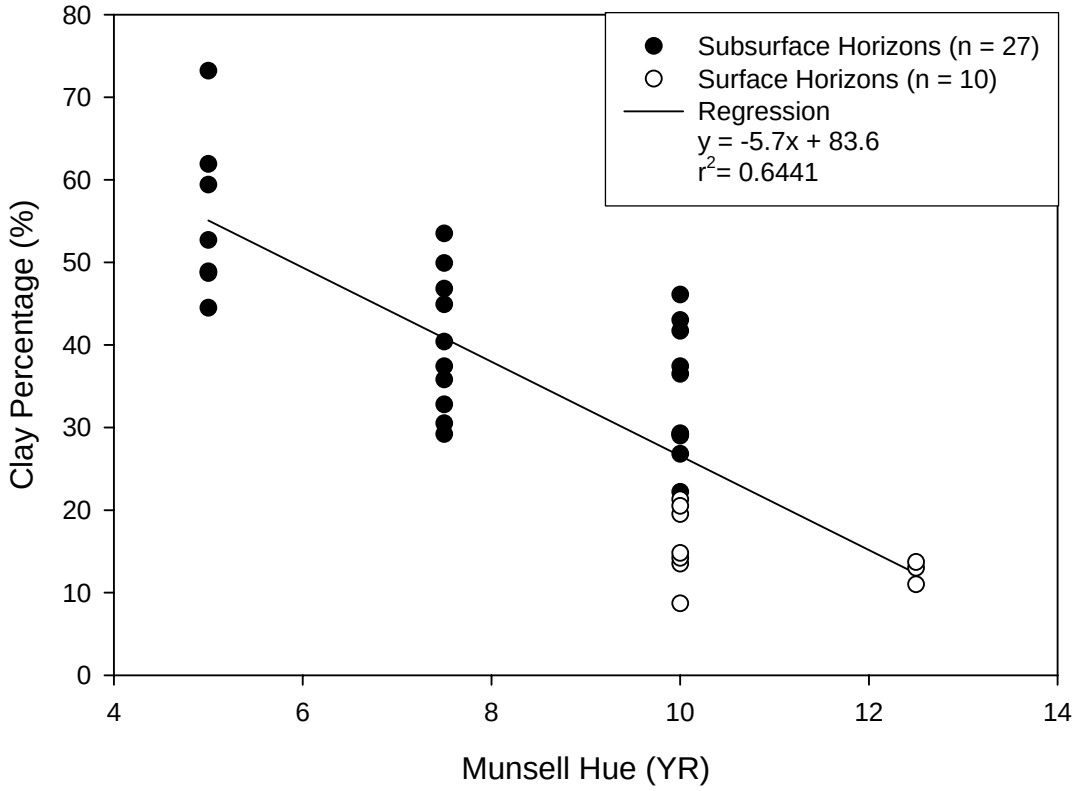

Fig. 4.13. Regression of the clay percentage in the soil trench samples, versus their Munsell Hue designation (n = 37). The 12.5 YR designation is actually 2.5 Y on the Munsell scale.

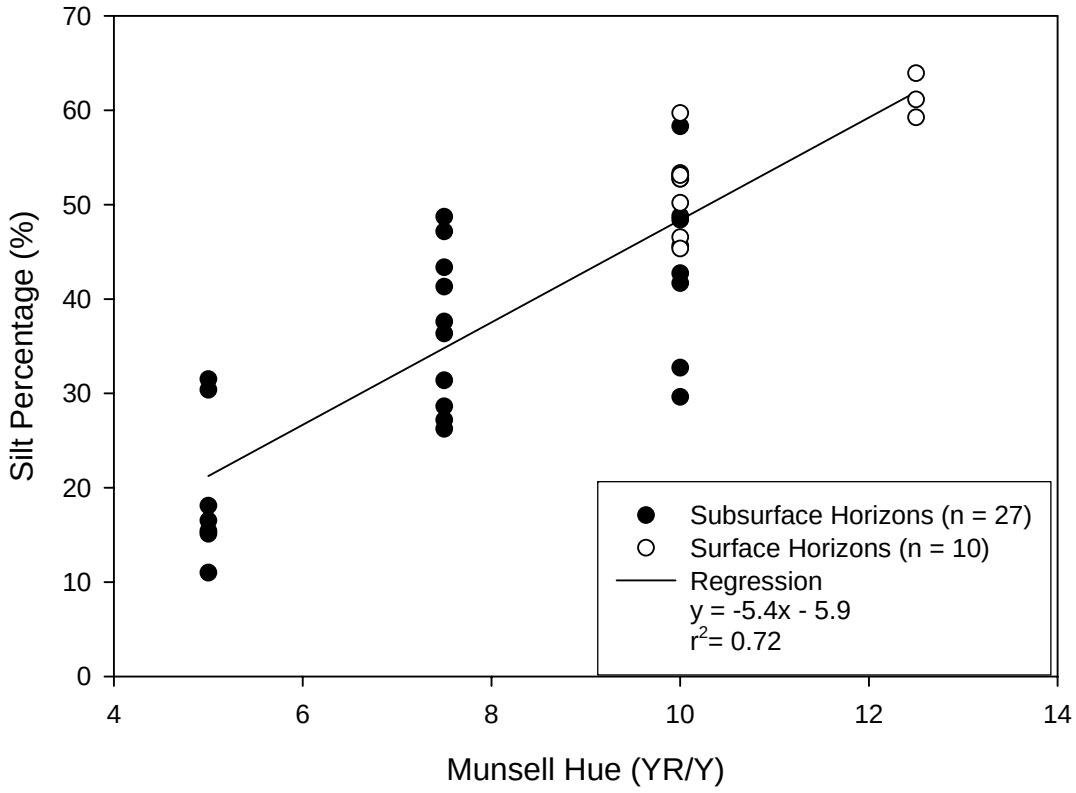

Fig. 4.14. Regression of the silt percentage in the soil trench samples, versus their Munsell Hue designation (N = 37). The 12.5 YR designation is actually 2.5 Y on the Munsell scale.

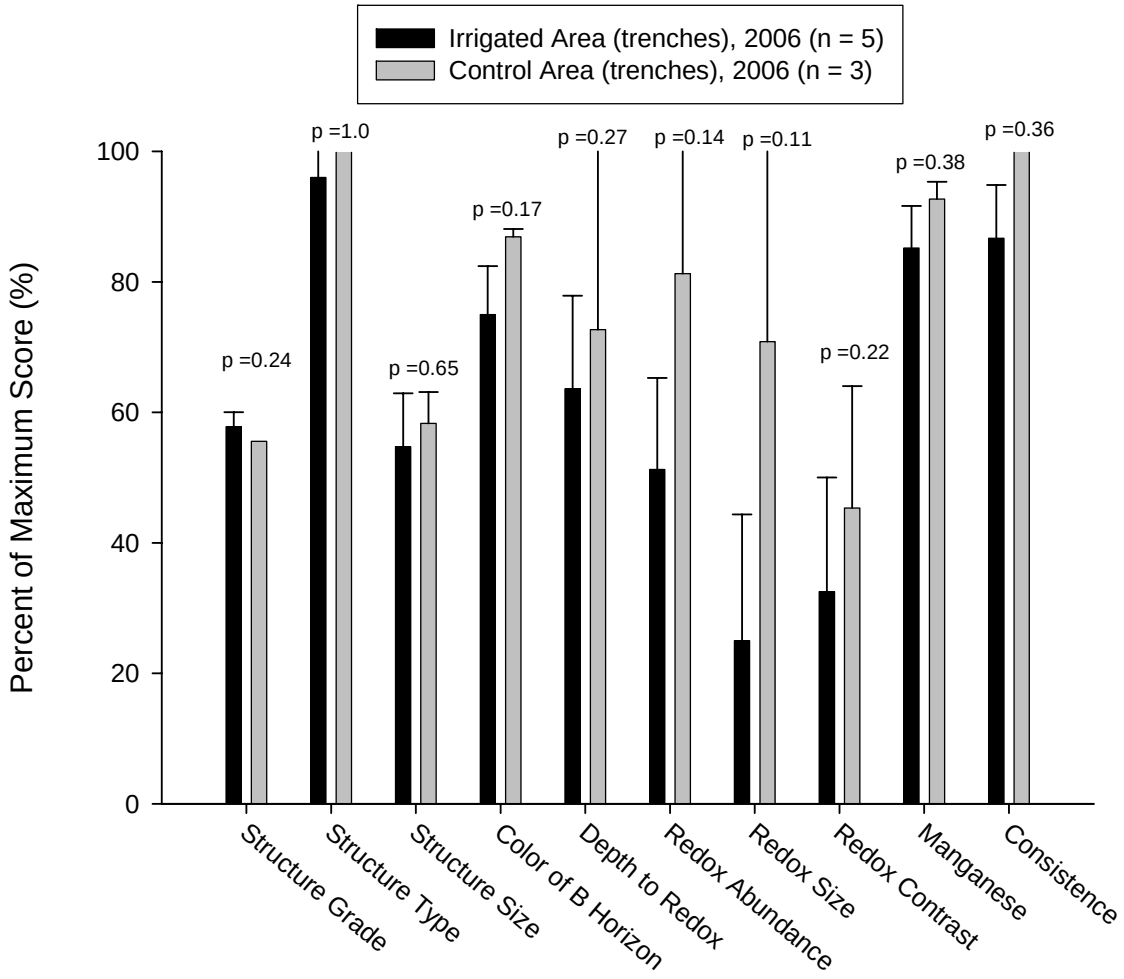

Fig. 4.15. 2006 trench descriptions for the irrigated area (40 + years of irrigation) and the control area (22 Years of irrigation). The percent maximum score was based on Simpson and Cunningham's (1978) morphological rating scale. High scores indicate a better capability for transmitting the irrigation water. For example, a score of 100 would mean there were no redoximorphic features present in the redoximorphic feature category. Error bars represent standard error of the mean.

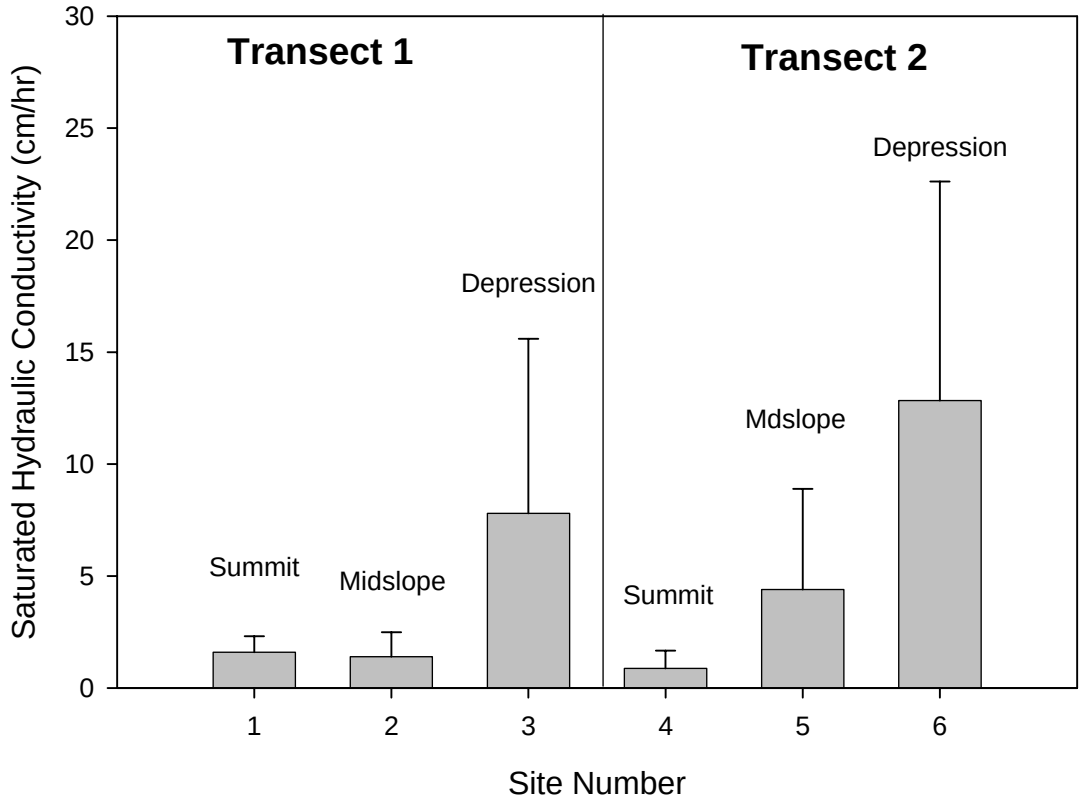

Fig. 4.16. Surface saturated hydraulic conductivity for the six trenches at the irrigation site, measured using the new constant head laboratory method as described in chapter 3. Each bar is the average of triplicate measurements for the surface horizon. Error bars represent standard error of the mean.

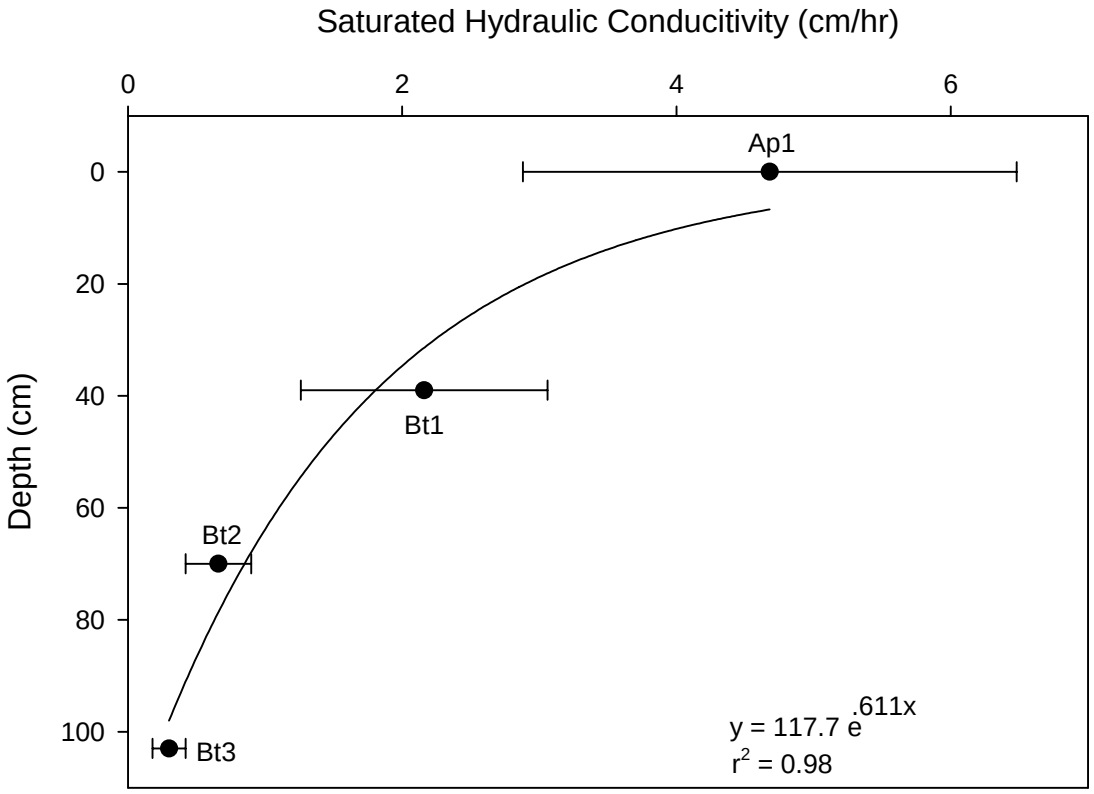

Fig. 4.17. Mean saturated hydraulic conductivity values for all six trenches at the irrigation site as a function of soil horizon using the new laboratory saturated hydraulic conductivity method described in chapter 3. Error bars represent standard error of the mean.

6 cm tension

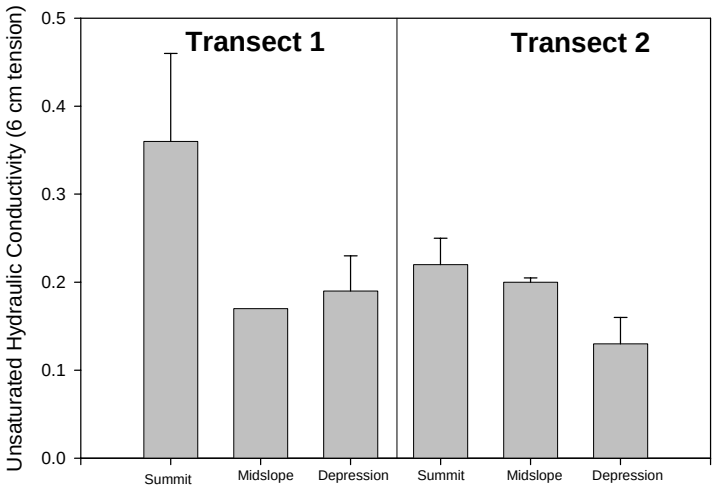

0 cm tension

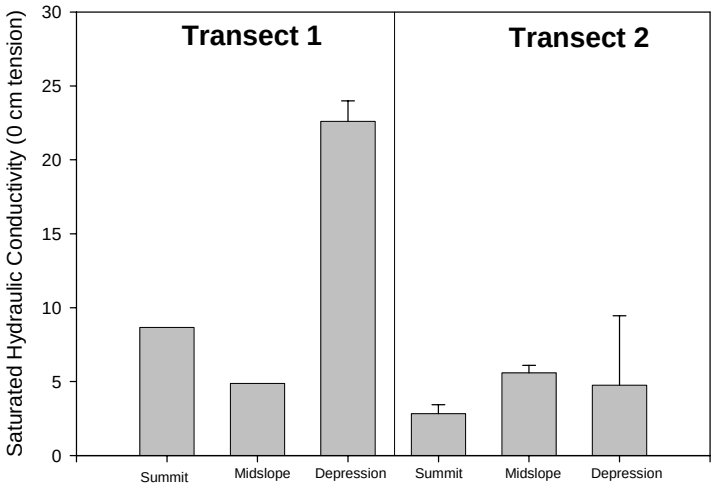

Fig. 4.18. Results from the tension infiltrometer measurements conducted at each trench in the irrigation area. The water potential is the tension that the infiltrometers were set in order to determine the contribution of different pore sizes to the conductivity values. The error bars represent standard error of the mean for the three replicates performed. Initial volumetric water contents for transect 1, were 22.7%, 22.3%, and 31.2% for the summit, midslope and depression respectively. Initial volumetric water contents for transect 2 were 30.6%, 30.3%, and 33.8% for the summit, midslope and depression, respectively.

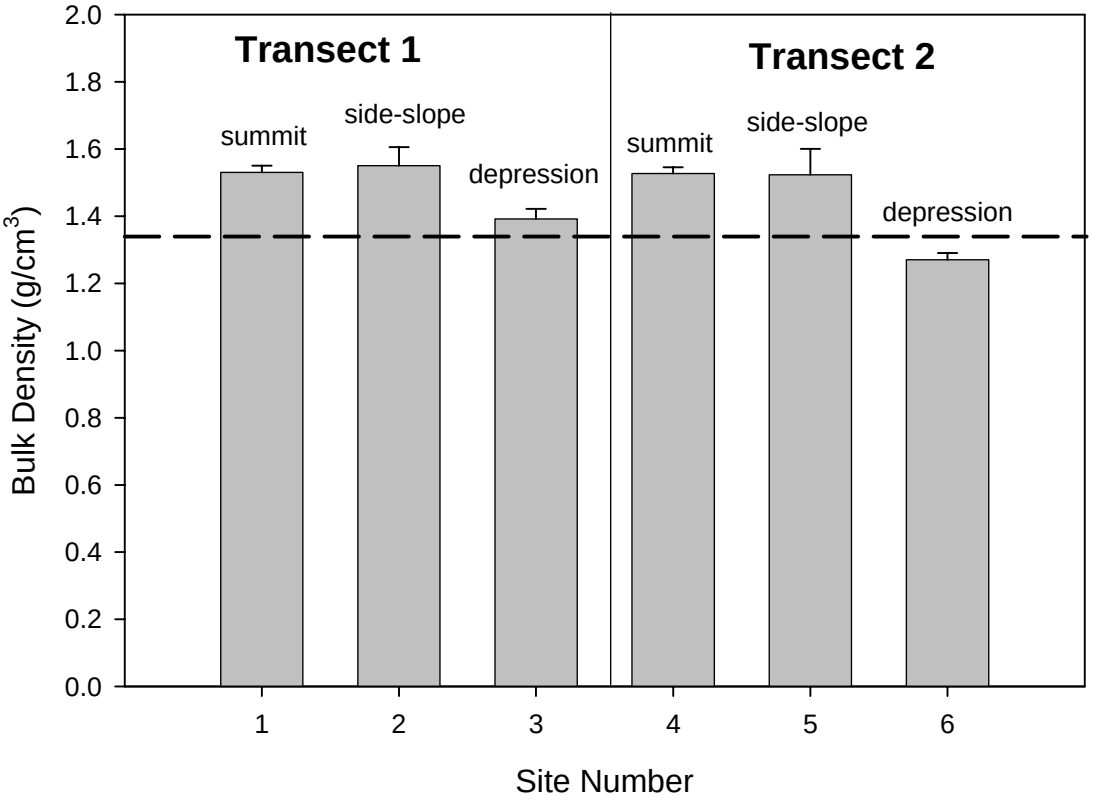

Fig. 4.19. Results from the bulk density analysis for each soil trench. The surface measurements were performed in triplicate and the error bars represent the standard error of the mean.

A-Horizon

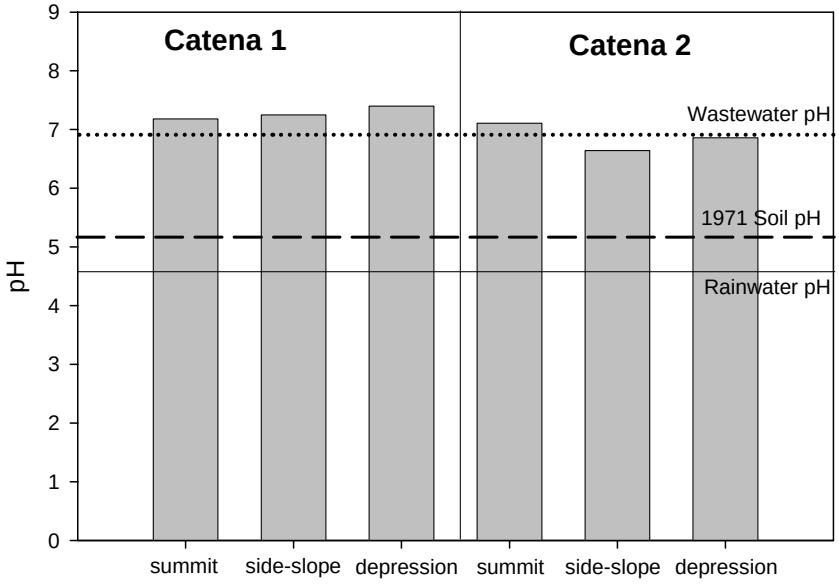

Upper B-Horizon

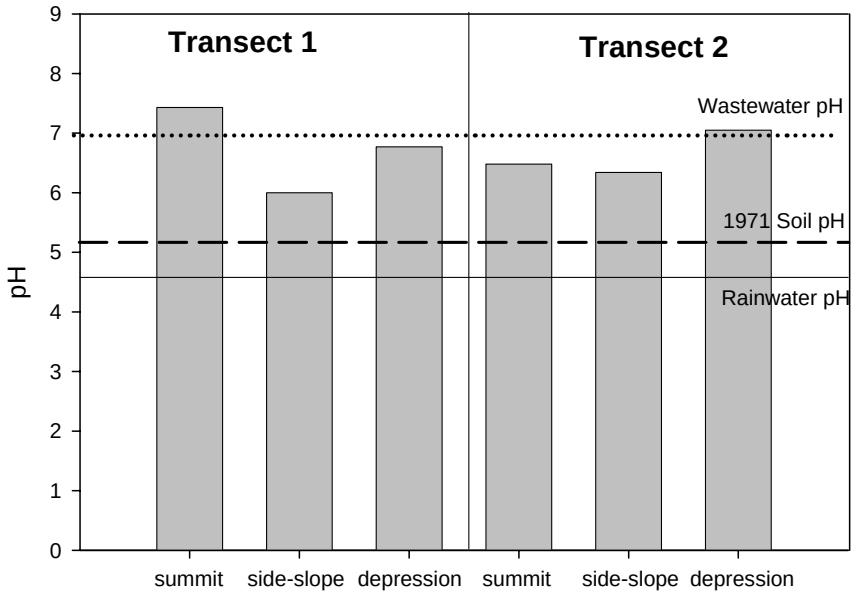

Fig. 4.20. Results from pH analysis (1:1 soil to water by mass) for each trench based on horizon. The control was based on data provided by Hook (1971). Wastewater pH was based on a 10 week average (Nov, 2005 – January, 2006) (Parizek et al., 2006). Rainfall pH was provided by the National Atmospheric Deposition Program (NADP, 2006).

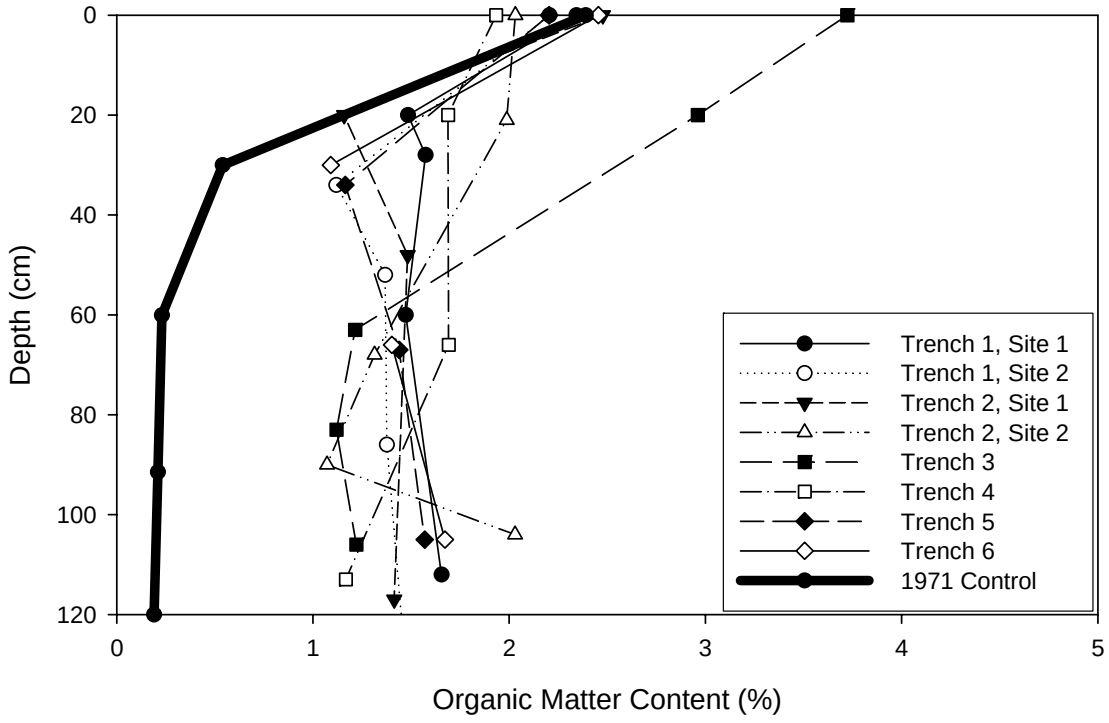

Fig. 4.21. Results for organic matter analysis (loss on ignition). The 1971 control was provided by Hook (1971).

CHAPTER 5

SUMMARY AND RECCOMENDATIONS

The main objective of this research was to determine how the Penn State Wastewater Irrigation System's soils have handled billions of gallons of water over the last forty years. To make such an assessment, a relatively new concept was employed, hydropedology. The hydropedology concept integrates pedology and hydrology to study soil-water interactions at multiple scales. This project incorporates this concept by describing the entire system of morphological, physical, and chemical properties at the irrigation area both at the pedon scale and at the landscape scale. Along with the descriptions and measurements, interactions between landscape positions, morphological features and soil physical properties were noted and used to describe the soil-water relationships on a systems basis.

Additional research performed during this project made an attempt to verify and improve a couple of common methods used to evaluate soil hydraulic properties. We were able to use samples and field experiments at the irrigation site not only to determine its properties, but also to improve on standard methods and instruments such as the tension infiltrometer and the laboratory constant head saturated hydraulic conductivity measurement.

The tension infiltrometer investigation was able to determine the constant tension assumption in most field situations, which is a key variable for solving the unsaturated hydraulic conductivity function. Experiments were conducted using a tension table to vary the flow rate at a given tension; on a sand column to have a laboratory controlled setting that resembled real world conditions; and out in the field with soils that had

contrasting textures and structures. Results from the tension table experiment indicated that as the flow increased past approximately 200 cubic centimeters per minute, the tension observed in the infiltration disc also increased, which voided the constant tension assumption. The sand column experiments exhibited similar trends. However, field experiments indicated that for the soils in this area, with flow under the 200 cubic centimeter per minute rate, the constant tension assumption was valid. This phenomenon was also proven through theoretical calculations based on the current tubing sizes. A retrofitting procedure was then provided to help improve the applicability of this instrument to the high flow situations.

Saturated hydraulic conductivity measurements performed in the laboratory are a common practice. However, there is a tendency for a preferential flow to occur between the soil core and the cylinder wall, which is commonly termed boundary or edge flow. A simple device was designed and manufactured to help separate out inner flow from the preferential flow at the edge. While measuring soil samples from the irrigation area, we found a significantly higher saturated hydraulic conductivity on the edge of soil core samples, than in the center. Brilliant blue dye experiments visually verified that edge flow was actually occurring.

The concept of steady-state flux through the core was also investigated. Constant head saturated hydraulic conductivity measurements were conducted on two cores for a period of eight days. An automated flow collection system was developed to measure the volume of effluent every 10 minutes from these cores. The results suggest that the cores did not reach steady-state conditions until approximately five days into the experiment. The results also indicated that the concept of steady-state is a function of the

time scale. Samples that appear to be at steady-state on minutes to hours time scale, are actually not at steady-state on the days to weeks time scale.

The presaturation process for the constant head saturated hydraulic conductivity technique was also evaluated during this research. Previous standard methods have recommended saturation periods from 12 hours to four days. Our results suggest that fine textured soil samples should be saturated for at least a week to achieve the maximum saturation percentage. Although saturation length did not have a significant effect on the saturated hydraulic conductivity values, evidence from brilliant blue dye experiments suggests that the flow is more uniform through the core after it has saturated for one to two weeks.

The results from investigating the standard constant head saturated hydraulic conductivity technique indicate there is a need develop a set of standardized methods based on soil properties to determine a representative value for saturated hydraulic conductivity. Future work should include the determination of time to steady-state conditions and presaturation time based on soil properties such as texture and structure.

All of the information and methods developed in the first two chapters were then utilized, along with additional investigations, to describe how the soils have changed at the Penn State Wastewater Irrigation Area after decades of wastewater irrigation. After investigating a wide array of properties, we found that morphological, physical and chemical soil properties had changed after receiving over forty years of wastewater irrigation. From a morphological standpoint, properties such as redoximorphic features appeared to become larger and more distinct and were found in the vicinity of coarse soil structure, which also increased in size. The depth of the A-horizon indicated that the area

was experiencing accelerated erosion. Manganese coatings provided a natural tracer to help determine where there was subsurface movement of water. The physical property that experienced the greatest change were areas of decreased saturated hydraulic conductivity. This coincided with an increase in bulk density. Chemical properties such as pH and also organic matter content also experienced a notable increase throughout the soil profile.

Soil properties varied within the study area primarily based on landscape position. There were three distinct positions recognized in this research, summit, midslope and depression. The summits were characterized as having the shallowest A-horizon, highest bulk density, low saturated hydraulic conductivity values and few signs of saturation. The midslope position, which normally has moderate values of measured properties, exhibited the highest percentage of manganese coatings within the profile. These coatings suggest that there is lateral flow occurring within this area, despite the relatively small amount of relief in the landscape. The depressional area, which is visibly the most affected position within the area, commonly exhibits A-horizon depths over 1 meter along with common distinct redoximorphic features. Despite being ponded sometimes, the upper portions of the depressions actually had the highest saturated conductivity values, which suggest these areas are experiencing very high amounts of run-on from the adjacent summit position. Therefore, remediation processes need to be concentrated on the summit position to be the most effective.

There are four different categories for potential run-off-reducing treatments at the Penn State Spray Irrigation System: operational, physical, chemical, and biological. To determine how these potential treatments will respond to the system, future studies will

have to be carried out in a systematic way to yield the most benefit for the cost of treatment. Sub-watersheds need to be chosen in order to evaluate the different treatments. Evaluations could be made on the basis of run-off amount and total solids within the run-off.

The first category for potential treatments is changes in the irrigation operation. These operational changes would require no soil treatment, but rather modify the current distribution system. The most obvious solution to the problem would be to add less water to the area, which was also recommended by Dadio (1998) specifically for the PSU irrigation system. Irrigating for a shorter period of time on any one area would help to reduce the run-off problem. There is also a potential benefit to turning off some of the sprinklers in the laterals that contribute to combined run-off. This could be achieved by performing a quick soil survey on the depth of the A-horizon mapped with elevation data to determine potential sprinklers that contribute significantly to high volumes of run-off. Finally, the most sophisticated way to determine irrigation scheduling would be to monitor the soil's moisture content electronically through wireless dataloggers and make the irrigation schedule based on the laterals that have the most room for additional moisture. These technologies are available and can be applicable to this situation.

The other treatments result in the alteration of the soils to better receive the irrigation water. The goal of the physical methods would be to make the surface horizon as receptive as possible to the irrigation water. This would most likely involve lowering the bulk density of the surface layer, and thereby increase the porosity and infiltration-capacity. This normally could be accomplished by tillage; research has shown the best type of tillage for infiltration is a mid-level conservation tillage (Akinyemi, 2004;

Hangen et al., 2002). However, precautions must be taken to avoid potential side-effects of plow-pans and increased erosion. Therefore it may be more desirable to use a soil aerator as is used in the turf grass industry. For example, products offered by Redixim Charterhouse (Pittston Township, PA) are designed especially for removing the effects of compaction and aerating the soil, with only minimal disturbance to the soil. Precautions would have to be taken since these machines are not specifically designed for farm applications.

In addition, there are a variety of chemical methods designed to increase the infiltration for irrigation areas. Organic matter additions have been shown to increase the infiltration rate on soils (Wuest, 2005). The addition of gypsum to the soil has also been shown to increase the soil's infiltrative capacity (Borselli, 1996; Miller, 1987). Another chemical, polyacrylamide, appears to be well suited to increase the infiltration in the area and reduce erosion (Bjorneberg et al., 2003; Flanagan et al., 2003; Lentz and D.Bjorneberg, 2003). Polyacrylamide may also be beneficial because it has been shown to reduce bacteria from animal wastewater, which could carry over to municipal wastewater (Spackman, 2003). It would be very important to have green house experiments on the addition of any chemicals to the soils to be sure that there are no negative reactions between the soil and the wastewater. Finally, biological treatment could be implemented through using plants that have large root systems, to provide for more macropores and help increase the porosity by breaking up the compacted surface.

REFERENCES

Akinyemi, J., A. Adedeji. 2004. Water Infiltration Under No-Tillage, Minimum Tillage and Conventional Tillage Systems on a Sandy Loam Alfisols. 2004 ASAE/CSAE Annual International Meeting.

Bjorneberg, D., F. Santos, N. Castanheira, O. Martins, J. Reis, J. Aase, and R. Sojka. 2003. Using polyacrylamide with sprinkler irrigation to improve infiltration. Journal of Soil and Water Conservation 58:283-289.

Borselli, L., S. Carnicelli, G. Ferrari, M. Pagliai, G. Lucamante. 1996. Effects of gypsum on hydrological, mechanical and porosity properties of a kaolinitic crusting soil. Soil Technology 9:39-54.

Dadio, S. 1998. Ponding and runoff dynamics of a closed hillslope system undergoing irrigation with treated wastewater. Master of Science, The Pennsylvania State University, University Park, PA.

Flanagan, D., L. Norton, J. Peterson, and K. Chaudhari. 2003. Using polyacrylamide to control erosion on agricultural and disturbed soils in rainfed areas. Journal of Soil and Water Conservation 58:301-311.

Hangen, E., U. Buczko, O. Bens, J. Brunotte, and E. Huttl. 2002. Infiltration patterns into two soils under conventional and conservation tillage: influence of the spatial distribution of plant root structures and soil animal activity. Soil and Tillage Research 63:181-186.

Lentz, R., and D.Bjorneberg. 2003. Polyacrylamide and straw residue effects on irrigation furrow erosion and infiltration. Journal of Soil and Water Conservation 58:312-319.

Miller, W. 1987. Infiltration and soil loss of three gypsum-amended ultisols under simulated rainfall. Soil Science Society of America 51:1314-1320.

Spackman, R., J.A. Entry, R.E. Sojka, and J.W. Ellsworth. 2003. Polyacrylamide for coliform bacteria removal from agricultural wastewater. Journal of Soil and Water Conservation 58:276 -283.

Wuest, S., T. Caesar-TonThat, S. Wright, J. Williams. 2005. Organic matter addition, N, and residue burning effects on infiltration, biological, and physical properties of an intensively tilled silt-loam soil. Soil and Tillage Research 84:154-167.

APPENDIX A

SOIL CORE DESCRIPTIONS

Core Number	1										
Horizon	Depth (top and bottom)	texture	% clay	Rock Fragments Vol	RF Kind	RF Size Shape	Rupture/Consistance (Moist)	R/C Dry	Stickiness	Plastic	
Ap1	0-17	SiL	17	2%	FG	0.3	VFR		SO	PO	
AP2	17-26	SiL	17	2	FG	0.3	VFI		SO	PO	
AP3	26-55	SiL	17	2	FG	0.3	FR		SO	PO	
Ab	55-63	SiL	17	2	FG	0.3	VFR		SO	PO	
BE	70-84	SiL	25	5	FG	0.3	FR		SS	SP	
bt1	84-104	SiCL	30	5	FG	0.3	FR		SS	SP	
bt2	104	SiCL	35	5	FG	0.3	FR		SS	SP	
Suspected Series	Hagerstown										
	Soil Color	Roots	Pores	Structure Grade	Structure Size	Structure type	Boundary	Manganese (%)	Mg Size		
Ap1	10 YR 4/3	C	F (1 mm)	1	M	SBK	AS				
AP2	10 YR 4/3	F		1	M	ABK	AS				
AP3	10 YR 4/4	F		1	M	SBK	CW	2	fine		
Ab	10 YR 3/3			1	M	SBK	CW	2	fine		
BE	10 YR 6/6			1	M	SBK	CW				
bt1	10 YR 5/8			1	M	SBK	CW	2	fine		
bt2	7.5 YR 5/8			1	M	SBK		15	medium		
	Mottles %	Size	Contrast	Concentrations	Concentration Size	C Cont	C Color	Redox %	Redox Size	Redox Cont	Color
Ap1											
AP2											
AP3											
Ab											
BE											
bt1											
bt2											

Core Number	3										
Horizon	Depth Top (cm)	Bottom (cm)	texture	% clay	Rock Fragments Vol	RF Kind	RF Size Shape (CM)	Rupture/Consistance (Moist)	R/C Dry	Stickiness	Plastic
Ap	0	20	SiL	20	2	FG	0.5	VFR		SS	SO
BE	20	36	SiL	25	5	FG	0.8	VFR		SS	SO
Bt1	36	55	SiCL	30	5	FG	0.5	FR		SS	SO
BT2	55	78	SiCL	30	5	FG	0.5	FR		SS	SP
BT3	78	94	SiC	45	2	FG	0.3	FI		MS	SP
B4	94	110	SiCL	35	20	MG	1.5	FR		SS	SP
Btx	110		CL	30	5	FG	0.3	FR		SS	SO
	Soil Color	Roots	Size	Pores	Size	Structure Grade	Structure Size	Structure type	Boundary	Manganese	Size
Ap	10YR 5/6	C	FINE	C	medium	1	M	SBK	CW		
BE	10YR 5/8	F	FINE	F	F	1	M	SBK	CW	30	COARSE
Bt1	10YR 5/8					2	TK	PLATY	CW	20	COARSE
BT2	10YR 5/6					1	M/TK	SBK PLATY	CW	30	COARSE
BT3	5YR 4/6					1	M	SBK	CW	2	FINE
B4	10YR 5/8					1	M	SBK	CW	15	COARSE
Btx	7.5YR 5/8					1	F	SBK		20	COARSE
Horizon	Mottles %	Size	Conc Color	Concentration Size	REDUCED	Redox Size	Color				
Ap											
BE											
Bt1											
BT2											
BT3											
B4											
Btx											

Core Number			4N						
Horizon	Depth top	Depth Bottom	texture	% clay	Rupture/Consistance (Moist)	Stickiness	Plastic		
Ap1	0	34	SiL	15	FR	SS	PO		
Ap2	34	74	SiL	20	FR	SS	SP		
Ap3	74	101	CL	30	FR	SS	SP		
2Ap1	101	110	SiL	20	VFR	SS	PO		
E	110	120	CL	30	FR	SS	SP		
Horizon	Soil Color	Roots	Pores	Structure Grade	Structure Size	Structure type	Boundary	Manganese	Size
Ap1	10 YR 4/3	FF	COMMON MED	WEAK	MED/THIN	SBK/PLATY			
Ap2	10 YR 5/4		COMMON MED	WEAK	MED/THIN	SBK/PLATY	CLEAR		
Ap3	10 YR 5/4			WEAK	MED/THIN	SBK/PLATY	CLEAR		
2Ap1	2.5 Y 4/4			WEAK	MED/THIN	SBK/PLATY	CLEAR	2%	FINE
E	10 YR 5/4			WEAK	MED/THIN	SBK/PLATY	CLEAR		
Horizon	Mottles %	Size	Conc Color	Concentration Size	REDUCED	Redox Size	Color		

Core Number			5							
Describer			chuck							
Horizon	Depth top	Depth Bottom	texture	% clay	Rock Fragments Vol	RF Kind	RF Size Shape (CM)	Rupture/Consistance (Moist)	Stickiness	Plastic
Ap	0	20	SiL	20	1	CHERT	MED GRAVEL	FR	SS	SP
BE	20	35	CL	35	2	CHERT	MED/COARSE	FR	SS	MP
B1	35	54	C	45	1	CHERT	MED GRAVEL	FIRM	MS	VP
B2	54	100	C	45	2	CHERT	MED/COARSE	FIRM	MS	VP
B3	100	118	C	45	1	CHERT	FINE/MED	FIRM	MS	VP
Horizon	Soil Color	Roots	Pores	Structure Grade	Structure Size	Structure type	Boundary	Manganese	Size	
Ap	10 YR 4/3	FF	FF	WEAK	MED	SBK/GRANULAR				
BE	10 YR 5/4			WEAK	MED	SBK	CLEAR			
B1	7.5 YR 5/8			MOD	THIN	PLATY	CLEAR	0.5	FINE	
B2	7.5 YR 5/6			MOD	THIN	PLATY	CLEAR	15	COARSE	
B3	7.5 YR 5/8			MOD	MED/THIN	SBK/PLATY	CLEAR	5	MED	
Horizon	Mottles %	Size	Conc Color	Concentration Size	REDUCED	Redox Size	Color			

Core Number			8							
Describer			chuck							
Horizon	Depth top	Depth Bottom	texture	% clay	Rock Fragments Vol	RF Kind	RF Size Shape (CM)	Rupture/Consistance (Moist)	Stickiness	Plastic
Ap1	0	21	SiL	17	1	chert	medium gravel	VFR	SO	PO
E	21	34	SiL	25	5	chert	medium/coarse gravel	VFR	SO	PO
Rock	34	43			90	chert	medium/coarse gravel			
B1	43	56	CL	35	2%	chert	fine gravel	VFR	SS	MP
B2	56	100	C	45	5%	chert/shale	fine gravel	VFR	SS	MP
Horizon	Soil Color	Roots	Pores	Structure Grade	Structure Size	Structure type	Boundary	Manganese	Size	
Ap1	10YR 4/3	FF		WEAK	MED	SBK/PLATY				
E	10YR 4/4			WEAK	MED	SBK/PLATY	ABRUPT			
Rock							ABRUPT			
B1	10YR 4/6			WEAK	MED	SBK/PLATY	ABRUPT	25%	MED	
B2	7.5YR 4/6			WEAK	MED	SBK/PLATY	CLEAR	5%	FINE	
	Mottles %	Size	Conc Color	Concentration Size	REDUCED	Redox Size	Color			

Core Number			16							
Describer			chuck							
Horizon	Depth top	Depth Bottom	texture	% clay	Rock Fragments Vol	RF Kind	RF Size Shape (CM)	Rupture/Consistance (Moist)	Stickiness	Plastic
Ap	0	5	SiL	20	1	chert	med	VFR	SO	SP
AB	5	21	CL	30	1	chert	med	FR/Firm	SS	SP
B1	21	53	C	45	2	sandstone	coarse	FR/Firm	MS	VP
B2	53	69	C	40				FR	MS	VP
B3	69	96	C	40	2	chert	med	FR/Firm	MS	MP
B4	96	108	C	45				FR	MS	VP
Horizon	Soil Color	Roots	Pores	Structure Grade	Structure Size	Structure type	Boundary	Manganese	Size	
Ap	7.5 YR 4/4	CF	FF	WEAK	MED	GRAN				
AB	7.5 YR 4/6	FF		WEAK	MED	SBK	CLEAR			
B1	5 YR 5/6		FF	MOD	MED	SBK	CLEAR			
B2	7.5 YR 5/6			WEAK	MED	SBK	CLEAR	10%	COARSE	
B3	10 YR 5/8			WEAK	MED	SBK	ABRUPT	15	COARSE	
B4	5 YR 4/6			WEAK	MED	SBK	CLEAR	2	FINE	
Horizon	Mottles %	Size	Conc Color	Concentration Size	REDUCED	Redox Size	Color			

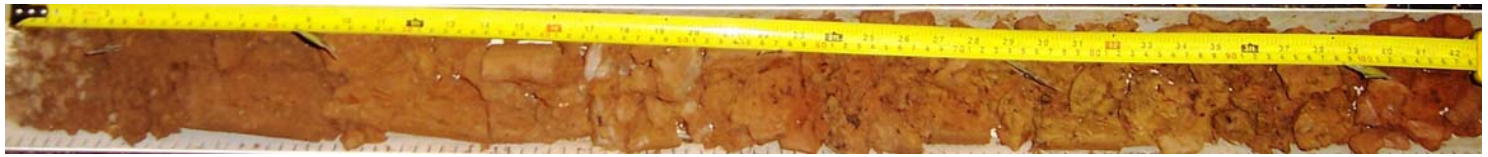

Core Number			17							
Describer			chuck							
Horizon	Depth top	Depth Bottom	texture	% clay	Rock Fragments Vol	RF Kind	RF Size Shape (CM)	Rupture/Consistance (Moist)	Stickiness	Plastic
Ap	0	31	SiL	15	1	chert	fine gravel	VFR	SO	PO
EB	31	41	SiL	25				VFR	SO	SP
B1	41	58	SiCL	30				VFR	SS	MP
B2	58	79	SiCL	35	5	chert	med gravel	VFR	SS	MP
B3	79	98	SiCL	35	1	chert	fine gravel	FR	SS	MP
B4	98	120	SiCL	38	1%	chert	fine gravel	FR	SS	MP
Horizon	Soil Color	Roots	Pores	Structure Grade	Structure Size	Structure type	Boundary	Manganese	Size	
Ap	10 YR 4/3	FEW FINE		WEAK	MED	SBK/PLATY				
EB	2.5 Y 5/4		COMMON FINE	WEAK	MED	SBK/PLATY	CLEAR			
B1	10 YR 5/6			WEAK	MED	SBK/PLATY	CLEAR	2%	FINE	
B2	10 YR 5/8			WEAK	THIN	PLATY	CLEAR			
B3	10 YR 5/8			MODERATE	THIN	PLATY	ABRUPT			
B4	10 YR 5/6			WEAK	THIN	PLATY	ABRUPT	30%	FINE/MEDIUM	
Horizon	Mottles %	Size	Conc Color	Concentration Size	REDUCED	Redox Size	Color			
Ap										
EB										
B1										
B2										
B3	50%	COARSE	7.5 YR 5/8	MED	15	MED	10 YR 6/2			
B4										

Core Number			18							
Describer			chuck							
Horizon	Depth top	Depth Bottom	texture	% clay	Rock Fragments Vol	RF Kind	RF Size Shape (CM)	Rupture/Consistance (Moist)	Stickiness	Plastic
Ap	0	35	SiL	17	1	chert	med/course	VFR	SS	SP
BE	35	56	CL	30	0.5	chert	fine	FR	SS	SP
B1	56	86	CL	38	0.5	chert	fine	FR	MS	MP
B2	86	120	C	45	0.5	chert	fine	FR/FIRM	MS	VP
Horizon	Soil Color	Roots	Pores	Structure Grade	Structure Size	Structure type	Boundary	Manganese	Size	
Ap	10 YR 4/3	FF	FF	WEAK	MED	SBK				
BE	10 YR 5/4	FF	FF	WEAK	MED	SBK	ABRUPT	1%	FINE	
B1	10 YR 5/6			WEAK	MED	SBK	CLEAR			
B2	5 YR 4/6			MOD	THIN	PLATY	GRADUAL			
Horizon	Mottles %	Size	Conc Color	Concentration Size	REDUCED	Redox Size	Color			

Core Number			19							
Describer			chuck							
Horizon	Depth top	Depth Bottom	texture	% clay	Rock Fragments Vol	RF Kind	RF Size Shape (CM)	Rupture/Consistance (Moist)	Stickiness	Plastic
Ap1	0	26	SiL	20	2	chert	fine	FR	SS	PO
BE	26	56	C	40	2	chert	med	Firm	SS	MP
B1	56	86	C	50	1	chert	fine	Very Firm	MS	P
B2	86	105	C	40	1	chert	fine	VFR	MS	MP
Horizon	Soil Color	Roots	Pores	Structure Grade	Structure Size	Structure type	Boundary	Manganese	Size	
Ap1	10 YR 4/4	FF		WEAK	MED	SBK/GRANULAR				
BE	5 YR 4/6			WEAK	MED	SBK	CLEAR			
B1	2.5 YR 4/6			WEAK	MED	SBK	GRADUAL	5%	MED	
B2	10 YR 6/8			MOD	THIN	PLATY	ABRUPT	1%	FINE	
Horizon	Mottles %	Size	Conc Color	Concentration Size	REDUCED	Redox Size	Color			

Core Number			21							
Describer			chuck							
Horizon	Depth top	Depth Bottom	texture	% clay	Rock Fragments Vol	RF Kind	RF Size Shape (CM)	Rupture/Consistance (Moist)	Stickiness	Plastic
Ap	0	10	SiL	15	2	chert	fine gravel	vfr	SO	PO
E	10	18	SiL	25	5	chert	coarse gravel	fr	SS	SP
B1	18	28	CL	30	5	chert	fine gravel	fr	SS	MP
B2	28	43	CL	30	2%	chert	fine gravel	fr	SS	MP
B3	43	66	C	47	2%	chert	fine gravel	firm	S	VP
B4	66	105	C	42	5	chert	coarse gravel	fr	SS	MP
Horizon	Soil Color	Roots	Pores	Structure Grade	Structure Size	Structure type	Boundary	Manganese	Size	
Ap	2.5 Y 4/4	FF		Weak	Med	SBK/jGranualr				
E	10 YR 4/6	FF		Weak	Med	SBK	Clear			
B1	7.5YR 5/8	FF		Weak	Med	SBK	Clear			
B2	7.5YR 5/8			Weak	Thin	Platy	Gradual	5%	Fine	
B3	7.5Yr 5/6			Weak	Med	SBK	Gradual	2	fine	
B4	7.5 YR 5/8			Weak	Med	SBK	Gradual	5	medium	
Horizon	Mottles %	Size	Conc Color	Concentration Size	REDUCED	Redox Size	Color			
Ap										
E										
B1										
B2										
B3										
B4										

Core Number			22							
Describer			chuck							
Horizon	Depth top	Depth Bottom	texture	% clay	Rock Fragments Vol	RF Kind	RF Size Shape (CM)	Rupture/Consistance (Moist)	Stickiness	Plastic
Ap 1	0	24	SiL	20	1	chert	fine gravel	Fr	SO	SP
Ap2	24	49	SiL	20	1	chert	fine gravel	Fr	SO	SP
2Ap1	49	62	SiL	20	2	chert	med gravel	VFR	SO	PO
E	62	96	CL	30	2%	chert	fine/med gravel	Fr	SS	SP
Bt	96	112	C	40	3%	chert	med/coarse gravel	Fr	MS	MP
Horizon	Soil Color	Roots	Pores	Structure Grade	Structure Size	Structure type	Boundary	Manganese	Size	
Ap 1	2.5Y 4/4	FF		Weak	med	SBK				
Ap2	2.5 Y 5/4			Weak	med	SBK	gradual			
2Ap1	2.5 Y 3/3			Weak	med	SBK	abrupt			
E	2.5 Y 5/3			Weak	med	SBK	abrupt			
Bt	10 YR 5/6			Weak	med	SBK	abrupt			
Horizon	Mottles %	Size	Conc Color	Concentration Size	REDUCED	Redox Size	Color			
Ap 1										
Ap2										
2Ap1										
E										
Bt	25	med	5 YR 4/6	med						

Core Number			23							
Describer			chuck							
Horizon	Depth top	Depth Bottom	texture	% clay	Rock Fragments Vol	RF Kind	RF Size Shape (CM)	Rupture/Consistance (Moist)	Stickiness	Plastic
Ap	0	15	SIL	20	1	chert	med gravel	FR	SO	SP
B/E or B1	15	30	C	40	2	chert	fine/coarse	Firm	SS	MP
B1	30	57	C	45	0.5	chert	fine	Firm	SS	VP
B2	57	77	CL	38	0.5	chert	fine	FR	SS	MP
B3	77	99	C	40	2	sandstone/chert	med/coarse	Firm	SS	MP
B4	99	105	CL	38						
Horizon	Soil Color	Roots	Pores	Structure Grade	Structure Size	Structure type	Boundary	Manganese	Size	
Ap	10 YR 4/4	FF	FF	WEAK	MED	SBK				
B/E or B1	5 YR 5/6	FF	FF	WEAK	MED	SBK	CLEAR			
B1	5 YR 5/8			WEAK	THIN/MED	PLATY/SBK	GRADUAL	20%	COARSE	
B2	7.5 YR 5/8			MODERATE	THIN	PLATY	CLEAR	2%	fine	
B3	7.5 YR 6/8			WEAK	MED	SBK	ABRUPT	2	fine	
B4	10 YR 5/8						ABRUPT	10	COARSE	
Horizon	Mottles %	Size	Conc Color	Concentration Size	REDUCED	Redox Size	Color			

Core Number			24							
Describer			chuck							
Horizon	Depth top	Depth Bottom	texture	% clay	Rock Fragments Vol	RF Kind	RF Size Shape (CM)	Rupture/Consistance (Moist)	Stickiness	Plastic
Ap	0	36	SiL	20	1	chert	fine	FR	SO	SP
E/B	36	55	CL	35	1	chert	med	FR	SS	SP
B1	55	73	C	40	1	chert	med	FR	SS	MP
B2	73	103	C	45	1%	chert	med	Firm	SS	MP
B3	103	123	C	47	1%	chert	med	Firm	SS	MP
Horizon	Soil Color	Roots	Pores	Structure Grade	Structure Size	Structure type	Boundary	Manganese	Size	
Ap	10 YR 4/3	FF	FF	WEAK	MED	SBK				
E/B	10 YR 5/8	FF		WEAK	MED	SBK	CLEAR			
B1	7.5 YR 5/6			MODERATE	THIN	PLATY	CLEAR			
B2	7.5 YR 5/6			MODERATE	THIN	PLATY	GRADUAL	2%	FINE	
B3	5 yr 5/6			WEAK	THIN	PLATY	GRADUAL	2	FINE	
Horizon	Mottles %	Size	Conc Color	Concentration Size	REDUCED	Redox Size	Color			

Core Number			25							
Describer			chuck							
Horizon	Depth top	Depth Bottom	texture	% clay	Rock Fragments Vol	RF Kind	RF Size Shape (CM)	Rupture/Consistance (Moist)	Stickiness	Plastic
Ap	0	15	CL	30	1	chert	med	FR	SS	SP
B1	15	48	C	45	1	chert	coarse	Firm	MS	VP
B2	48	76	CL	38	1	chert	coarse	FR	SS	MP
B3	76	108	CL	32	1%	chert	coarse	VFR	SS	MP
B4	108	125	C	50				Very Firm	MS	VP
Horizon	Soil Color	Roots	Pores	Structure Grade	Structure Size	Structure type	Boundary	Manganese	Size	
Ap	10 YR 4/6	FF	FF	WEAK	MED	SBK				
B1	5 YR 5/6	FF		WEAK	MED	SBK	CLEAR			
B2	7.5 YR 5/8			WEAK	THIN	PLATY	ABRUPT	5%	FINE	
B3	10 YR 5/8			MOD	THIN	PLATY	GRADUAL	10%	COARSE	
B4	5 YR 4/6			MOD	MED	SBK	ABRUPT	2	FINE	
Horizon	Mottles %	Size	Conc Color	Concentration Size	REDUCED	Redox Size	Color			

Core Number			26							
Describer			chuck							
Horizon	Depth top	Depth Bottom	texture	% clay	Rock Fragments Vol	RF Kind	RF Size Shape (CM)	Rupture/Consistance (Moist)	Stickiness	Plastic
Ap1	0	21	SiL	17	1	chert	fine	VFR	SO	SP
E	21	27	CL	35	2	chert	med	FR	SS	SP
B1	27	47	C	40	1	chert	med	FIRM	MS	MP
B2	47	87	C	50	4	chert	fine/med	VERY FIRM	MS	P
B3	87	101	C	45	2	chert	med	FR/FIRM	MS	MP
Horizon	Soil Color	Roots	Pores	Structure Grade	Structure Size	Structure type	Boundary	Manganese	Size	
Ap1	10 YR 4/3	CF	FF	WEAK	MED	SBK/GRAN				
E	7.5 YR 5/6			WEAK	MED	SBK	CLEAR			
B1	5 YR 4/6			MOD	MED	SBK	CLEAR			
B2	5 YR 4/6			MOD	MED	SBK	GRADUAL			
B3	7.5 YR 5/8			WEAK	MED	SBK	CLEAR			
Horizon	Mottles %	Size	Conc Color	Concentration Size	REDUCED	Redox Size	Color			

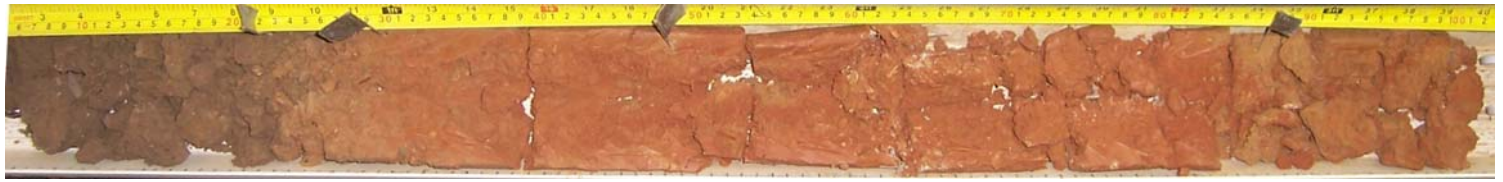

Core Number		28							
Describer		chuck							
Horizon	Depth (top and bottom)	texture	% clay	Rock Fragments Vol	RF Kind	RF Size Shape (CM)	Rupture/Consistance (Moist)	Stickiness	Plastic
A	0-20	SIL	15	5	FG	2	FR	SO	PO
BE	20-50	SIL	25	5	FG	0.5	FR	SS	SP
Bt1	50-74	SICL	30	5	FG	0.5	FR	SS	SP
Bt2	74-108	SICL	33	5	FG	0.5	FI	SS	SP
BT3	108	SIC	42	5	FG	0.5	FI	SS	SP
	Soil Color	Roots	Pores	Structure Grade	Structure Size	Structure type	Boundary	Manganese	Size
A	2.5 YR 4/3	F	F	1	M	SBK	AIR		
BE	10 YR 6/8	F		1	M	SBK	CW		
Bt1	7.5 YR 6/8	F		1	M	SBK	CW		
Bt2	7.5 YR 5/8	F		1	F	SBK	CW	8	coarse
BT3	5 YR 5/8			1	M	SBK			
Horizon	Mottles %	Size	Conc Color	Concentration Size	REDUCED	Redox Size	Color		
A									
BE									
Bt1									
Bt2									
BT3									

Core Number			29							
Describer			chuck							
Horizon	Depth top	Depth Bottom	texture	% clay	Rock Fragments Vol	RF Kind	RF Size Shape (CM)	Rupture/Consistance (Moist)	Stickiness	Plastic
Ap	0	20	SiL	20	2	chert	MED/COARSE	FR	SS	SP
BE	20	32	CL	35	1	chert	MED/COARSE	FR	SS	MP
B1	32	66	C	45	3	chert	MED	FIRM	MS	VP
B2	66	86	C	50				FIRM	MS	VP
B3	86	102	C	50				FIRM	MS	VP
B4	102	123	C	50	2	chert	MED	FR	MS	MP
Horizon	Soil Color	Roots	Pores	Structure Grade	Structure Size	Structure type	Boundary	Manganese	Size	
Ap	10 YR 4/3	FF	FF	WEAK	MED	SBK				
BE	10 YR 5/6			WEAK	MED	SBK	ABRUPT	30%	MED	
B1	10 YR 5/8			WEAK	MED/THIN	SBK/PLATY	ABRUPT	2%	MED	
B2	7.5 YR 5/6			MOD/STRONG	THIN	PLATY	ABRUPT	20%	COARSE	
B3	7.5 YR 5/6			MOD	THIN	PLATY	GRADUAL	1	MED	
B4	10 YR 5/8			WEAK	MED/THIN	SBK/PLATY	GRADUAL	2	MED	
Horizon	Mottles %	Size	Conc Color	Concentration Size	REDUCED	Redox Size	Color			
Ap										
BE										
B1										
B2										
B3										
B4										

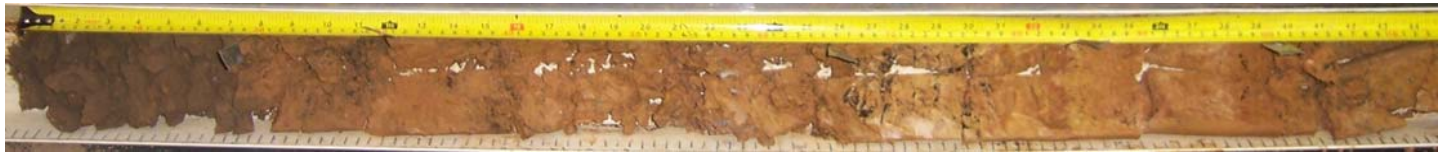

Core Number			30							
Describer			chuck							
Horizon	Depth top	Depth Bottom	texture	% clay	Rock Fragments Vol	RF Kind	RF Size Shape (CM)	Rupture/Consistance (Moist)	Stickiness	Plastic
Ap1	0	19	CL	30	1	chert	med	FR	SS	MP
B1	19	51	C	50	1	chert	med	Firm	MS	MP
B2	51	84	SC	40	2	sandstone	coarse	FR	SS	MP
B3	84	125	SC	45				FR	SS	MP
Horizon	Soil Color	Roots	Pores	Structure Grade	Structure Size	Structure type	Boundary	Manganese	Size	
Ap1	7.5 YR 4/6	FF	FF	WEAK	MED	SBK				
B1	5 YR 4/6			MOD	MED	SBK	ABRUPT			
B2	5 YR 5/6			WEAK	MED	SBK	CLEAR			
B3	5 YR 5/6			WEAK	MED	SBK	GRADUAL			
Horizon	Mottles %	Size	Conc Color	Concentration Size	REDUCED	Redox Size	Color			

Core Number			31							
Describer			chuck							
Horizon	Depth top	Depth Bottom	texture	% clay	Rock Fragments Vol	RF Kind	RF Size Shape (CM)	Rupture/Consistance (Moist)	Stickiness	Plastic
Ap	0	14	SiL	25	1	chert	medium gravel	VFR	SS	SP
B/E	14	40	C	40	2	chert	medium gravel	FR	SS	MP
B1	40	59	C	45	0.5	chert	fine	FIRM	MS	VP
B2	59	78	C	45				FR	MS	VP
B3	78	125	C	50				FR/FIRM	MS	VP
Horizon	Soil Color	Roots	Pores	Structure Grade	Structure Size	Structure type	Boundary	Manganese	Size	
Ap	10 YR 5/4	FF	FF	WEAK	MED	SBK/GRANULAR				
B/E	10 YR 5/8			WEAK	MED	SBK	ABRUPT			
B1	7.5 YR 5/8			WEAK	MED	SBK	CLEAR			
B2	5 YR 4/6			WEAK	MED	SBK	CLEAR	40%	COARSE	
B3	2.5 YR 4/6			WEAK	MED	SBK	CLEAR	2	MED	
Horizon	Mottles %	Size	Conc Color	Concentration Size	REDUCED	Redox Size	Color			
Ap										
B/E										
B1	1	COARSE	5 YR 5/8	MEDIUM		MEDIUM	10 YR 7/1			
B2										
B3										

Core Number			32							
Describer			chuck							
Horizon	Depth top	Depth Bottom	texture	% clay	Rock Fragments Vol	RF Kind	RF Size Shape (CM)	Rupture/Consistance (Moist)	Stickiness	Plastic
Ap1	0	27	SiL	15				FR	SO	PO
Ap2	27	51	SiL	20	1	chert	med gravel	FR	SO	PO
Ap3	51	83	SiL	25				VFR	SS	SP
Ap4	83	104	CL	30				VFR	SS	SP
Bg	104	120	C	50	1%	chert	med gravel	FIRM	MS	VP
Horizon	Soil Color	Roots	Pores	Structure Grade	Structure Size	Structure type	Boundary	Manganese	Size	
Ap1	2.5y 4/4	Common Fine	Common Fine	weak	thin	platy				
Ap2	2.5y 5/3	Common Fine	Common Fine	weak	thin	platy	gradual			
Ap3	2.5 Y 5/3		common medium	mod	thin	platy	gradual			
Ap4	2.5Y 4/3		common medium	weak	med	sbk	clear			
Bg	2.5 Y 5/2			can't determine			clear			
Horizon	Mottles %	Size	Conc Color	Concentration Size	REDUCED	Redox Size	Color			
Ap1										
Ap2	10	fine	5YR 4/6	FINE						
Ap3	15	FINE	5YR 5/8	FINE						
Ap4	20	MEDIUM	5YR 5/8	MEDIUM						
Bg				MEDIUM	ALL		2.5 Y 5/2			

Core Number			33							
Describer			chuck							
Horizon	Depth top	Depth Bottom	texture	% clay	Rock Fragments Vol	RF Kind	RF Size Shape (CM)	Rupture/Consistance (Moist)	Stickiness	Plastic
Ap	0	33	SiL	20	1	chert	med gravel	FR	SO	PO
E/B	33	53	CL	35	1	chert	fine gravel	Firm	SS	SP
B1	53	98	C	40	1	chert	fine gravel	Firm	SS	MP
B2	98	127	C	45	10%	chert	med/coarse	Firm	SS	MP
Horizon	Soil Color	Roots	Pores	Structure Grade	Structure Size	Structure type	Boundary	Manganese	Size	
Ap	10 YR 4/3	FF		WEAK	MED	SBK				
E/B	7.5 YR 5/6			WEAK	MED	SBK	ABRUPT	%		
B1	7.5 YR 5/8			MOD	THIN	PLATY	CLEAR	5%	FINE	
B2	10 YR 5/8			MOD	MED	SBK	CLEAR	3%	FINE	
Horizon	Mottles %	Size	Conc Color	Concentration Size	REDUCED	Redox Size	Color			

Core Number			34							
Describer			chuck							
Horizon	Depth top	Depth Bottom	texture	% clay	Rock Fragments Vol	RF Kind	RF Size Shape (CM)	Rupture/Consistance (Moist)	Stickiness	Plastic
Ap	0	20	L	18	2%	chert	medium gravel	VFR	SO	PO
B1	20	64	SiCL	35	2%	chert	fine/medium	FR/FI	SO	MP
B2	64	89	C	45	1%	chert	medium gravel	FR/FI	SS	VP
B3	89	110	SCL	30	5%	chert	fine/medium	FR/FI	SS	VP
B4	110	127	C	40	0%			FR	SS	VP
	Soil Color	Roots	Pores	Structure Grade	Structure Size	Structure type	Boundary	Manganese	Size	
Ap	10 YR 4/2	FF	FF	WEAK	MED	SBK				
B1	7.5 YR 5/6	FF	FM	WEAK	MED	SBK	ABRUPT	2%	VERY COARSE	
B2	5 YR 5/6	FF	FM	WEAK	MED	SBK	CLEAR			
B3	7.5 YR 5/6			WEAK	MED	SBK	CLEAR			
B4	5 YR 5/6			WEAK	MED	SBK	CLEAR	5%	MEDIUM	
Horizon	Mottles %	Size	Conc Color	Concentration Size	REDUCED	Redox Size	Color			
Ap										
B1										
B2										
B3										
B4										

Core Number			35	test core						
Describer			chuck							
Horizon	Depth top	Depth Bottom	texture	% clay	Rock Fragments Vol	RF Kind	RF Size Shape (CM)	Rupture/Consistance (Moist)	Stickiness	Plastic
Ap	0	20	SiL	15	2	chert	fine gravel	VFR	SO	PO
E	20	39	CL	30	10	chert	fine gravel	VFR	SS	SP
B1	39	104	CL	30	2	chert	fine gravel	FR	SS	MP
B2	104	120	C	50	5%	chert	fine gravel	F	SS	VP
Horizon	Soil Color	Roots	Pores	Structure Grade	Structure Size	Structure type	Boundary	Manganese	Size	
Ap	10YR 5/6	FF		WEAK	MED	SBK/PLATY				
E	10 YR 5/8	FF		WEAK	THIN/MED	PLATY/SBK	ABRUPT	10%	FINE	
B1	10 YR 5/8			WEAK	THIN/MED	PLATY/SBK	CLEAR	30%	FINE/COARSE	
B2	10 YR 5/8			WEAK	THIN/MED	PLATY/SBK	ABRUPT	5%	MED	
Horizon	Mottles %	Size	Conc Color	Concentration Size	REDUCED	Redox Size	Color			
Ap										
E										
B1										
B2										

Core Number			36							
Describer			chuck							
Horizon	Depth top	Depth Bottom	texture	% clay	Rock Fragments Vol	RF Kind	RF Size Shape (CM)	Rupture/Consistance (Moist)	Stickiness	Plastic
Ap1	0	24	SiL	25				FR	SS	SP
Ap2	24	48	SiL	20				VFR	SO	PO
2Ap1	48	63	SiL	17				VFR	SO	PO
2Ap2	63	79	SiL	25	10%	LIMYSANDSTONE	COARSE GRAVEL	FR	SS	SP
B1	79	94	C	40				F	MS	VP
B2	94	105	C	45				F	MS	VP
Horizon	Soil Color	Roots	Pores	Structure Grade	Structure Size	Structure type	Boundary	Manganese	Size	
Ap1	10 YR 4/3	FF		W	MEDIUM	PLATY				
Ap2	10 YR 4/3	FF		W	MEDIUM	PLATY	CLEAR	1%	FINE	
2Ap1	10 YR 2/2			W	MEDIUM	PLATY/SBK	CLEAR			
2Ap2	10 YR 5/3			W	MEDIUM	PLATY/SBK	CLEAR			
B1	10 YR 6/3			W	MEDIUM	PLATY/SBK	CLEAR			
B2	10 YR 6/2			W	MEDIUM	PLATY/SBK	ABRUPT			
Horizon	Mottles %	Size	Conc Color	Concentration Size	REDUCED	Redox Size	Color			
Ap1										
Ap2										
2Ap1										
2Ap2										
B1	5%	FINE	7.5 YR 5/8	FINE						
B2	10%	FINE	7.5 YR 5/8							

Core Number			37							
Describer			chuck							
Horizon	Depth top	Depth Bottom	texture	% clay	Rock Fragments Vol	RF Kind	RF Size Shape (CM)	Rupture/Consistance (Moist)	Stickiness	Plastic
Ap	0	34	SiL	20	0.5	CHERT	MED GRAVEL	VFR	SS	PO
B1	34	68	C	40	0.5	CHERT	MED GRAVEL	FR/FIRM	SS	MP
B2	68	95	C	45	0.5	CHERT	MED GRAVEL	FR/VRF	SS	VP
B3	95	125	C	45	0.5	CHERT	MED GRAVEL	VFR	SS	VP
Horizon	Soil Color	Roots	Pores	Structure Grade	Structure Size	Structure type	Boundary	Manganese	Size	
Ap	10 YR 3/3	CF	C M/F	WEAK	MED	SBK/GRAN				
B1	10 YR 5/4		C M/F	WEAK	MED	SBK/GRAN	CLEAR			
B2	10 YR 6/6			MOD	THIN	PLATY	CLEAR	5	COARSE	
B3	10 YR 5/6			MOD	THIN	PLATY	CLEAR	70	COARSE	
Horizon	Mottles %	Size	Conc Color	Concentration Size	REDUCED	Redox Size	Color			

Core Number			38	test core						
Describer			chuck							
Horizon	Depth top	Depth Bottom	texture	% clay	Rock Fragments Vol	RF Kind	RF Size Shape (CM)	Rupture/Consistance (Moist)	Stickiness	Plastic
Ap	0	22	L	15	2	chert	med gravel	FR	SO	PO
BE	22	54	CL	27	1	chert	fine gravel	FR	SO	MP
B1	54	80	CL	30	2	chert	med gravel	FR	SO	MP
B2	80	120	C	40	1	chert	fine gravel	FI	SS	VP
Horizon	Soil Color	Roots	Pores	Structure Grade	Structure Size	Structure type	Boundary	Manganese	Size	
Ap	10 YR 4/3	FEW FINE		WEAK	MED	SBK				
BE	10 YR 5/8	FEW FINE		WEAK	MED	SBK	ABRUPT	5%	MED	
B1	10 YR 6/6			WEAK	MED	SBK	CLEAR	15%	COARSE	
B2	10 YR 5/8			WEAK	MED	SBK	CLEAR	5%	MED	
Horizon	Mottles %	Size	Conc Color	Concentration Size	REDUCED	Redox Size	Color			
Ap										
BE										
B1										
B2	30	coarse				coarse	10 YR 6/3			

Core Number			39 Nearest Road							
Describer			chuck							
Horizon	Depth top	Depth Bottom	texture	% clay	Rock Fragments Vol	RF Kind	RF Size Shape (CM)	Rupture/Consistance (Moist)	Stickiness	Plastic
Ap1	0	18	CL	30	8	CHERT	COARSE GRAVEL	VFR	SS	SP
B1	18	50	C	40	1	CHERT	MED/COARSE	FR	SS	MP
B2	50	75	C	40	1	CHERT	MED/COARSE	VFR	SS	MP
B3	75	83	C	50	0.5	CHERT	MED	FIRM	MS	VP
Horizon	Soil Color	Roots	Pores	Structure Grade	Structure Size	Structure type	Boundary	Manganese	Size	
Ap1	10 YR 5/4	FF	FF	WEAK	MED	SBK				
B1	7.5 YR 5/6		1- 7MM PORE	WEAK	THIN	PLATY	ABRUPT			
B2	10 YR 5/6		1- 7MM PORE	MOD	THIN	PLATY	CLEAR	5%	COARSE	
B3	5 YR 5/6			MOD	MED	SBK	ABRUPT			
Horizon	Mottles %	Size	Conc Color	Concentration Size	REDUCED	Redox Size	Color			

Core Number			39A							
Describer			chuck							
Horizon	Depth top	Depth Bottom	texture	% clay	Rock Fragments Vol	RF Kind	RF Size Shape (CM)	Rupture/Consistance (Moist)	Stickiness	Plastic
A	0	27	L	15	1	CHERT	MED GRAVEL	VFR	SO	SP
BE	27	45	CL	27	0			VFR	SS	MP
B1	45	65	CL	33	1	CHERT	FINE	VFR	SS	MP
B2	65	112	CL	33	0			VFR/LOOSE	SS	MP
B3	112	120	CL	40	0			VFR	SS	MP
Horizon	Soil Color	Roots	Pores	Structure Grade	Structure Size	Structure type	Boundary	Manganese	Size	
A	10 YR 4/3	FEW FINE		WEAK	MEDIUM	SBK/PLATY				
BE	10 YR 5/6	FEW FINE		WEAK	MEDIUM	SBK	GRAD			
B1	10 YR 5/6			WEAK	MEDIUM	PLATY	CLEAR	10%	MED	
B2	10 YR 4/6			MODERATE	THIN	PLATY	CLEAR	40%	FINE	
B3	10 YR 6/6			WEAK	THIN	PLATY	CLEAR	15%	COARSE	
Horizon	Mottles %	Size	Conc Color	Concentration Size	REDUCED	Redox Size	Color			
A										
BE										
B1										
B2	80	COARSE	5 YR 5/8	MED	40	MED	10 YR 6/3			
B3										

Core Number			40							
Describer			chuck							
Horizon	Depth top	Depth Bottom	texture	% clay	Rock Fragments Vol	RF Kind	RF Size Shape (CM)	Rupture/Consistance (Moist)	Stickiness	Plastic
Ap1	0	30	SiL	15				VFR	SS	PO
Ap2	30	54	SiL	20	0.5	chert	med	FR	SS	PO
AB	54	70	CL	28				VFR	SS	SP
B1	70	98	CL	38	1	chert	med	FR	SS	MP
B2	98	124	C	45	1	chert	med	FR/FIRM	MS	MP
Horizon	Soil Color	Roots	Pores	Structure Grade	Structure Size	Structure type	Boundary	Manganese	Size	
Ap1	10 YR 4/3	FF	FF	WEAK	MED	SBK/GRAN				
Ap2	10 YR 4/3	FF		WEAK	MED	SBK/GRAN	GRADUAL			
AB	7.5 YR 4/4			WEAK	MED	SBK	CLEAR			
B1	7.5 YR 5/8			WEAK	MED	SBK	ABRUPT			
B2	7.5 YR 5/8			MOD	MED	SBK	GRADUAL	2	MED	
Horizon	Mottles %	Size	Conc Color	Concentration Size	REDUCED	Redox Size	Color			

Core Number			41							
Describer			chuck							
Horizon	Depth top	Depth Bottom	texture	% clay	Rock Fragments Vol	RF Kind	RF Size Shape (CM)	Rupture/Consistance (Moist)	Stickiness	Plastic
Ap	0	26	SiL	20	3	Chert	med/coarse gravel	FR	SS	SP
E	26	46	CL	30	10	chet/sandstone	coarse gravel	FR	SS	SP
B1	46	68	C	45	2	chert	fine gravel	Firm	MS	VP
B2	68	92	C	50	5%	chert	fine/medium gravel	Firm	MS	VP
B3	92	111	C	50	2%	chert	fine gravel	Very Firm	MS	VP
Horizon	Soil Color	Roots	Pores	Structure Grade	Structure Size	Structure type	Boundary	Manganese	Size	
Ap	10 YR 4/4	FF		WEAK	MED	SBK				
E	10 YR 5/6			WEAK	MED	SBK	CLEAR			
B1	5 YR 5/8			WEAK	MED	SBK	CLEAR	10%	FINE	
B2	5 YR 4/6			WEAK	MED	SBK	GRADUAL	5%	MED	
B3	5 YR 5/8			WEAK	MED	SBK/AB	GRADUAL	7	MED	
Horizon	Mottles %	Size	Conc Color	Concentration Size	REDUCED	Redox Size	Color			
Ap										
E										
B1										
B2										
B3	5	FINE, PROMINENT	7.5 YR 6/8	2 mm		2mm	7.5 YR 6/1	root channels?		

Core Number			42							
Describer			chuck							
Horizon	Depth top	Depth Bottom	texture	% clay	Rock Fragments Vol	RF Kind	RF Size Shape (CM)	Rupture/Consistance (Moist)	Stickiness	Plastic
Ap	0	27	SiL	20	1	chert	med gravel	FR	SS	SP
B/E	27	44	CL	37				Firm	SS	MP
B1	44	70	C	45	1	chert	med gravel	Firm	SS	MP
B2	70	107	C	45	2%	chert	coarse gravel	VFR	SS	MP
Horizon	Soil Color	Roots	Pores	Structure Grade	Structure Size	Structure type	Boundary	Manganese	Size	
Ap	10 YR 4/3	FF	FF	WEAK	MED	SBK				
B/E	10 YR 5/4			WEAK	MED	SBK	ABRUPT			
B1	10 YR 5/6			WEAK	MED	SBK	CLEAR			
B2	10 YR 5/8			MODERATE	THIN	PLATY	ABRUPT	50%	FINE/MEDIUM	
Horizon	Mottles %	Size	Conc Color	Concentration Size	REDUCED	Redox Size	Color			

Core Number		43								
Describer		chuck								
Horizon	Depth (top and bottom)	texture	% clay	Rock Fragments Vol	RF Kind	RF Size Shape (CM)	Rupture/Consistance (Moist)	R/C Dry	Stickiness	Plastic
AP	0-8	CL	28	2%	chert	fine gravel	friable		NS	NP
AB	8 18	CL	35	2	chert	fine gravel	firm		SS	SP
B1	18-32	SICL	41	2	chert	fine gravel	firm		MS	MP
B2	32-52	SICL	45	25%	chert	coarse gravel	firm		MS	mp
B3	52-69	SICL	45	2	chert	fine gravel	firm		ss	sp
B4	69-84	CL	45	2	sandstone	medium gravel	friable		ms	mp
B5	84-108	CL	42	5	chert/sandstone	fine/medium gravel	friable		ss	sp
	Soil Color	Roots	Pores	Structure Grade	Structure Size	Structure type	Boundary	Manganese	Size	
AP	10 YR 4/3	F F		WEAK	MED	SBK PLATY		NO		
AB	10 YR 5/6	FF		MOD	MED	SBK	CLEAR	5%	FINE	
B1	10 YR 5/8	NO		WEAK	MED	SBK	CLEAR	20%	COARSE	
B2	7.5 YR 5/6	NO		WEAK	MED	SBK	CLEAR	5%	FINE	
B3	7.5 YR 5/8	NO		WEAK	MED	SBK	CLEAR	10%	FINE	
B4	5 YR 4/6	NO		WEAK	MED	SBK	CLEAR	5%	FINE	
B5	10 YR 5/8	NO		WEAK	MED	SBK	CLEAR	5%	FINE	
Horizon	Mottles %	Size	Conc Color	Concentration Size	REDUCED	Redox Size	Color			
AP										
AB										
B1										
B2										
B3										
B4										
B5										

Core Number			44							
Describer			chuck							
Horizon	Depth top	Depth Bottom	texture	% clay	Rock Fragments Vol	RF Kind	RF Size Shape (CM)	Rupture/Consistance (Moist)	Stickiness	Plastic
Ap1	0	22	SiL	20	1%	chert	med gravel	vfr	so	mp
E1	22	49	SiL	23	1	chert	med gravel	vfr	so	mp
E2	49	74	SiL	20	0			vfr	so	mp
2Ap	74	97	SiL	20	0%			vfr	so	mp
2E	97	110	SiL	20	1	chert	fine/med	vfr	so	mp
Horizon	Soil Color	Roots	Pores	Structure Grade	Structure Size	Structure type	Boundary	Manganese	Size	
Ap1	10YR 4/4	FEWFINE		weak	med	platy/sbk		3%	fine	
E1	10YR 5/4	FEWFINE		weak	med	platy	clear	1%	fine	
E2	10YR5/6	FEWFINE	FEWCOARSE	weak	med	platy	clear	1%	fine	
2Ap	10YR3/2			weak	med to fine	sbk	abrupt	20%	med	
2E	10YR4/3			weak	med	sbk	abrupt	0%		
Horizon	Mottles %	Size	Conc Color	Concentration Size	REDUCED	Redox Size	Color			
Ap1										
E1										
E2										
2Ap										
2E										

Core Number			45							
Describer			chuck							
Horizon	Depth top	Depth Bottom	texture	% clay	Rock Fragments Vol	RF Kind	RF Size Shape (CM)	Rupture/Consistance (Moist)	Stickiness	Plastic
Ap1	0	27	SiL	20	1	chert	med gravel	FR	SO	PO
Ap2	27	52	SiL	25	1	chert	med gravel	FR	SS	SP
2Ap1	52	65	SiL	25	10	chert	coarse gravel	VFR	SS	SP
E	65	83	CL	30	2%	chert	coarse gravel	VFR	SS	SP
B1	83	98	C	40	0%			FR	SS	MP
B2	98	108	C	45	5	chert	coarse gravel	FR/Firm	MS	MP
Horizon	Soil Color	Roots	Pores	Structure Grade	Structure Size	Structure type	Boundary	Manganese	Size	
Ap1	10 YR 4/4	FF	FF	WEAK	MED	SBK				
Ap2	2.5 Y 4/4			WEAK	MED	SBK	GRADUAL			
2Ap1	10 YR 3/3			WEAK	MED	SBK	GRADUAL			
E	10 YR 4/4			WEAK	MED	SBK	GRADUAL			
B1	10 YR 5/6			WEAK	MED	SBK	CLEAR			
B2	10 YR 5/8			WEAK	MED	SBK	CLEAR			
Horizon	Mottles %	Size	Conc Color	Concentration Size	REDUCED	Redox Size	Color			

Core Number			46	test core						
Describer			chuck							
Horizon	Depth top	Depth Bottom	texture	% clay	Rock Fragments Vol	RF Kind	RF Size Shape (CM)	Rupture/Consistance (Moist)	Stickiness	Plastic
Ap	0	20	L	15	1	chert	fine gravel	VFR	SO	PO
AB	20	43	CL	27	0.5	chert	fine gravel	FR	SS	SP
B1	43	57	C	40	4	chert	med gravel	FR	SS	MP
B2	57	95	C	40	3	chert	med gravel	FR	SS	VP
B3	95	120	CL	35	0.5	chert	fine gravel	VFR	SS	VP
	Soil Color	Roots	Pores	Structure Grade	Structure Size	Structure type	Boundary	Manganese	Size	
Ap	10 YR 4/3	FEW FINE		WEAK	MED	SBK				
AB	10 YR 4/6			WEAK	MED	SBK	CLEAR	FEW	FINE	
B1	10 YR 5/8			WEAK	MED	SBK	CLEAR			
B2	10 YR 5/8			WEAK	THIN	PLATY	CLEAR	FEW	FINE	
B3	10 YR 5/8			WEAK	THIN	PLATY	ABRUPT	COMMON	COARSE	
	Mottles %	Size	Conc Color	Concentration Size	REDUCED	Redox Size	Color			
Ap										
AB										
B1										
B2	50	COARSE	7.5 YR 5/8	COARSE	20	MED	10YR 6/3			
B3	60	COARSE	7.5 YR 5/8	COARSE	30	MED	10YR 6/3			

Core Number			47	test core						
Describer			chuck							
Horizon	Depth top	Depth Bottom	texture	% clay	Rock Fragments Vol	RF Kind	RF Size Shape (CM)	Rupture/Consistance (Moist)	Stickiness	Plastic
Ap	0	18	L	15	2	chert	fine/med gravel	vfr	SO	SP
BE	18	28	CL	35	2	chert	fine/med gravel	fr	SS	MP
B1	28	50	C	40	0.5	chert	fine	fr	SS	MP
B2	50	75	SCL	35	0.5	chert	fine	fr	SS	SP
B3	75	100	SCL	35	0.5	chert	fine	fr	SS	SP
Horizon	Soil Color	Roots	Pores	Structure Grade	Structure Size	Structure type	Boundary	Manganese	Size	
Ap	10 YR 4/3	FEW FINE		WEAK	MED	SBK				
BE	7.5 YR 5/6	FEW FINE		WEAK	MED	SBK	CLEAR			
B1	5 YR 5/8			WEAK	MED	SBK	CLEAR			
B2	5 YR 5/8			WEAK	MED	SBK/PLATY	ABRUPT	30%	COARSE	
B3	5 YR 5/6			WEAK	MED	SBK	CLEAR	30%	COARSE	
Horizon	Mottles %	Size	Conc Color	Concentration Size	REDUCED	Redox Size	Color			
Ap										
BE										
B1										
B2										
B3										

Core Number			48							
Describer			chuck							
Horizon	Depth top	Depth Bottom	texture	% clay	Rock Fragments Vol	RF Kind	RF Size Shape (CM)	Rupture/Consistance (Moist)	Stickiness	Plastic
Ap1	0	25	SiL	17	0			FR	SO	PO
Ap2	25	63	SiL	24	0			FR	SS	SP
Ap3	63	80	SiL	20	0			VFR	SS	SP
2Ap1	80	92	SiL	20	3%	chert	med/coarse gravel	VFR	SS	SP
E/B	92	116	CL	35	2%	chert	medium gravel	FR/FIRM	SS	MP
Horizon	Soil Color	Roots	Pores	Structure Grade	Structure Size	Structure type	Boundary	Manganese	Size	
Ap1	2.5 Y 4/4	FEW FINE	FEW MED	WEAK	THIN/MED	PLATY/SBK				
Ap2	2.5Y 4/4	FEW FINE	FEW MED	WEAK	THIN/MED	PLATY/SBK	GRADUAL			
Ap3	2.5 Y 3/3			WEAK	THIN/MED	PLATY/SBK	CLEAR			
2Ap1	2.5 Y 3/2			WEAK	MED	SBK	CLEAR			
E/B	10 YR 5/6			WEAK	MED	SBK	CLEAR			
Horizon	Mottles %	Size	Conc Color	Concentration Size	REDUCED	Redox Size	Color			

Core Number			49							
Describer			chuck							
Horizon	Depth top	Depth Bottom	texture	% clay	Rock Fragments Vol	RF Kind	RF Size Shape (CM)	Rupture/Consistance (Moist)	Stickiness	Plastic
Ap1	0	35	SiL	20	1	chert	fine/med	FR	SO	SP
E/B	35	56	CL	35	1	chert	fine/med	FR	SS	MP
B1	56	91	C	45	0.5	chert	fine	FR	MS	MP
B2	91	120	C	45	0.5	chert	fine	Firm	MS	VP
Horizon	Soil Color	Roots	Pores	Structure Grade	Structure Size	Structure type	Boundary	Manganese	Size	
Ap1	10YR 4/3	FF		WEAK	MED	SBK				
E/B	10 YR 5/6			WEAK	MED	SBK	CLEAR			
B1	10 YR 5/8			WEAK	MED	SBK	CLEAR			
B2	10 YR 5/6			WEAK	MED	SBK	ABRUPT	20%	COARSE	
Horizon	Mottles %	Size	Conc Color	Concentration Size	REDUCED	Redox Size	Color			
Ap1										
E/B										
B1										
B2	5	MED	7.5 YR 5/8							

Core Number			51							
Describer			chuck							
Horizon	Depth top	Depth Bottom	texture	% clay	Rock Fragments Vol	RF Kind	RF Size Shape (CM)	Rupture/Consistance (Moist)	Stickiness	Plastic
Ap	0	10	SCL	25	5%	chert	med gravel	VFR	SO	P
B1	10	47	CL	30	0%			VFR	SO	VP
B2	47	85	CL	30	3%	chert	fine/med	VFR	SO	VP
B3	85	103	CL	30	1%	chert	fine gravel	VFR	SO	P
B4	103	111	CL	30	1%	chert	fine gravel	VFR	SO	P
B5	111	118	CL	40	1%	chert	fine gravel	VFR	SS	P
Horizon	Soil Color	Roots	Pores	Structure Grade	Structure Size	Structure type	Boundary	Manganese	Size	
Ap	10YR 4/6	FF		W	M	SBK				
B1	10YR 5/6			W	THIN	PLATY	CLEAR	7%	COARSE	
B2	7.5YR 5/6			W	THIN	PLATY	CLEAR	5%	COARSE	
B3	7.5YR 5/8			W	M	SBK	CLEAR	5%	COARSE	
B4	10YR 5/3			W	M	SBK	CLEAR	10%	COARSE	
B5	5 YR 5/6			W	M	SBK	ABRUPT	1%	MEDIUM	
Horizon	Mottles %	Size	Conc Color	Concentration Size	Redox %	Redox Size	Color			
Ap										
B1	80	COARSE	10YR 5/8	MED		VERY COARSE	10YR 6/3			
B2	60	COARSE	10YR 5/8	MED		VERY COARSE	10YR 6/3			
B3										
B4	80	COARSE	1OYR 5/8	MED		VERY COARSE	10YR 6/3			
B5										

Core Number			52							
Describer			chuck							
Horizon	Depth top	Depth Bottom	texture	% clay	Rock Fragments Vol	RF Kind	RF Size Shape (CM)	Rupture/Consistance (Moist)	Stickiness	Plastic
Ap1	0	20	SiL	20	1%	chert	med gravel	VFR	SO	PO
Ap2	20	45	SiL	20	1	chert	med gravel	VFR	SO	PO
Ap3	45	72	SiL	20	1	chert	med gravel	FR	SO	PO
Ap4	72	80	SiL	20	1%	chert	med gravel	FR	SO	PO
E1	80	110	SiL	20	1	chert	med gravel	FR	SS	MP
E2	110	120+	SiL	20	1%	chert	med gravel	FR	SS	MP
Horizon	Soil Color	Roots	Pores	Structure Grade	Structure Size	Structure type	Boundary	Manganese	Size	
Ap1	10 YR 4/4	few fine	few fine and medium	weak	med	sbk		1%	fine	
Ap2	2.5 Y 4/4	few fine	few fine and medium	weak	med	sbk				
Ap3	10 YR 5/4	few fine	few fine and medium	med	med	platy				
Ap4	10 YR 3/2	few fine	few fine and medium	weak	med	platy				
E1	10 YR 5/6	few fine	few fine and medium	weak	med	sbk				
E2	10 YR 5/6	few fine	few fine and medium	weak	med	sbk				
Horizon	Mottles %	Size	Conc Color	Concentration Size	REDUCED	Redox Size	Color			
Ap1										
Ap2										
Ap3										
Ap4										
E1										
E2										

Core Number		53	test core						
Describer		chuck							
Horizon	Depth (top and bottom)	texture	% clay	Rock Fragments Vol	RF Kind	RF Size Shape (CM)	Rupture/Consistance (Moist)	Stickiness	Plastic
Ap	0 - 21	L	20	3%	chert/sandstone	med gravel	VFR	NS	NP
EB1	21 -32	CL	35	2	chert	med gravel	FR	SS	SP
EB2	32 -38	CL	30	2	chert	med gravel	FR	SS	SP
EB3	38 - 61	SCL	30	5%	chert	fine gravel	L/FR	NS	NP
B1	61 - 73	C	41	1	chert	fine gravel	FR	SS	SP
B2	73 -106	C	45	3%	chert	med gravel	FR	SS	SP
B3	106-114	SCL	30	5%	chert	fine gravel	L/FR	NS	NP
Horizon	Soil Color	Roots	Pores	Structure Grade	Structure Size	Structure type	Boundary	Manganese	Size
Ap	10 YR 3/4	F F		WEAK	FINE	SBK			
EB1	7.5 YR 5/8	F F		WEAK	MED	SBK	CLEAR	5%	FINE
EB2	10 YR 5/4			WEAK	MED	SBK	CLEAR	5%	FINE
EB3	10 YR 5/6			WEAK	FINE	SBK	ABRUPT	50%	COARSE
B1	7.5 YR 5/8			WEAK	MED	SBK	ABRUPT	10%	MED
B2	7.5 YR 5/8			WEAK	MED	SBK	CLEAR	7%	MED
B3	10 YR 5/4			WEAK	FINE	SBK	ABRUPT	60%	COARSE
Horizon	Mottles %	Size	Conc Color	Concentration Size	REDUCED	Redox Size	Color		
Ap									
EB1									
EB2									
EB3									
B1									
B2									
B3									

Core Number			54							
Describer			chuck							
Horizon	Depth top	Depth Bottom	texture	% clay	Rock Fragments Vol	RF Kind	RF Size Shape (CM)	Rupture/Consistance (Moist)	Stickiness	Plastic
Ap1	0	25	SiL	17	1	chert	fine/coarse gravel	FR	SS	SP
Ap2	25	50	SiL	17	1	chert	fine/coarse gravel	FR	SS	SP
Ap3	50	90	SiL	17	1	chert	fine/coarse gravel	FR	SS	SP
2Ap1	90	110	SiL	15	1%	chert	fine/coarse gravel	VFR	SO	PO
Horizon	Soil Color	Roots	Pores	Structure Grade	Structure Size	Structure type	Boundary	Manganese	Size	
Ap1	10YR 5/3	FEW FINE	FEW MEDIUM	MOD	THIN	PLATY				
Ap2	10 YR 4/3	FEW FINE	FEW FINE	WEAK	THIN	PLATY	GRADUAL			
Ap3	10YR 4/3			WEAK	THIN/MED	PLATY/SBK	GRADUAL			
2Ap1	10YR 2/2			WEAK	MED	SBK	CLEAR			
Horizon	Mottles %	Size	Conc Color	Concentration Size	REDUCED	Redox Size	Color			

Core Number			55							
Describer			chuck							
Horizon	Depth top	Depth Bottom	texture	% clay	Rock Fragments Vol	RF Kind	RF Size Shape (CM)	Rupture/Consistance (Moist)	Stickiness	Plastic
Ap1	0	35	SiL	20	2	chert	coarse	VFR	NS	SP
E	35	50	CL	30	1	chert	med	FR	SS	SP
B1	50	77	C	40	0.5	chert	fine	FR	SS	MP
B2	77	96	C	40	0.5	chert	fine	VFR	SS	MP
B3	96	120	C	40	0.5	chert	fine	FR	SS	MP
Horizon	Soil Color	Roots	Pores	Structure Grade	Structure Size	Structure type	Boundary	Manganese	Size	
Ap1	10 YR 4/3	FF	FF	WEAK	MED	SBK/GRAN				
E	10 YR 5/6	FF	FF	WEAK	MED	SBK	CLEAR			
B1	10 YR 5/8			WEAK	THIN/MED	PLATY/SBK	CLEAR			
B2	10 YR 5/6			MOD	THIN	PLATY	ABRUPT	20%	COARSE	
B3	7.5 YR 5/8			WEAK	MED	SBK	CLEAR			
Horizon	Mottles %	Size	Conc Color	Concentration Size	REDUCED	Redox Size	Color			
Ap1										
E										
B1										
B2	5	MED	7.5 YR 5/8							
B3	5					MED	7.5 YR 6/2			

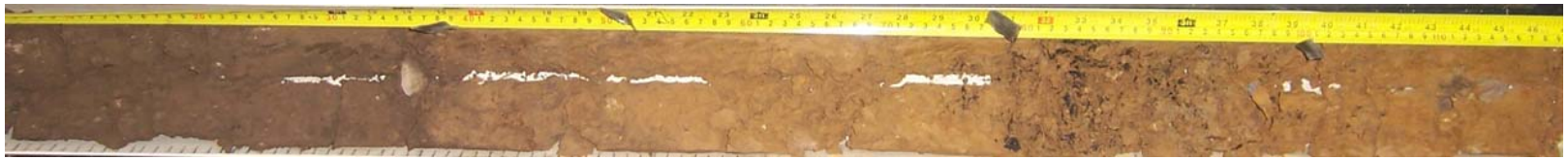

Core Number		56	test core							
Describer		chuck								
Horizon	Depth (top and bottom)	texture	% clay	Rock Fragments Vol	RF Kind	RF Size Shape (CM)	pH (water 1:1)	pH(CaCl2 1:1)	Stickiness	Plastic
Ap	0-15			15	chert	gravel	6.65	6.43		
Ap2	15-26			10	chert	gravel	6.93	6.43		
EB	26-36			5			7.12	6.45		
B1	36-63			5			7.16	6.48		
B2	63-80			5			6.77	6.23		
B3	80-85			5			5.43	4.95		
	Soil Color	Roots	Pores	Structure Grade	Structure Size	Structure type	Boundary	Manganese	Size	
Ap	10 YR 4/6			mod	coarse	platy		no		
Ap2	10 YR 4/6			mod	coarse	platy		no		
EB	10 YR 5/8			weak	med	sbk		no		
B1	7.5 YR 5/8			mod	med	bk		no		
B2	7.5 YR 5/8			mod	med	bk		yes	med	
B3	7.5 YR 5/8									
Horizon	Mottles %	Size	Conc Color	Concentration Size	REDUCED	Redox Size	Color			
Ap										
Ap2										
EB										
B1										
B2										
B3										

Core Number			57										
Describer			chuck										
Horizon	Depth top	Depth Bottom	texture	% clay	Rock Fragments Vol	RF Kind	RF Size Shape (CM)	pH (water 1:1)	pH(CaCl2 1:1)	Rupture/Consistance (Moist)	R/C Dry	Stickiness	Plastic
Ap	0	36	SiL	20	1	chert	med gravel			FR		SS	SP
E/B	36	48	CL	30	2	chert	coarse gravel			FR		SS	MP
B1	48	76	C	40	1	chert	fine gravel			Firm		MS	MP
B2	76	106	C	42	1%	chert	fine gravel			Firm		MS	VP
B3	106	116	C	45	1%	chert	fine gravel			FR/Firm		MS	VP
Horizon	Soil Color	Roots	Pores	Structure Grade	Structure Size	Structure type	Boundary	Manganese	Size				
Ap	10 YR 4/3	FF	FF	WEAK	MED	SBK							
E/B	10 YR 4/6			WEAK	MED	SBK	CLEAR						
B1	10 YR 5/6			WEAK	MED	SBK	CLEAR	2%	MEDIUM				
B2	10 YR 5/8			WEAK	THIN	PLATY	GRADUAL	15%	COARSE				
B3	10 YR 5/8			MOD	THIN	PLATY	CLEAR	50-60	COARSE				
Horizon	Mottles %	Size	Conc Color	Concentration Size	REDUCED	Redox Size	Color						

Core Number			58							
Describer			chuck							
Horizon	Depth top	Depth Bottom	texture	% clay	Rock Fragments Vol	RF Kind	RF Size Shape (CM)	Rupture/Consistance (Moist)	Stickiness	Plastic
Ap	0	20	SiL	20	0.5	chert	fine gravel	VFR	SS	SP
B1	20	32	C	45				FIRM	SS	VP
B2	32	60	C	40	2	chert	med gravel	VFR/FR	MS	VP
B3	60	85	C	50	0.5	chert	med gravel	FIRM	MS	VP
Horizon	Soil Color	Roots	Pores	Structure Grade	Structure Size	Structure type	Boundary	Manganese	Size	
Ap	10 YR 4/4	FF	FF	WEAK	MED	SBK/GRANULAR				
B1	7.5 YR 5/6			MOD	MED	SBK	CLEAR			
B2	7.5 YR 5/6			MOD	THIN	PLATY	CLEAR	2	MED	
B3	5 YR 4/6			MOD	MED	SBK	CLEAR	1	MED	
Horizon	Mottles %	Size	Conc Color	Concentration Size	REDUCED	Redox Size	Color			

Core Number			59							
Describer			chuck							
Horizon	Depth top	Depth Bottom	texture	% clay	Rock Fragments Vol	RF Kind	RF Size Shape (CM)	Rupture/Consistance (Moist)	Stickiness	Plastic
Ap1	0	30	SiL	17	1	chert	med gravel	FR	SO	PO
Ap2	30	70	SiL	17	1	chert	med gravel	FR	SO	SP
Ap3	70	100	SiL	20	1	chert	med gravel	FR	SO	SP
2Ap1	100	120	SiL	20	1%	chert	coarse gravel	VFR	SO	SP
Horizon	Soil Color	Roots	Pores	Structure Grade	Structure Size	Structure type	Boundary	Manganese	Size	
Ap1	10YR 4/4	FEWFINE	FEW FINE	MOD	THIN	PLATY				
Ap2	10YR 4/3	FEWFINE	FEW FINE	WEAK	THIN	PLATY	GRADUAL			
Ap3	10YR 4/3	FEWFINE		WEAK	MED	SBK	GRADUAL			
2Ap1	10YR 3/3			WEAK	MED	SBK	CLEAR			
Horizon	Mottles %	Size	Conc Color	Concentration Size	REDUCED	Redox Size	Color			

APPENDIX B

SOIL TRENCH DESCRIPTIONS

Pit Number	1	Site Number	1						
Describer			Jake						
Horizon	Depth top	Depth Bottom	texture	% clay	Rupture/Consistance (Moist)	Stickiness	Plastic		
1 Ap	0	20	Silt Loam	20	Very Friable	NS	NP		
2 B/Ap	20	28	Silty Clay Loam	33	Friable	SS	SP		
3 Bt1	28	60	Clay Loam	37	Friable	SS	P		
4 Bt2	60	112	Clay Loam	37	Friable	SS	P		
5 Bt3	112	152+	Clay Loam	35	Friable	SS	P		
Horizon	Soil Color	Roots	Pores	Structure Grade	Structure Size	Structure type	Boundary	Manganese	Size
1 Ap	2.5 YR 4/3	M, VF	M	S	M/F	Granular	abrupt/smooth		
2 B/Ap	10 YR 5/6	C, VF	C, M	M	M	SBK	clear/smooth		
3 Bt1	10 YR 5/6	C, VF	C, M	M	M	SBK	clear/wavy		
4 Bt2	7.5 YR 5/8	F, VF	F, M	M	M	SBK	clear/smooth	7%	C
5 Bt3	5 YR 5/8	none	None	W	C	SBK		<2%	C
Horizon	Mottles %	Size	Conc Color	Concentration Size	REDUCED	Redox Size	Color		
1 Ap									
2 B/Ap									
3 Bt1	Common	Coarse	5YR 5/8				10 YR 6/3		
4 Bt2	Few	Medium	7.5 YR 5/8				10YR 5/4		
5 Bt3									

Pit Number	1	Site Number	2						
Describer			Jake						
Horizon	Depth top	Depth Bottom	texture	% clay	Rupture/Consistance (Moist)	Stickiness	Plastic		
1 Ap1	0	34	Silt Loam	20	Very Friable	NS	NP		
2 Bt1	34	52	Silty Clay Loam	33	Friable	SS	SP		
3 Bt2	52	86	Clay Loam	35	Friable	SS	SP		
4 Bt3	86	137	Clay Loam	35	Friable	SS	SP		
5 Bt4	137	145+	Clay Loam	35	Friable	SS	SP		
Horizon	Soil Color	Roots	Pores	Structure Grade	Structure Size	Structure type	Boundary	Manganese	Size
1 Ap1	2.5 YR 4/4	M VF	C M	Strong	M/F	Granular	Abrupt/Smooth		
2 Bt1	7.5 YR 5/6	C F	C M	Medium	M	SBK	Clear/Smooth		
3 Bt2	5 YR 5/8	C F	C M	Medium	M	SBK	Clear/Smooth	2%	Coarse
4 Bt3	5 YR 5/6	F F	none	Medium	M	SBK	Clear/Smooth	2%	Coarse
5 Bt4	5 YR 5/8	None	none	Weak	M	SBK			
Horizon	Mottles %	Size	Conc Color	Concentration Size	REDUCED	Redox Size	Color		
1 Ap1									
2 Bt1									
3 Bt2									
4 Bt3									
5 Bt4									

Pit Number	2	Site Number	1						
Describer			Jake						
Horizon	Depth top	Depth Bottom	texture	% clay	Rupture/Consistance (Moist)	Stickiness	Plastic		
1 Ap1	0	20	Silt Loam	20	Friable	NS	NP		
2 Bt1	20	48	Silty Clay Loam	30	Friable	SS	SP		
3 Bt2	48	117	Clay Loam	25	Friable	SS	SP		
4 Bt3	117	143+	Clay	50 to 55	Firm	S	P		
Horizon	Soil Color	Roots	Pores	Structure Grade	Structure Size	Structure type	Boundary	Manganese	Size
1 Ap1	10 YR 4/4	M, very fine	none	Strong	M/F	Granular			
2 Bt1	10 YR 5/8	F, very fine	none	Moderate	M	SBK		15%	Coarse
3 Bt2	7.5 YR 5/8	none	none	Moderate	C	SBK		15%	Coarse
4 Bt3	10 YR 5/8	none	none	Weak	VC	SBK		2%	Coarse
Horizon	Mottles %	Size	Conc Color	Concentration Size	REDUCED	Redox Size	Color		
1 Ap1									
2 Bt1	15%	Coarse	7.5 YR 5/8	Coarse		10 YR 6/3			
3 Bt2									
4 Bt3									

Pit Number	2	Site Number	2						
Describer			Jake						
Horizon	Depth top	Depth Bottom	texture	% clay	Rupture/Consistance (Moist)	Stickiness	Plastic		
1 Ap1	0	21	Silt Loam	20	FR	NS	NP		
2 Bt1	21	68	Silty Clay Loam	32	FR	SS	SP		
3 Bt2	68	90	Silty Clay Loam	32	FR	SS	SP		
4 Bt3	90	104	Clay Loam	32	FR	SS	SP		
5 Bt 4	104	136	Silty Clay Loam	37	FR	S	P		
Horizon	Soil Color	Roots	Pores	Structure Grade	Structure Size	Structure type	Boundary	Manganese	Size
1 Ap1	10 YR 5/6	M, VF		Strong	M/F	Gran	Abrupt, Smooth		
2 Bt1	7.5 YR 6/8	F, VF	Common med	Mod	Coarse/M	SBK	Gradual Wavy	30	Coarse
3 Bt2	7.5 YR 5/8			Mod	Med	SBK	Clear Wavy	2%	Medium
4 Bt3	10 YR 5/8			Mod	Med	SBK	Clear Wavy	30%	Medium
5 Bt 4	5 YR 5/8			Weak	Coarse	SBK		2	Medium
Horizon	Mottles %	Size	Conc Color	Concentration Size	REDUCED	Redox Size	Color		
1 Ap1									
2 Bt1									
3 Bt2									
4 Bt3									
5 Bt 4									

Pit Number	3	Site Number	1						
Describer			Jake						
Horizon	Depth top	Depth Bottom	texture	% clay	Rupture/Consistance (Moist)	Stickiness	Plastic		
1 Ap1	0	20	SiL	20	FR	NS	NP		
2 Ap2	20	63	SiL	20	FR	NS	NP		
3 ApB	63	83	SiL	25	FR	NS	NP		
Bt1b	83	106	Silty Clay Loam	33	FR	SS	SP		
Bt2b	106	138+	Silty Clay Loam	38	FR	SS	SP		
Horizon	Soil Color	Roots	Pores	Structure Grade	Structure Size	Structure type	Boundary	Manganese	Size
1 Ap1	2.5 Y 4/4	C C	C C	Strong	Med/fine	Granular	Clear Smooth		
2 Ap2	2.5 Y 5/4	C C	C C	Mod	med	SBK	Clear Smooth		
3 ApB	2.5 Y 5/3	F F	F F	Weak	Med/fine	SBK	Gradual Smooth		
Bt1b	10 YR/54			Mod	Med/fine	SBK	Clear Smooth		
Bt2b	10 YR/54			Mod	Med/fine	SBK			
Horizon	Mottles %	Size	Conc Color	Concentration Size	REDUCED	Redox Size	Color		
1 Ap1									
2 Ap2									
3 ApB									
Bt1b									
Bt2b	30%	Coarse	7.5 YR 5/8				10 YR 5/1		

Pit Number	4	Site Number							
Describer			Jake						
Horizon	Depth top	Depth Bottom	texture	% clay	Rupture/Consistance (Moist)	Stickiness	Plastic		
Ap	0	20	Silt Loam	21	Friable	NS	NP		
Bt1	20	66	Clay Loam	38	Friable	SS	SP		
Bt2	66	113	Silty Clay Loam	33	Friable	SS	SP		
Bt3	113	140+	Silty Clay Loam	35	Friable	SS	SP		
Horizon	Soil Color	Roots	Pores	Structure Grade	Structure Size	Structure type	Boundary	Manganese	Size
Ap	10 YR 4/4	3 vf/f		Strong	M & F	SBK	Abrupt Smooth		
Bt1	5 YR 5/8	1 f	1, M, Tu	Moderate	M	SBK	Clear Wavy	< 2	medium
Bt2	7.5 YR 5/6			Moderate	C & M	SBK	Gradual Wavy	15%	coarse/medium
Bt3	7.5 YR 5/6			Weak	C	SBK		15%	coarse
Horizon	Mottles %	Size	Conc Color	Concentration Size	REDUCED	Redox Size	Color		
Ap									
Bt1									
Bt2									
Bt3									

Pit Number	5	Site Number							
Describer			Jake						
Horizon	Depth top	Depth Bottom	texture	% clay	Rupture/Consistance (Moist)	Stickiness	Plastic		
Ap	0	34	Silt Loam	21	Friable	NS	NP		
BE	34	67	Silty Clay Loam	30	Friable	SS	SP		
Bt1	67	105	Clay Loam	30-35	Friable	SS	SP		
Bt2	105	144	Silty Clay	45-50	Friable	S	P		
Horizon	Soil Color	Roots	Pores	Structure Grade	Structure Size	Structure type	Boundary	Manganese	Size
Ap	10 YR 4/3	Many VF		Strong	Fine/Med	Gran/SBK	Abrupt Smooth		
BE	10 YR 5/4	Few VF	Few Medium	Moderate	Med/Coarse	SBK	Coarse Smooth		
Bt1	7.5 YR 5/6			Moderate	Coarse	SBK	Gradual Wavy	15%	Med/Coarse
Bt2	5 YR 5/6			Moderate	Coarse	SBK		25%	Coarse/VC
Horizon	Mottles %	Size	Conc Color	Concentration Size	REDUCED	Redox Size	Color		
Ap									
BE									
Bt1	2	Coarse	5YR 5/8		10YR 5/4				
Bt2	15	Coarse	5YR 5/8		10YR 5/4				

Pit Number	6	Site Number							
Describer			Jake						
Horizon	Depth top	Depth Bottom	texture	% clay	Rupture/Consistance (Moist)	Stickiness	Plastic		
Ap	0	36	SiL	22	Friable	NS	NP		
BE	35	44	SiL	25	Friable	NS	NP		
Bt1	44	66	CL	32	Friable	SS	SP		
Bt2	66	105	CL	37	Friable	SS	SP		
Bt3	105	146+	C	45	Firm	S	P		
Horizon	Soil Color	Roots	Pores	Structure Grade	Structure Size	Structure type	Boundary	Manganese	Size
Ap	10YR 3/3	Many F & VF		Stong	M & F	GR	AS		
BE	10YR 4/6	Few F	Few M	Moderate	C & M	SBK	GS	2	Medium
Bt1	7.5YR 5/6			Moderate	C & M	SBK	CW	25%	C and VC
Bt2	7.5YR 5/6			Moderate	M & F	SBK	GW	25%	C and VC
Bt3	10YR 5/8			Moderate/Weak	M&C/M&T	SBL/PL			
Horizon	Mottles %	Size	Conc Color	Concentration Size	REDUCED	Redox Size	Color		
Ap									
BE									
Bt1									
Bt2									
Bt3	<2%					Med	7.5YR 7/3		

VITA
CHARLES W. WALKER

BIRTH LOCATION/ DATE: Philipsburg (Hawk Run), Pennsylvania. January 14, 1978.

FAMILY: Susan Walker (wife), William and Alice Walker (parents).

EDUCATION:

The Pennsylvania State University, University Park, PA
Soil Science
Doctor of Philosophy

The Pennsylvania State University, University Park, PA
Environmental Pollution Control
Master of Science August 2002

The Pennsylvania State University, University Park, PA
Environmental Resource Management
Bachelor of Science May 2000
Minor: Environmental Engineering
Graduated with Distinction

PUBLICATIONS:

Walker, C., H. Lin and D.D. Fritton. 2006. Is the tension beneath the tension infiltrometer what we think it is? Vadose Zone Journal 5: 860-866.

Walker C. and R. Shannon. 2006. Nitrate and phosphate removal effects of compost amendments in wetland mesocosms. Transactions of the ASABE 49(6): (In print).

Lin, H., W. Kogelmann, **C. Walker**, and M. A. Bruns. 2006. Soil moisture patterns in a forested catchment: A hydropedological perspective. Geoderma 131: 345-368

HONORS:

Dean's List
Gamma Sigma Delta, Honorary Agricultural Fraternity
2nd place in NEBASA Oral Presentation Contest
2nd and 3rd place in Penn State University's Research Poster Expo
Honorary Mention, College of Agriculture Poster Contest